

COMPARATIVE BIOCHEMISTRY AND GENETIC ANALYSIS OF
NUCLEOSIDE HYDROLASE IN *Escherichia coli*, *Pseudomonas aeruginosa*, AND
Pseudomonas fluorescens

Christopher J. Fields

Dissertation Prepared for the Degree of

DOCTOR OF PHILOSOPHY

UNIVERSITY OF NORTH TEXAS

December 2002

APPROVED:

Gerard A. O'Donovan, Major Professor
Robert C. Benjamin, Committee Member
Mark A. Farinha, Committee Member
John Knesek, Committee Member
Mark S. Shanley, Committee Member
Earl G. Zimmerman, Chair of the of Biological Sciences
C. Neal Tate, Dean of the Robert B. Toulouse School of
Graduate Studies

Fields, Christopher J., Comparative biochemistry and genetic analysis of nucleoside hydrolase in *Escherichia coli*, *Pseudomonas aeruginosa*, and *Pseudomonas fluorescens*. Doctor of Philosophy (Biology), December 2002, 139 pp., 7 tables, 39 illustrations, 208 references, 3 chapters

The pyrimidine salvage enzyme, nucleoside hydrolase, catalyzes the irreversible hydrolysis of nucleosides into the free nucleic acid base and D-ribose. Nucleoside hydrolases have varying degrees of specificity towards purine and pyrimidine nucleosides. In *E. coli*, three genes were found that encode homologues of several known nucleoside hydrolases in protozoa. All three genes (designated *yaaF*, *yeiK*, and *ybeK*) were amplified by PCR and cloned. Two of the gene products (*yeiK* and *ybeK*) encode pyrimidine-specific nucleoside hydrolases, while the third (*yaaF*) encodes a nonspecific nucleoside hydrolase. All three were expressed at low levels and had different modes of regulation.

As a comparative analysis, the homologous genes of *Pseudomonas aeruginosa* and *P. fluorescens* (designated *nuh*) were cloned. Both were determined to encode nonspecific nucleoside hydrolases. The nucleoside hydrolases of the pseudomonads exhibited markedly different modes of regulation. Both have unique promoter structures and genetic organization. Furthermore, both pseudomonad nucleoside hydrolases were found to contain an N-terminal extension of 30-35 amino acids that is shown to act as a periplasmic-signaling sequence. These are the first two nucleoside hydrolases, to date, that have been conclusively demonstrated to be exported to the periplasmic space. The physiological relevance of this is explained.

ACKNOWLEDGMENTS

To my wife Tasha, who has always supported me; my extensive family, who were there when I needed them; and for my dad, who would smile at this.

TABLE OF CONTENTS

ACKNOWLEDGMENTS	ii
LIST OF TABLES	v
LIST OF ILLUSTRATIONS	vi
CHAPTER 1 – INTRODUCTION	1
Pyrimidine biosynthesis	1
Synopsis of the <i>de novo</i> pathway	1
Carbamoyl phosphate synthetase	3
Aspartate transcarbamoylase.....	4
Dihydroorotase	9
Dihydroorotate dehydrogenase	9
Orotate phosphoribosyltransferase	10
Orotidine-5'-monophosphate (OMP) decarboxylase	10
Uridine-5'-monophosphate kinase	11
Nucleoside diphosphate kinase	11
Cytidine-5'-triphosphate synthase	11
Overview of pyrimidine salvage reactions.....	12
Degradation of RNA	12
Breakdown of monophosphates	13
Transport of nucleosides and bases.....	14
Deaminations.....	14
Nucleoside kinases	15
Cytidine-monophosphate (CMP) kinase	15
Uracil phosphoribosyltransferase.....	15
Nucleoside phosphorylases	15
Nucleoside hydrolase	16
The crystal structure of the <i>Crithidia fasciculata</i> IUNH.....	18
The purine-specific IAGNH of <i>Trypanosoma vivax</i>	19
Conclusion.....	21
References	22

CHAPTER 2 – CLONING AND CHARACTERIZATION OF THREE ISOGENIC
NUCLEOSIDE HYDROLASES FROM *Escherichia coli* K-12..... 37

Introduction	37
Materials and Methods	41
Abbreviations and common names used	41
Chemicals and Supplies	41
Bacterial strains and media	42
Chromosomal DNA Isolation.....	47
Cloning and sequence determination	48
Nucleoside hydrolase enzyme assay	52
Software used	53
Results and Discussion.....	56
Cloning and expression of <i>yeiK</i> , <i>ybeK</i> , and <i>yaaF</i>	56
Induction and expression of the cloned nucleoside hydrolase genes.....	57
Multiple alignment and analysis of the translated nucleoside hydrolase genes.....	61
Structural analysis	61
Analysis of the genes and promoter regions	69
References	80

CHAPTER 3 – CLONING AND CHARACTERIZATION OF *nuh* ENCODING
NUCLEOSIDE HYDROLASE IN *Pseudomonas aeruginosa* PAO1
AND *Pseudomonas fluorescens* Pf0-1..... 86

Introduction	86
Materials and Methods	87
Abbreviations used.....	87
Bacterial strains and media	87
Determination of cellular localization.....	94
Cloning and sequence determination	95
Nucleoside hydrolase enzyme assay	98
Aspartate transcarbamoylase assay	99
Alkaline phosphatase assay.....	100
Phospholipase C assay	103
Software used	103
Results and Discussion.....	107
Analysis of <i>nuh</i> genes in <i>Pseudomonas aeruginosa</i> and <i>Pseudomonas fluorescens</i>	107
Enzyme specificity and regulation of NH expression.....	110
Multiple alignment and analysis of the N-terminal signaling peptide	120
Cellular localization studies of <i>Pseudomonas</i> NHs	120
Conclusions	127
References	131

LIST OF TABLES

<u>Table</u>	<u>Page</u>
Table 2.1: List of abbreviations.....	42
Table 2.2: List of strains, plasmids, and primers	46
Table 2.3: Statistical analysis of <i>E. coli</i> NHs.....	64
Table 2.4: Analysis of <i>E. coli</i> open reading frames	76
Table 3.1: List of abbreviations.....	89
Table 3.2: Strains, plasmids, and primers	93
Table 3.3: Summary of enzyme induction studies	119

LIST OF ILLUSTRATIONS

Figure	Page
Figure 1.1: The <i>E. coli</i> pyrimidine biosynthetic pathway	1
Figure 1.2: Classes of bacterial ATCases.....	5
Figure 1.3: Three-fold symmetry of the aspartate transcarbamoylase from <i>E. coli</i>	7
Figure 2.1: Pyrimidine salvage pathway reactions in <i>E. coli</i> K-12.....	39
Figure 2.2: Hydrolytic and phosphorylytic breakdown of uridine and UMP	40
Figure 2.3: Outline of cloning procedure	49
Figure 2.4: PCR reaction products	50
Figure 2.5: Standard determination for the reducing sugar assay	54
Figure 2.6: Bradford protein concentration assay, using lysozyme as a standard	55
Figure 2.7: Plasmid constructs pCJF2, pCJF3, pCJF4r	58
Figure 2.8: Hypothetical plasmid construct of <i>yeiK</i> gene in orientation with the promoter	59
Figure 2.9: Specific activity of induced nucleoside hydrolase clones from plasmids pCJF2, pCJF3, pCJF4r	60
Figure 2.10: Multiple alignment of nucleoside hydrolase homologues	62
Figure 2.11: Proposed catalytic site of the <i>E. coli</i> YbeK nucleoside hydrolase	66
Figure 2.12: Surface layering of the <i>E. coli</i> YbeK active site.....	67
Figure 2.13: <i>C. fasciculata</i> binding site	72
Figure 2.14: Genetic organization of <i>yaaF</i> a) Upstream region of <i>yaaF</i>	71
b) Putative rho-independent terminator of <i>yaaF</i>	71

Figure 2.15: Genetic organization of <i>ybeK</i>	
a) Upstream region of <i>ybeK</i>	72
b) Downstream region of <i>ybeK</i>	73
Figure 2.16: Genetic organization of <i>yeiK</i>	
a) Promoter region of <i>yeiK</i>	74
b) Downstream terminator region of <i>yeiK</i>	75
Figure 2.17: Alignment of potential transcription factor binding sites	76
Figure 3.1: Pyrimidine salvage circuits of <i>E. coli</i> and <i>P. aeruginosa</i>	95
Figure 3.2: <i>Pseudomonas aeruginosa</i> PAO1 PCR reactions	97
Figure 3.3: Plasmid maps	97
Figure 3.4: Standards determined using the DC microtiter plate assay	101
Figure 3.5: Standards used for the determination of carbamoyl aspartate concentration	102
Figure 3.6: Genetic organization of the <i>P. aeruginosa nuh</i> gene.....	105
Figure 3.7: Potential terminator located 3' of the <i>nuh</i> gene.....	106
Figure 3.8: Alignment of the putative P1 and P2 of <i>P. aeruginosa nuh</i> to other known σ^{54} promoters.....	108
Figure 3.9: Genetic organization of the <i>P. fluorescens nuh</i> gene	109
Figure 3.10: Alignment of upstream of <i>Pseudomonas rbs</i> operons, revealing the operator binding site and the promoter.....	111
Figure 3.11: Nucleoside specificity of <i>P. aeruginosa</i> NH	112
Figure 3.12: Regulation of <i>P. aeruginosa</i> nucleoside hydrolase expression	113
Figure 3.13: Regulation of <i>P. fluorescens</i> nucleoside hydrolase expression.....	117
Figure 3.14: Multiple alignment of nucleoside hydrolase from <i>Pseudomonas</i> and several other species	121
Figure 3.15: Alignments of signal peptide sequences	
a) Alignments of signal peptide sequences showing sequence conservation.....	123
b) Alignment showing conservation of amino acid characteristics between sequences	123

Figure 3.16: SignalP prediction.....	124
Figure 3.17: Localization of <i>P. aeruginosa</i> NH.....	125
Figure 3.18: Localization of <i>P. fluorescens</i> NH.....	126
Figure 3.19: Proposed mode of nucleoside breakdown in <i>Pseudomonas</i>	130

CHAPTER 1

INTRODUCTION

Pyrimidine biosynthesis

The biosynthesis of pyrimidines is a pathway that is present in all but the most parasitic of organisms. Biosynthesis of uridine-5'-triphosphate (UTP) and cytidine-5'-triphosphate (CTP) is essential because they are required precursors of RNA; if these compounds are not synthesized *de novo*, then they must be supplied through various salvage routes. Furthermore, CTP also acts as a precursor of 2'-deoxycytidine-5'-triphosphate (dCTP), while UTP is the precursor of 2'-deoxythymidine-5'-triphosphate (dTTP). Both dTTP and dCTP (pyrimidine deoxyribonucleotides) are required precursors of DNA synthesis.

Enzymes involved in pyrimidine metabolism have continuously been explored, to various degrees of success (Gero et al., 1984; Seymour et al., 1994; Parkin et al., 1997), as therapeutic targets due to their importance in cellular metabolism. Here, a brief synopsis of the steps leading to the biosynthesis of the ribonucleoside triphosphates is presented using *Escherichia coli* as a model.

Synopsis of the *de novo* pathway

Here we will discuss the *de novo* pathway leading to the formation of UTP and CTP, as shown in Figure 1.1.

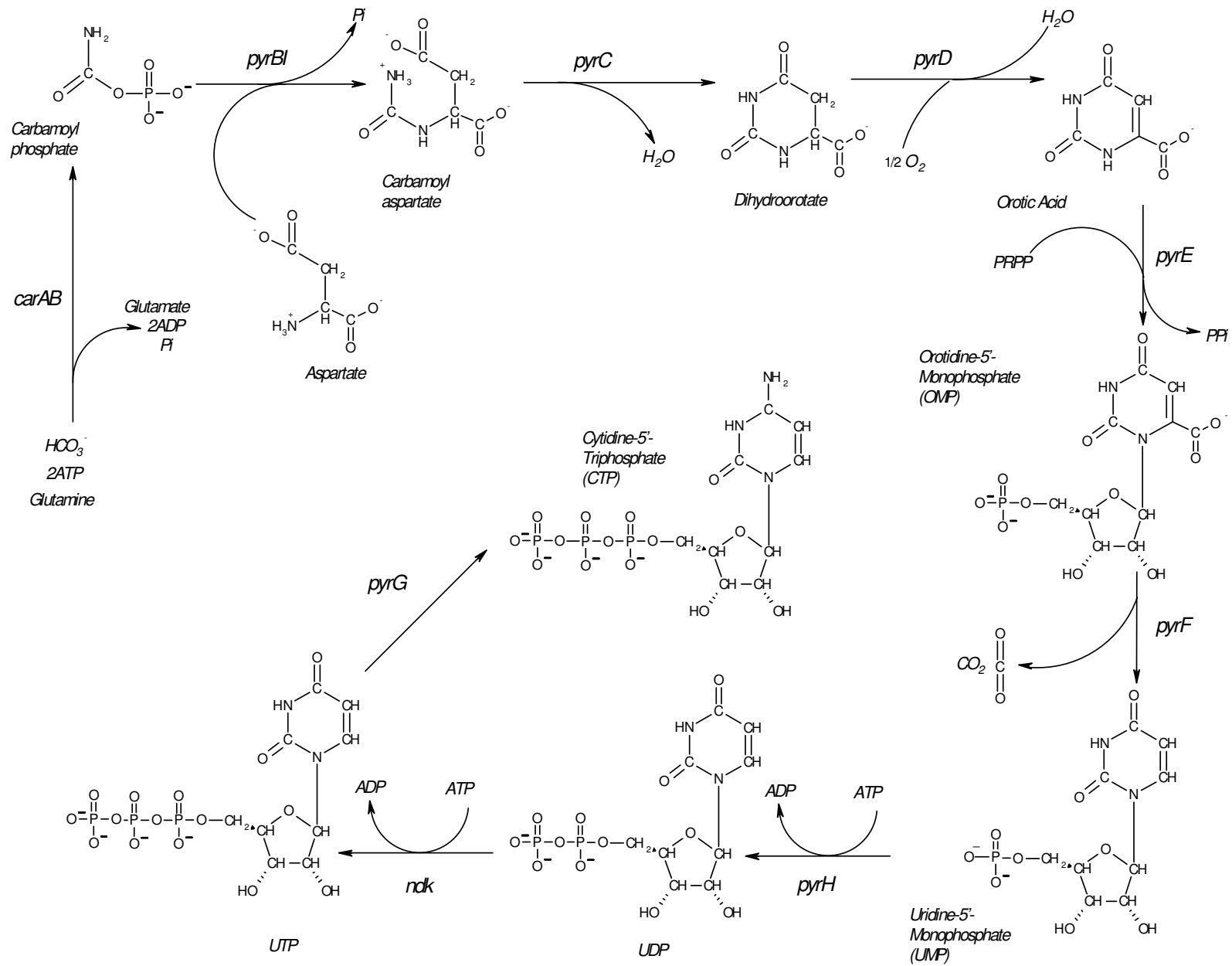


Figure 1.1 - The *E. coli* pyrimidine biosynthetic pathway.

Carbamoyl phosphate synthetase (CPSase, *carA* and *carB*, EC 6.3.5.5)

The first reaction leading to the formation of pyrimidines is the formation of the high-energy compound carbamoyl phosphate (CP). This compound is also the precursor of arginine and therefore represents a branch point in the pyrimidine pathway. This reaction, catalyzed by the enzyme carbamoyl phosphate synthetase, is extremely energy-intensive, requiring two molecules of adenosine-5'-triphosphate (ATP) to form carbamoyl phosphate from the precursors bicarbonate and glutamine or ammonium (Anderson and Meister, 1965). CPSase is a large enzyme complex composed of two subunits; subunit A (encoded by *carA*) is a glutaminase, which acts to remove the R-group amide from the glutamine donor, while subunit B (encoded by *carB*) acts as the general synthetase domain. The synthetase domain has two distinct ATP binding sites, one for each catalyzed in the reaction (Rubio and Cervera, 1995). The first domain catalyzes the phosphorylation of the CP precursor carboxyphosphate from bicarbonate and ATP, while the second domain combines the carboxyphosphate with the glutaminase-formed carbamate. The two CarB subunit domains appear to be an internal gene duplication, as the N-terminal and C-terminal domains have a high degree of similarity to one another (Nyunoya and Lusty, 1983). The crystal structure has been solved for the *E. coli* enzyme and represents one of the more complex protein structures solved to date, detailing how CP is synthesized in a long, tunnel-like pathway through the molecule (Thoden et al., 1997) and has several novel mechanisms for allosteric regulation and substrate-channeling (Liu et al., 1994b). The *E. coli* CPSase is allosterically regulated by several effectors. UMP (uridine-5'-monophosphate) negatively regulates the enzyme, while ornithine and IMP (inosine-5'-monophosphate) both activate (Anderson, 1977). Each of the effectors has a specific binding site. The allosteric effector-binding sites for UMP and IMP overlap the ATP-binding site in the carboxy-terminal

domain of the synthetase subunit, leading to sigmoidal kinetics for Mg-ATP (Boettcher and Meister, 1982).

In *E. coli*, the *carAB* genes are expressed as an operon and are negatively regulated at the transcriptional level in a complex interaction several transcription factors. Two promoters are present upstream of the operon. Promoter P2 is regulated by ArgR (Charlier et al., 1988; Kilstrup et al., 1988), while the other, P1, is regulated by a more complex interaction between the UMP kinase product (PyrH), IHF, and the protein CarP (also known as PepA) (Charlier et al., 1995a; Charlier et al., 1995b).

Aspartate transcarbamoylase (ATCase, *pyrB* and *pyrI*, EC 2.1.3.2)

The reaction leading to the formation of N-carbamoyl aspartate is catalyzed by the enzyme aspartate transcarbamoylase, arguably the most characterized and studied enzyme in biology. The *E. coli* enzyme is one of the two original models for end-product (allosteric) regulation and transcriptional repression (Roof et al., 1982; Roland et al., 1985; Gouaux and Lipscomb, 1988a; Gouaux and Lipscomb, 1988b). Several reviews have been written about this enzyme (O'Donovan and Neuhard, 1970; Kantrowitz and Lipscomb, 1988; Kantrowitz and Lipscomb, 1990; Stevens et al., 1991a; Lipscomb, 1994; Neuhard and Kelln, 1996), therefore a detailed discussion will not be made here. However, several key points need to be made.

ATCase in bacteria has been separated into three classes (Figure 1.2, Bethell and Jones, 1969). The first group, Class A, is represented by the enzyme complex found in a wide range of phylogenetically distinct bacteria and is a large (~480 kDa) dodecameric holoenzyme composed of two subunits: two trimers made up of the catalytic polypeptide (*pyrB*, 36 kDa) and three

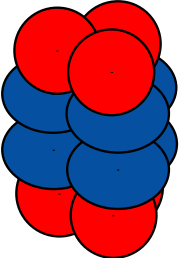
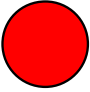
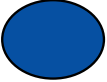
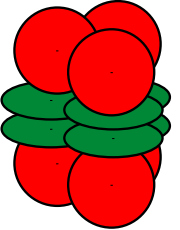
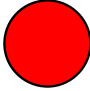

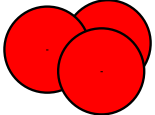
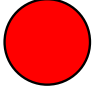
ATCase Class	Holoenzyme	Polypeptide structure	Representative organisms
Class A (480 kDa)		 = <i>pyrB</i> (catalytic) (36 kDa)  = <i>pyrC'</i> (active or inactive dihydroorotase) (45 kDa)	Inactive DHOase <i>Pseudomonas putida</i> <i>Pseudomonas aeruginosa</i> Active DHOase <i>Thermus</i> sp. <i>Deinococcus radiophilus</i> <i>Mycobacterium smegmatis</i> <i>Streptomyces coelicolor</i>
Class B (300 kDa)		 = <i>pyrB</i> (catalytic) (34 kDa)  = <i>pyrI</i> (regulatory) (17 kDa)	<i>Escherichia coli</i> <i>Salmonella typhimurium</i> <i>Serratia marcescens</i> <i>Erwinia herbicola</i> <i>Proteus vulgaris</i> <i>Citrobacter freundii</i> <i>Pyrococcus abyssi</i> <i>Neisseria meningitidis</i> <i>Vibrio natriegens</i>
Class C (100 kDa)		 = <i>pyrB</i> (catalytic) (34 kDa)	<i>Bacillus subtilis</i> <i>Bacillus cauldolyticus</i> <i>Streptococcus pyogenes</i> <i>Stenotrophomonas maltophila</i>

Figure 1.2 - Classes of bacterial ATCases.

dimers composed of dihydroorotase or a dihydroorotase-like polypeptide (*pyrC* or *pyrC'*, respectively, 45 kDa). The active dihydroorotase subunit would likely play a role in substrate channeling (Van de Casteele et al., 1997). However, the purpose of the *pyrC'*-encoded subunit remains to be elucidated. It is currently hypothesized to play a role as structural “glue” for the two catalytic trimers as the trimers are inactive when expressed alone. A regulatory role may also exist for this subunit (C. J. Fields, work in progress). This group has a disparate mode of regulation, with ATP normally acting as an inhibitor (Bergh and Evans, 1993; Shepherdson and McPhail, 1993; Schurr et al., 1995; Kenny et al., 1996; Vickrey et al., 2002). ATP binds to the catalytic subunit (Bergh and Evans, 1993), unlike the class B enzymes.

The second group, Class B, is the most characterized and best represented by the ATCase holoenzyme found in *E. coli* and other enteric bacteria and in the Archaea. This class is structurally similar to Class A above, with a dodecameric structure composed of two catalytic trimers (polypeptide size of 34 kDa) and three dimers (polypeptide size of 17 kDa) (Bothwell and Schachman, 1974). The dimers, in this case, are the product of the *pyrI* gene and act as regulatory subunits (Roof et al., 1982). ATP, UTP (uridine 5'-triphosphate) and CTP (cytidine 5'-triphosphate) bind to the N-terminal region on the PyrI polypeptide (Figure 1.3, Xi et al., 1994), allowing for allosteric activation of ATCase in the case of ATP, or inhibition in the case of CTP and UTP (the latter acting only in the presence of CTP) (Wild et al., 1989). The allosteric transition can be seen by the sigmoidal kinetics noted for the substrate aspartate. The crystal structure for the native holoenzyme and several mutants has been solved to 1.8 Å, allowing for the mechanism of allosteric inactivation to be viewed (Figure 1.3, Honzatko et al., 1982; Lipscomb, 1994). Unlike the Class A enzymes, Class B ATCases are able to form a

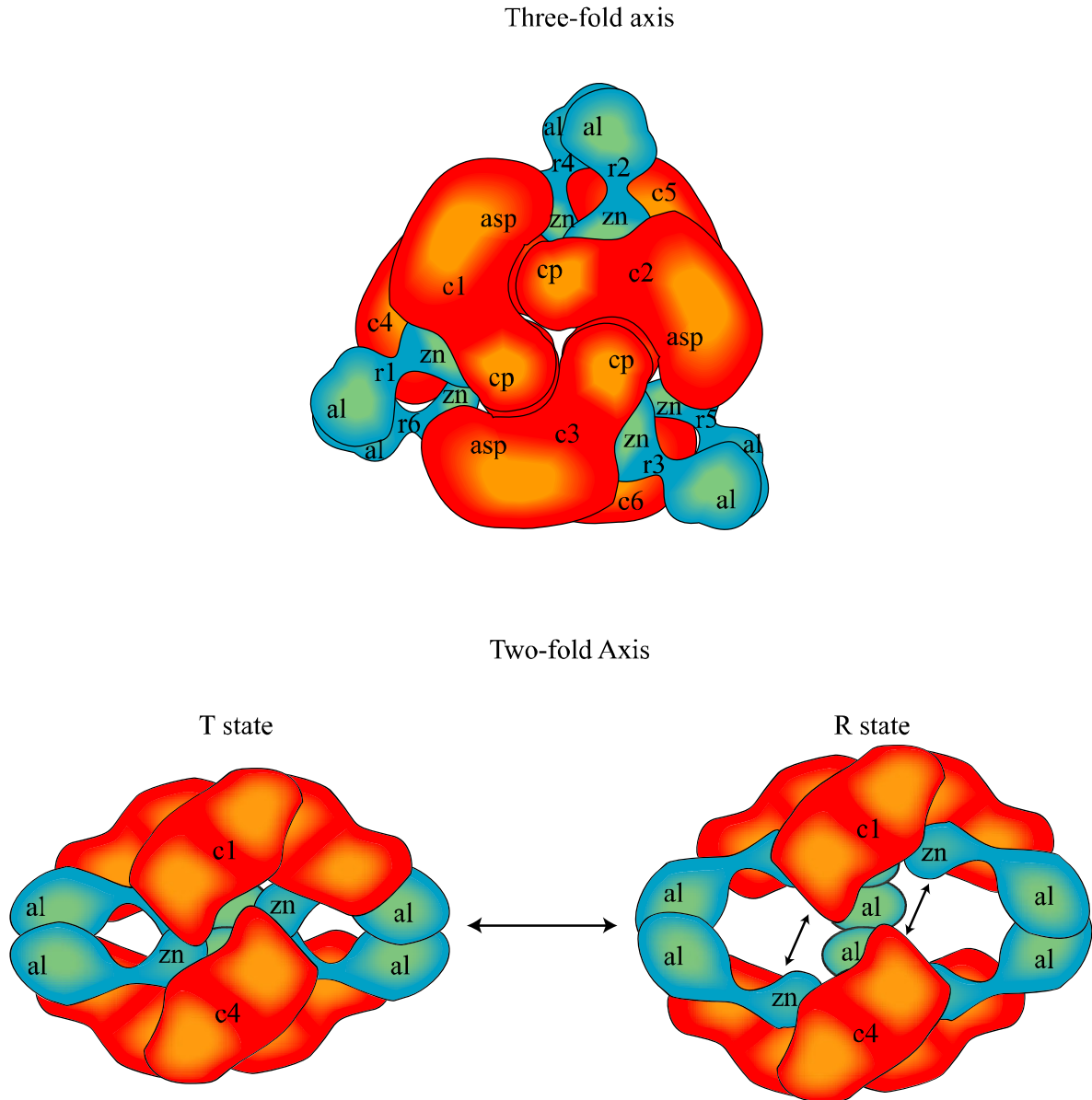


Figure 1.3 - Aspartate transcarbamoylase from *E. coli*. In the three-fold axis, the numbered subunits r and c designate the regulatory and catalytic subunits, respectively. In the two-fold axis, the allosteric transition from the T state (tight, or less active) to R (relaxed, or more active) is shown. zn – zinc- binding; cp –carbamoyl-phosphate binding; asp – aspartate-binding, al – allosteric binding site. Modified, with permission, from Gouaux et al., 1989; Gouaux and Lipscomb, 1989.

functional trimer that lacks allosteric regulation due to the loss of the PyrI regulatory dimers and, therefore, exhibits Michaelis-Menten kinetics. An unusual variant of this class is found in the bacteria *Thermotoga maritima* and *Treponema denticola*, both of which have a regulatory subunit fused to the catalytic subunit (Chen et al., 1998). The *T. maritima* enzyme is still currently being characterized and is in the process of having its structure elucidated by X-ray crystallography (R. Cunin, personal communication).

Class C, best characterized by *Bacillus*, is a simple trimer of three catalytic polypeptides of ~34 kDa. This class, much like the *E. coli* trimer, lacks allosteric regulation and has Michaelis-Menten kinetics for aspartate (Baker et al., 1995). The enzyme has been crystallized to 3.0 Å (Stevens et al., 1991b), revealing a structure is similar to the *E. coli* trimer.

A fourth class (Class D) is currently being proposed to include the unusually large ATCase from *Burkholderia cepacia* and other related bacteria. This holoenzyme is composed of two catalytic trimers and three DHOase dimers, much like the Class A enzymes. In this case, the catalytic PyrB polypeptide has an N-terminal extension of ~80 amino acid residues that increases the total polypeptide size to 47 kDa (Farinha et al., 2000). The total size of the enzyme is thought to be 550 kDa; smaller sizes have been seen that likely arise from the active trimer dissociating from the DHOase dimers (Linscott et al., 1994). The N-terminal extension represents a unique feature for this group of enzymes that continues to be investigated (G. A. O'Donovan, unpublished results).

The *pyrBI* genes in *E. coli* are located in a single operon and are controlled by the concentration of UTP in the cell through an attenuation mechanism involving a leader peptide, a rho-independent terminator, and UMP-rich regions in the transcript (Roof et al., 1982; Navre and Schachman, 1983; Roland et al., 1985). Transcriptional initiation of the *pyrBI* operon is further

regulated by transcriptional slippage, referred to as reiterated transcription, due to high UTP concentrations (Liu et al., 1994a).

Dihydroorotase (DHOase, *pyrC*, EC 3.5.2.3)

The enzyme DHOase catalyzes the cyclization of N-carbamoyl-aspartate to form the first ringed structure, dihydroorotate. The enzyme from *E. coli* has been cloned and characterized (Sander and Heeb, 1971; Washabaugh and Collins, 1984; Washabaugh and Collins, 1986; Brown and Collins, 1986; Collins and Brown, 1990; Brown and Collins, 1991) and is a homodimer. The crystal structure has been recently determined (Thoden et al., 2001). A full review has been published on the evolutionary history of this enzyme (Fields et al., 1999) and is currently in revision for an update to include current genome sequences.

Dihydroorotate dehydrogenase (DHOdehase, *pyrD*, EC 1.3.3.1)

The enzyme dihydroorotate dehydrogenase catalyzes the only redox reaction involved in pyrimidine metabolism, removing two hydrogens from the substrate dihydroorotate to form the first true pyrimidine, orotate. DHOdehase is a membrane-bound enzyme complex that has bound a flavin mononucleotide cofactor (Larsen and Jensen, 1985). The electron acceptor for the *E. coli* enzyme is thought to be ubiquinone or menaquinone, which carries the electrons from dihydroorotate to fumarate (Kerr and Miller, 1968; Andrews et al., 1977).

The *E. coli pyrC* and *pyrD* genes are regulated in a similar manner (Vial et al., 1993; Sorensen et al., 1993; Liu and Turnbough, Jr., 1994a; Liu and Turnbough, Jr., 1994b). Increased CTP pools in the cell cause transcriptional initiation to occur at a site which enables the formation of a stem-loop structure. The stem-loop structure sequesters the ribosomal binding

site, shutting down gene expression. In low levels of CTP, the transcript starts at the downstream G residue, destabilizing the stem-loop and allowing translation of the gene products to occur. Furthermore, the PurR repressor has been found to regulate gene expression for both *pyrC* and *pyrD*; in high purine nucleotide pools, DHOase and DHODEhase are slightly repressed due to the action of the PurR repressor (Choi and Zalkin, 1990).

Orotate phosphoribosyltransferase (OPRTase, *pyrE*, EC 2.2.4.10)

The addition of 5'-phosphoribosyl-1'pyrophosphate (PRPP) to the pyrimidine ring is catalyzed by the enzyme orotate phosphoribosyltransferase. OPRTase belongs to a much larger family of enzymes, the phosphoribosyltransferases (PRTases), that catalyze similar reactions (Jensen, 1983). The primary sequence of OPRTases, like most other PRTases, contain a motif known to bind PRPP (Carrey, 1994).

The regulation of *pyrE* expression occurs through a mechanism similar to that seen for the *E. coli pyrBI* operon. However, the leader peptide is actually an expressed protein, *rphH*, encoding the enzyme RNase pH, involved with tRNA modification (Andersen et al., 1991; Andersen et al., 1992).

Orotidine-5'-monophosphate (OMP) decarboxylase (OMPdecase, *pyrF*, EC 4.1.1.23)

One of the most efficient enzymes known is OMP decarboxylase, which removes the carboxylate group at position 6 on the pyrimidine intermediate OMP. This is the single step in the pathway that is truly irreversible and helps drive the pathway towards biosynthesis of UMP (Beak and Siegel, 1976). The *pyrF* gene in *Salmonella typhimurium* is in a small operon containing the gene *orfF*, which is translationally coupled to *pyrF* (Theisen et al., 1987). The

expression of *pyrF* is negatively regulated by a uridine nucleotide and a guanosine nucleotide (Kelln et al., 1975; Kelln et al., 1975; Jensen, 1989).

Uridine-5'-monophosphate kinase (UMP kinase, *pyrH*, EC 2.7.4.3)

The *E. coli pyrH* gene product is a UMP-specific kinase that is identical to the *E. coli* gene *smbA* (Smallshaw and Kelln, 1992). UMP kinase converts UMP to UDP (uridine-5'-diphosphate); however, it has recently been implicated in the pyrimidine-specific regulation of the *carAB* operon. In this case, UMP kinase is thought to act as a signaling protein that enables the CarP protein to bind to the P1 region when the UMP levels are high (Kholti et al., 1998).

Nucleoside diphosphate kinase (Ndk, *ndk*, EC EC 2.7.4.6)

The nonspecific enzyme nucleoside diphosphate kinase catalyzes the conversion of any nucleoside diphosphate to its respective triphosphate. The enzyme can utilize any NTP or dNTP as a phosphate donor for any NDP or dNDP (Ohtsuki et al., 1984).

Cytidine-5'-triphosphate synthase (CTP synthase, *pyrG*, EC 6.3.4.2)

The last step in pyrimidine biosynthesis is the formation of cytidine-5'-triphosphate (CTP) by the enzyme CTP synthetase. The enzyme acts as a glutamine amidotransferase in order to supply the amino group to form CTP, utilizing one ATP in the process (von der et al., 1985).

Overview of pyrimidine salvage reactions

The salvage of pyrimidines is an important series of reactions present, in some form, in all organisms. The ability to utilize and recycle preformed pyrimidines and purines prevents the energetically expensive route to forming these compounds through coordinate regulation of both biosynthetic and salvage reactions. Furthermore, the breakdown products of RNA and DNA can be utilized in many organisms as a source of carbon, nitrogen, and energy.

Here, a brief synopsis of the pathways involved in the salvage and regeneration of pyrimidines is presented.

Degradation of RNA

The half-life ($t_{1/2}$) of bacterial messenger RNA (mRNA) transcripts, in comparison, to eukaryotic mRNA, is extremely short. The average $t_{1/2}$ is 2.4 minutes at 37°C but can range from 20 seconds to as long as 50 minutes (Regnier and Arraiano, 2000). Various mechanisms are responsible for the targeting and degradation of mRNA. Here, I cover the pathways leading to the generation of nucleoside monophosphates; a full review is available which is more comprehensive (Regnier and Arraiano, 2000).

Bacterial mRNA is targeted for degradation by various means. The addition of a poly(A) tail by the bacterial poly (A) polymerase leads to the degradation of the targeted RNA by a large complex called the “degradosome” (Miczak et al., 1996). This complex consists of several enzymes, including the single-stranded endonuclease RNase E, polynucleotide phosphorylase (PNPase), and RhlB, a DEAD-box protein (a family of proteins having the motif aspartate-glutamate-alanine-aspartate, or DEAD) that specifically binds RNA (Py et al., 1996). The rate of

degradation depends on many factors, not limited to the secondary structure of the message, presence of a poly(A) tail, and ribosomal protection of the message during translation (Py et al., 1996).

RNase E degradation acts to cleave at A-U-rich regions in the RNA sequence, normally proceeding from the 5' to the 3' end of the mRNA. Secondary structures that stabilize the mRNA at the 5' or 3' end can be cleaved by the double-stranded endonuclease RNase III, thus freeing up the exposed ends for further breakdown. Fragments cleaved by RNase E and RNase III are rapidly broken down by an exonuclease reaction; normally this can be phosphorolysis by the "degradasome"-associated PNPase to the nucleoside diphosphates, or by hydrolysis from RNase II, releasing nucleoside monophosphates (Regnier and Arraiano, 2000). These are then subject to further degradation, as seen below.

Breakdown of monophosphates

Nucleoside monophosphates liberated during mRNA degradation can be reutilized through the action of specific NMP kinase, such as CMP or UMP kinase. Nucleoside diphosphates can also be reutilized through the nonspecific enzyme reaction catalyzed by nucleoside diphosphate kinase. However, little is known about the breakdown of NMPs to unphosphorylated nucleosides or bases in the cytoplasm.

In some bacteria, the nucleoside monophosphates can be cleaved into the base and D-ribose-5-phosphate. The enzyme AMP nucleosidase is one well-characterized example (Leung and Schramm, 1984). Pyrimidine nucleoside 5' monophosphate (NMP)-specific nucleosidases have been reported for some bacteria, including *Neisseria meningitidis* (Jyssum, 1989), *Pseudomonas oleovorans* (Sakai et al., 1971), and *E. coli* (Neuhard, 1983).

The removal of the 5' phosphate is also possible; this reaction is attributed to the action of 5'-nucleotidase (EC 3.1.3.5, Knofel and Strater, 1999). 5'-nucleotidase activity has been reported for *Pseudomonas aeruginosa* (Bhatti et al., 1976). The role that these play in the control of cytoplasmic nucleotide pools is dubious, however, as 5'-nucleotidases are generally exported outside of the cell or are localized in the periplasmic space. However, it can't be ruled out that some activity may occur prior to export.

Transport of nucleosides and bases

Nucleosides and bases may also be imported into the cell through various transport routes. They must be also be able to negotiate the outer and inner membrane for Gram-negative cells. Outer membrane nucleoside transport in *E. coli* requires the channel-forming protein Tsx (Hantke, 1976), but there have been no reports describing how bases traverse the outer membrane.

Transport of pyrimidine bases across the inner membrane requires one of the two systems encoded by *nupG* and *nupC* (Munch-Peterson and Mygind, 1983). Transport of bases requires the more substrate-specific permeases; separate transporters have been found for cytosine and uracil (Munch-Peterson and Mygind, 1983).

Deaminations

The enzymes cytidine deaminase (*cdd*) and cytosine deaminase (*codA*) are able to hydrolyze the amino group of cytidine and cytosine to form uridine and uracil, respectively. The *E. coli* cytidine deaminase (EC 3.5.4.5) is the main route for the conversion of cytidine to uridine

(Ashley and Bartlett, 1984). Cytosine deaminase (EC 3.5.4.1), although not as active, is able to convert cytosine hydrolytically to uracil (Katsuragi et al., 1987).

Nucleoside kinases

A single enzyme in *E. coli*, uridine kinase (*udk*, EC 2.7.1.48), is capable of adding a phosphate to the 5' hydroxyl group of both pyrimidine ribonucleosides (Valentin-Hansen, 1978). This enzyme, in effect, bypasses the need for 5'-phosphoribosyl-1'pyrophosphate in the uracil phosphoribosyltransferase reaction.

Cytidine-monophosphate (CMP) kinase

Cytidine 5'-monophosphate (CMP), catalyzed by uridine kinase, can be converted to cytidine 5' diphosphate by the specific enzyme CMP kinase (*cmk*, EC.2.7.4.14) (Beck et al., 1974). This is considered a salvage enzyme as it is not required for growth.

Uracil phosphoribosyltransferase

The regeneration of intracellular UMP pools occurs through the action of uracil phosphoribosyltransferase (*upp*, EC 2.4.2.9) (Rasmussen et al., 1986). The enzyme in *E. coli* is specific for uracil; no other nucleic acids are catalyzed, although 5-substituted uracil analogues such as 5-fluorouracil are easily converted.

Nucleoside phosphorylases

Breakdown of nucleosides occurs through two separate routes. The first, described here briefly, is the action of uridine phosphorylase (*udp*, EC 2.4.2.3). This enzyme is able to carry out

the reversible cleavage of the β -N-glycosyl bond to release ribose-1-phosphate and uracil (Leer et al., 1977). The enzyme has no action for cytidine.

The second enzyme, nucleoside hydrolase, is the focus of this dissertation and is described in much greater detail below.

Nucleoside hydrolase

The enzyme nucleoside hydrolase (NH, EC 3.2.2.1) catalyzes the hydrolysis of the β -N-glycosyl bond in nucleosides. The NHs are characterized based on their substrate specificity and their ability to hydrolyze ribo- or deoxyribonucleotides, the former by far the more prevalent. The enzyme is found in a wide range of organisms, including bacteria (Takagi and Horecker, 1957; Lee, 1991; Beck, 1995), plants (Camici et al., 1979), fungi (Magni, 1978), protozoa (Degano et al., 1998; Shi et al., 1999), and insects (GenPept #AAG22352, among others). They have not been found in higher organisms, including humans, and therefore have been exploited as possible targets for antimicrobial chemotherapy, mainly for some of the parasitic protozoans. Some organisms may have more than one gene encoding NHs. In these cases, the paralogous NHs normally display a difference in substrate specificity that allow for the degradation of a wide range of nucleosides.

Several different protozoan nucleoside hydrolases have been cloned and sequenced. Many of the first were cloned in an attempt to exploit them as targets for antimicrobial action as many parasitic protozoans, such as *Leishmani major*, *Crithidia fasciculata*, and *Trypanosoma brucei*, do not have a purine *de novo* pathway and thus require extracellular purines for RNA and DNA synthesis. The first cloned and characterized protozoan NH was the inosine-uridine preferring nucleoside hydrolase (IUNH) from the protozoan *Crithidia fasciculata* (Parkin et al.,

1991). As the name suggests, the most activity has been recorded for the purine nucleoside inosine (I) and the pyrimidine nucleoside uridine (U); however, some activity still remains for the other nucleosides and therefore it is considered relatively nonspecific. Several more NHs from protozoans were cloned more recently, including an IUNH from *Leishmania major*, a nonspecific nucleoside hydrolase from *Leishmania donovani* (Cui et al., 2001), and purine-specific nucleoside hydrolases from several trypanosomes, such as *Trypanosoma brucei* (Parkin, 1996) and *Trypanosoma vivax* (Versees et al., 2001). The trypanosomal NHs are all purine-specific and designated as IAGNH, for inosine-adenosine-guanosine specific nucleoside hydrolases. This finding led to a detailed structural comparison of the *T. vivax* enzyme to that of *C. fasciculata*

Several nucleoside hydrolases from other organisms have been studied. The nucleosidase from *Saccharomyces cerevisiae* has been characterized as a copper-containing enzyme (Magni et al., 1976) that is uridine-specific. The gene that encoded the enzyme has been recently cloned (Mitterbauer et al., 2002) and has a significant degree of similarity to the protozoan nucleoside hydrolases. Bacterial nucleoside hydrolases have been characterized from several *Pseudomonas* (Lee, 1991) species and have been found to have little specificity for nucleosides but are recalcitrant to deoxynucleosides. The notable exception to this is the report of a pyrimidine-preferring nucleoside hydrolase from *Pseudomonas fluorescens* (Terada et al., 1967); this may be a strain-specific issue, however as most have been found to have a wide substrate specificity. The NH from *Ochrobactrum anthropi* (Ogawa et al., 2001) has been classified as a purine-specific NH.

The catalytic mechanism of nucleoside hydrolysis catalyzed by NHs was first described by Schramm and others (reviewed in Schramm, 1997). The mechanism relies on an

oxocarbenium intermediate structure. The reaction mechanism is similar to that seen for the enzyme AMP nucleosidase (Leung and Schramm, 1984) and the powerful cytotoxin Ricin A-chain, the castor bean-derived toxin that became infamous when it was used to assassinate the Bulgarian dissident Georgi Markov in 1978 (Schramm, 1997).

The crystal structure of the *Crithidia fasciculata* IUNH

The crystal structure for the *Crithidia fasciculata* IUNH, the *Leishmania major* IUNH, and the *Trypanosoma vivax* IAGNH (see below) have been solved. Comparisons between IUNH structures revealed that the *C. fasciculata* and *L. major* nucleoside hydrolases were practically identical in structure, including several key residues involved in catalysis and in the tetrameric quaternary structure (Shi et al., 1999). A Rossmann-like fold was found at the N-terminus; this fold, known to bind nucleotides, is missing the phosphate-binding consensus GXGXXG. This missing consensus is replaced by two of the five residues (Asp-, Asp-, Asp-, Asp-, Thr-), which coordinate a calcium ion in order to stabilize the oxocarbenium transition state and activate the water nucleophile (Schramm, 1997). The bound calcium ion acts also to hold the oxocarbenium transition state by coordinating the 2' and 3' hydroxyls as well as the water nucleophile, which is used to attack the β -N-glycosyl bond. Furthermore all the hydroxyl groups are multiply hydrogen-bonded, stabilizing the structure in the binding pocket. Protonation of the leaving group is accomplished by the proton-donating residue His-241 prior to oxocarbenium activation (Gopaul et al., 1996) revealing that ribonucleosides would more likely be catalyzed than deoxyribonucleosides due to a lack of the 2' hydroxyl group. The 5' hydroxyl group was held by several key hydrogen bonds; the addition of a phosphate group in this position is thought to prevent binding due to the repelling charge and could explain why many nucleotides cannot act

as substrates for this enzyme (Degano et al., 1998). Another discovery was that the base portion of the nucleoside made no specific contacts with the IUNH enzymes; rather, several key hydrophobic interactions were present that held the nucleoside in place, including several that resembled base stacking interactions, such as seen in DNA and RNA, likely explaining the lack of substrate specificity (Parkin et al., 1997).

The purine-specific IAGNH of *Trypanosoma vivax*

The *Trypanosoma vivax* IAGNH crystal structure (Versees et al., 2001) has added a new dimension about substrate specificity. The enzyme is 1000-10000 times more specific towards the naturally occurring purine bases inosine, adenosine, and guanosine over the pyrimidine bases due to a faster turnover rate and a higher substrate affinity for the purine. Furthermore, they are relatively resistant to the transition-state inhibitors constructed for the *Crithidia* IUNH (Versees et al., 2001). The colorimetric substrate *p*-nitrophenyl- β -D-ribofuranoside (*p*-nitrophenylriboside) was a relatively poor substrate (Versees et al., 2001). Moreover, the enzyme is thought to require either multiple protonations or other electron-leaving effects in order to reach the transition state (Versees et al., 2001). The IAGNH and the IUNH differ substantially in the primary sequence; these differences are mainly in the regions that surround the pocket known to sequester the base portion of the nucleoside. All the above characteristics suggested that that the enzyme catalyzes nucleoside hydrolysis by a slightly different mechanism. The crystal structure (Versees et al., 2001) revealed that the enzyme quaternary structure also differs; the IAGNH is a dimer as opposed to a tetramer. The calcium ion is coordinated by four aspartate residues and a threonine residue, as found with the IUNHs. The pK_a range of k_{cat} (maximal enzymatic turnover) indicates that two residues are likely to act as

proton donors, with pK_a values of 5.5 and 8.5. Therefore, both must be protonated during enzyme catalysis. The likely acidic proton donor (pK_a or 5.5) is Asp-40; however, the more basic proton donor ($pK_a = 8.5$) has not been determined.

The purine moiety of the nucleoside is involved in a base-stacking interaction that involves two tryptophan residues (Trp-83 and Trp-260) in the IAGNH; since the purine is heterocyclic, this stacking interaction enhances the enzyme's specificity for purine nucleosides. In other words, this interaction leads to a "sandwiching" effect in which the purine base is stacked, edge-to-edge, between the tryptophan residues. Pyrimidine nucleosides are not heterocyclic and will not stack edge-to-edge, but edge-to-face. Therefore, pyrimidine nucleosides would be much more difficult to accommodate in the binding pocket compared to purine nucleosides (Versees et al., 2001). This is evidenced in more recent work (Versees et al., 2001), which has determined that mutants lacking the two tryptophan residues also lack purine substrate specificity. Furthermore, the natural substrate inosine was determined to bind in an *anti*-conformation in IAGNH, in contrast to the *syn*-conformation that has been found for the substrate analogue 3-deaza-adenosine in previous crystal structures for IUNH and IAGNH (Versees et al., 2001). Both tryptophan residues still interact with the purine base in a base-stacking arrangement. Notably, no other residues have been found close to the purine base that would protonate it as a leaving group. Therefore, it has been suggested that the base-stacking interaction itself might allow for partial activation due interactions between the molecular orbitals surrounding the tryptophan residues and the purine base. Orbital interactions would strengthen the base-stacking interaction upon protonation of the purine base by Asp-40; this would then stabilize the transition state and allow catalysis to proceed (Versees et al., 2001). This represents a major difference in catalysis between the two different nucleoside hydrolases

and adds to the that fact that, while the two enzymes may have similarity in their primary sequence, several key differences in their substrate specificity and catalytic mechanism demonstrate the continual evolution of this enzyme.

Conclusion

In this dissertation, I will detail the substrate specificity and regulation of the cloned genes encoding nucleoside hydrolases from three bacteria.

In *Escherichia coli*, I determine the presence of three nucleoside hydrolases through scanning of the genome sequence. The individual genes were amplified by the polymerase chain reaction and cloned. The substrate specificity and possible modes of regulations for each gene were determined

In a comparative analysis, nucleoside hydrolases are also cloned and characterized from *Pseudomonas aeruginosa* and *Pseudomonas fluorescens*. The substrate specificity and modes of regulation were determined for each enzyme. Furthermore, a model is elucidated involving the potential physiological role for the nucleoside hydrolase involving nucleoside degradation.

References

- Andersen, J. T., K. F. Jensen, and P. Poulsen.** 1991. Role of transcription pausing in the control of the *pyrE* attenuator in *Escherichia coli*. *Mol.Microbiol.* **5**:327-333.
- Andersen, J. T., P. Poulsen, and K. F. Jensen.** 1992. Attenuation in the *rph-pyrE* operon of *Escherichia coli* and processing of the dicistronic mRNA. *Eur.J.Biochem.* **206**:381-390.
- Anderson, P. M.** 1977. Binding of allosteric effectors to carbamyl-phosphate synthetase from *Escherichia coli*. *Biochemistry* **16**:587-593.
- Anderson, P. M. and A. Meister.** 1965. Evidence for an activated form of carbon dioxide in the reaction catalyzed by *Escherichia coli* carbamoyl phosphate synthetase. *Biochemistry* **4**:2803-2808.
- Andrews, S., G. B. Cox, and F. Gibson.** 1977. The anaerobic oxidation of dihydroorotate by *Escherichia coli* K-12. *Biochim.Biophys.Acta* **462**:153-160.
- Ashley, G. W. and P. A. Bartlett.** 1984. Purification and properties of cytidine deaminase from *Escherichia coli*. *J.Biol.Chem.* **259**:13615-13620.
- Baker, D. P., J. M. Aucoin, M. K. Williams, L. A. deMello, and E. R. Kantrowitz.** 1995. Overexpression and purification of the trimeric aspartate transcarbamoylase from *Bacillus subtilis*. *Protein Expr.Purif.* **6**:679-684.
- Beak, P. and B. Siegel.** 1976. Mechanism of decarboxylation of 1,3-dimethylorotic acid. A model for orotidine 5'-phosphate decarboxylase. *J.Am.Chem.Soc.* **98**:3601-3606.

- Beck, C. F., J. Neuhard, E. Thomassen, J. L. Ingraham, and E. Kleker.** 1974. *Salmonella typhimurium* mutants defective in cytidine monophosphate kinase (*cmk*). J.Bacteriol. **120**:1370-1379.
- Beck, D. E.** 1995. Pyrimidine salvage enzymes in microorganisms : labyrinths of enzymatic diversity. Ph.D. dissertation. The University of North Texas.
- Bergh, S. T. and D. R. Evans.** 1993. Subunit structure of a class A aspartate transcarbamoylase from *Pseudomonas fluorescens*. Proc.Natl.Acad.Sci.U.S.A. **90**:9818-9822.
- Bethell, M. R. and M. E. Jones.** 1969. Molecular size and feedback-regulation characteristics of bacterial aspartate transcarbamylases. Arch.Biochem.Biophys. **134**:352-365.
- Bhatti, A. R., I. W. DeVoe, and J. M. Ingram.** 1976. The release and characterization of some periplasm-located enzymes of *Pseudomonas aeruginosa*. Can.J.Microbiol. **22**:1425-1429.
- Boettcher, B. and A. Meister.** 1982. Regulation of *Escherichia coli* carbamyl phosphate synthetase. Evidence for overlap of the allosteric nucleotide binding sites. J.Biol.Chem. **257**:13971-13976.
- Bothwell, M. and H. K. Schachman.** 1974. Pathways of assembly of aspartate transcarbamoylase from catalytic and regulatory subunits. Proc.Natl.Acad.Sci.U.S.A. **71**:3221-3225.
- Brown, D. C. and K. D. Collins.** 1986. Dihydroorotase from *Escherichia coli*. Cloning the *pyrC* gene and production of tryptic peptide maps. J.Biol.Chem. **261**:5917-5919.

- Brown, D. C. and K. D. Collins.** 1991. Dihydroorotase from *Escherichia coli*. Substitution of Co(II) for the active site Zn(II). J.Biol.Chem. **266**:1597-1604.
- Camici, M., G. Cercignani, U. Mura, and P. L. Ipata.** 1979. Enzymologic characterization of adenosine nucleosidase of medicinal plants (*Medicago sativa*). Boll.Soc.Ital.Biol Sper. **55**:1001-1007.
- Carrey, E. A.** 1994. The PRPP-binding site in phosphoribosyltransferases. Paths Pyr.:An Int'l Nwsltr. **2**:15-16.
- Charlier, D., D. Gigot, N. Huysveld, M. Roovers, A. Pierard, and N. Glansdorff.** 1995a. Pyrimidine regulation of the *Escherichia coli* and *Salmonella typhimurium carAB* operons: CarP and integration host factor (IHF) modulate the methylation status of a GATC site present in the control region. J.Mol.Biol. **250**:383-391.
- Charlier, D., G. Hassanzadeh, A. Kholti, D. Gigot, A. Pierard, and N. Glansdorff.** 1995b. *carP*, involved in pyrimidine regulation of the *Escherichia coli* carbamoylphosphate synthetase operon encodes a sequence-specific DNA- binding protein identical to XerB and PepA, also required for resolution of ColEI multimers. J.Mol.Biol. **250**:392-406.
- Charlier, D., G. Weyens, M. Roovers, J. Piette, C. Bocquet, A. Pierard, and N. Glansdorff.** 1988. Molecular interactions in the control region of the *carAB* operon encoding *Escherichia coli* carbamoylphosphate synthetase. J.Mol.Biol. **204**:867-877.
- Chen, P., F. Van Vliet, M. Van de Castele, C. Legrain, R. Cunin, and N. Glansdorff.** 1998. Aspartate transcarbamylase from the hyperthermophilic eubacterium *Thermotoga*

- maritima*: fused catalytic and regulatory polypeptides form an allosteric enzyme. J.Bacteriol. **180**:6389-6391.
- Choi, K. Y. and H. Zalkin.** 1990. Regulation of *Escherichia coli pyrC* by the purine regulon repressor protein. J.Bacteriol. **172**:3201-3207.
- Collins, K. D. and D. C. Brown.** 1990. Dihydroorotase from *Escherichia coli*: Substitution of cobalt for the active site zinc. FASEB J. **4**.
- Cui, L., G. R. Rajasekariah, and S. K. Martin.** 2001. A nonspecific nucleoside hydrolase from *Leishmania donovani*: implications for purine salvage by the parasite. Gene **280**:153-162.
- Degano, M., S. C. Almo, J. C. Sacchettini, and V. L. Schramm.** 1998. Trypanosomal nucleoside hydrolase. A novel mechanism from the structure with a transition-state inhibitor. Biochemistry **37**:6277-6285.
- Farinha, M. A., Hooshdaran, M. Z., Houghton, J. E., Linscott, A. J., Kumar, A. P., Combs, M., and O'Donovan, G. A.** 2000. Aspartate transcarbamoylase (*pyrB*) of *Burkholderia cepacia* assembles as both an active trimer and as a dodecamer with attendant dihydroorotase (*pyrC*) activity. Unpublished Work.
- Fields, C. J., D. M. Brichta, M. Shepherdson, M. A. Farinha, and G. A. O'Donovan.** 1999. Phylogenetic analysis and classification of dihydroorotases: a complex history for a complex enzyme. Paths Pyr.:An Int'l Nwsltr. **7**:1-20.

- Gero, A. M., G. V. Brown, and W. J. O'Sullivan.** 1984. Pyrimidine de novo synthesis during the life cycle of the intraerythrocytic stage of *Plasmodium falciparum*. *J.Parasitol.* **70**:536-541.
- Gopaul, D. N., S. L. Meyer, M. Degano, J. C. Sacchettini, and V. L. Schramm.** 1996. Inosine-uridine nucleoside hydrolase from *Crithidia fasciculata*. Genetic characterization, crystallization, and identification of histidine 241 as a catalytic site residue. *Biochemistry* **35**:5963-5970.
- Gouaux, J. E. and W. N. Lipscomb.** 1988b. Three-dimensional structure of carbamoyl phosphate and succinate bound to aspartate carbamoyltransferase. *Proc.Natl.Acad.Sci.U.S.A.* **85**:4205-4208.
- Gouaux, J. E. and W. N. Lipscomb.** 1988a. Three-dimensional structure of carbamoyl phosphate and succinate bound to aspartate carbamoyltransferase. *Proc.Natl.Acad.Sci.U.S.A.* **85**:4205-4208.
- Gouaux, J. E. and W. N. Lipscomb.** 1989. Structural transitions in crystals of native aspartate carbamoyltransferase. *Proc.Natl.Acad.Sci.U.S.A.* **86**:845-848.
- Gouaux, J. E., R. C. Stevens, H. M. Ke, and W. N. Lipscomb.** 1989. Crystal structure of the Glu-239->Gln mutant of aspartate carbamoyltransferase at 3.1Å resolution: an intermediate quaternary structure. *Proc.Natl.Acad.Sci.U.S.A.* **86**:8212-8216.
- Hantke, K.** 1976. Phage T6-colicin K receptor and nucleoside transport in *Escherichia coli*. *FEBS Lett.* **70**:109-112.

- Honzatko, R. B., J. L. Crawford, H. L. Monaco, J. E. Ladner, B. F. Edwards, D. R. Evans, S. G. Warren, D. C. Wiley, R. C. Ladner, and W. N. Lipscomb.** 1982. Crystal and molecular structures of native and CTP-liganded aspartate carbamoyltransferase from *Escherichia coli*. *J.Mol.Biol.* **160**:219-263.
- Jensen, K. F.** 1983. Metabolism of 5-phosphoribosyl-1-pyrophosphate (PRPP) in *Escherichia coli* and *Salmonella typhimurium*, p. 1-25. In A. Munch-Peterson (ed.), *Metabolism of Nucleotides, Nucleosides, and Nucleobases in Microorganisms*. Academic Press, London.
- Jensen, K. F.** 1989. Regulation of *Salmonella typhimurium pyr* gene expression: effect of changing both purine and pyrimidine nucleotide pools. *J.Gen.Microbiol.* **135**:805-815.
- Jyssum, S.** 1989. Pyrimidine 5'-nucleosidase in *Neisseria meningitidis*. An enzyme specific for uridine 5'-monophosphate. *APMIS* **97**:343-346.
- Kantrowitz, E. R. and W. N. Lipscomb.** 1988. *Escherichia coli* aspartate transcarbamylase: the relation between structure and function. *Science* **241**:669-674.
- Kantrowitz, E. R. and W. N. Lipscomb.** 1990. *Escherichia coli* aspartate transcarbamoylase: The molecular basis for a concerted allosteric transition. *Trends Biochem.Sci.* **15**:53-59.
- Katsuragi, T., T. Sakai, and K. Tonomura.** 1987. Implantable enzyme capsules for cancer chemotherapy from bakers' yeast cytosine deaminase immobilized on epoxy-acrylic resin and urethane prepolymer. *Appl.Biochem.Biotechnol.* **16**:61-69.

- Kelln, R. A., J. J. Kinahan, K. F. Foltermann, and G. A. O'Donovan.** 1975. Pyrimidine biosynthetic enzymes of *Salmonella typhimurium*, repressed specifically by growth in the presence of cytidine. *J.Bacteriol.* **124**:764-774.
- Kenny, M. J., D. McPhail, and M. Shepherdson.** 1996. A reappraisal of the diversity and class distribution of aspartate transcarbamoylases in gram-negative bacteria. *Microbiology* **142**:1873-1879.
- Kerr, C. T. and R. W. Miller.** 1968. Dihydroorotate-ubiquinone reductase complex of *Escherichia coli* B. *J.Biol.Chem.* **243**:2963-2968.
- Kholtzi, A., D. Charlier, D. Gigot, N. Huysveld, M. Roovers, and N. Glansdorff.** 1998. *pyrH*-encoded UMP-kinase directly participates in pyrimidine-specific modulation of promoter activity in *Escherichia coli*. *J.Mol.Biol.* **280**:571-582.
- Kilstrup, M., C. D. Lu, A. Abdelal, and J. Neuhard.** 1988. Nucleotide sequence of the *carA* gene and regulation of the *carAB* operon in *Salmonella typhimurium*. *Eur.J.Biochem.* **176**:421-429.
- Knofel, T. and N. Strater.** 1999. X-ray structure of the *Escherichia coli* periplasmic 5'-nucleotidase containing a dimetal catalytic site. *Nat.Struct.Biol.* **6**:448-453.
- Larsen, J. N. and K. F. Jensen.** 1985. Nucleotide sequence of the *pyrD* gene of *Escherichia coli* and characterization of the flavoprotein dihydroorotate dehydrogenase. *Eur.J.Biochem.* **151**:59-65.

- Lee, Y.-S.** 1991. Pyrimidine metabolism in bacteria : physiological properties of nucleoside hydrolase and uridine kinase. Masters thesis. The University of North Texas.
- Leer, J. C., K. Hammer-Jespersen, and M. Schwartz.** 1977. Uridine phosphorylase from *Escherichia coli*. Physical and chemical characterization. *Eur.J.Biochem.* **75**:217-224.
- Leung, H. B. and V. L. Schramm.** 1984. The structural gene for AMP nucleosidase. Mapping, cloning, and overproduction of the enzyme. *J.Biol.Chem.* **259**:6972-6978.
- Linscott, A. J., D. E. Beck, A. P. Kumar, and G. A. O'Donovan.** 1994. Pyrimidine metabolism in the pseudomonads. Abstracts of the 94th General Meeting of the American Society for Microbiology **94**:282.
- Lipscomb, W. N.** 1994. Aspartate transcarbamylase from *Escherichia coli*: activity and regulation. *Adv.Enzymol.Relat.Areas.Mol.Biol.* **68**:67-151.
- Liu, C., L. S. Heath, and C. L. Turnbough, Jr.** 1994a. Regulation of *pyrBI* operon expression in *Escherichia coli* by UTP-sensitive reiterative RNA synthesis during transcriptional initiation. *Genes Dev.* **8**:2904-2912.
- Liu, J. and C. L. Turnbough, Jr.** 1994a. Effects of transcriptional start site sequence and position on nucleotide-sensitive selection of alternative start sites at the *pyrC* promoter in *Escherichia coli*. *J.Bacteriol.* **176**:2938-2945.
- Liu, J. and C. L. Turnbough, Jr.** 1994b. Identification of the Shine-Dalgarno sequence required for expression and translational control of the *pyrC* gene in *Escherichia coli* K-12. *J.Bacteriol.* **176**:2513-2516.

- Liu, X., H. I. Guy, and D. R. Evans.** 1994b. Identification of the regulatory domain of the mammalian multifunctional protein CAD by the construction of an *Escherichia coli*-hamster hybrid carbamyl-phosphate synthetase. *J.Biol.Chem.* **269**:27747-27755.
- Magni, G.** 1978. Uridine nucleosidase from yeast. *Methods Enzymol.* **51**:290-296.
- Magni, G., P. Natalini, S. Ruggieri, and A. Vita.** 1976. Bakers' yeast uridine nucleosidase is a regulatory copper containing protein. *Biochem.Biophys.Res.Comm.* **69**:724-730.
- Miczak, A., V. R. Kaberdin, C. L. Wei, and S. Lin-Chao.** 1996. Proteins associated with RNase E in a multicomponent ribonucleolytic complex. *Proc.Natl.Acad.Sci.U.S.A.* **93**:3865-3869.
- Mitterbauer, R., T. Karl, and G. Adam.** 2002. *Saccharomyces cerevisiae* URH1 (encoding uridine-cytidine N-ribohydrolase): functional complementation by a nucleoside hydrolase from a protozoan parasite and by a mammalian uridine phosphorylase. *Appl.Environ.Microbiol.* **68**:1336-1343.
- Munch-Peterson, A. and B. Mygind.** 1983. Transport of nucleic acid precursors, p. 259-305. *In* A. Munch-Peterson (ed.), *Metabolism of Nucleotides, Nucleosides, and Nucleobases in Microorganisms.* Academic Press, London.
- Navre, M. and H. K. Schachman.** 1983. Synthesis of aspartate transcarbamoylase in *Escherichia coli*: transcriptional regulation of the *pyrB-pyrI* operon. *Proc.Natl.Acad.Sci.U.S.A.* **80**:1207-1211.

- Neuhard, J.** 1983. Utilization of preformed pyrimidine bases and nucleosides, p. 95-148. *In* A. Munch-Peterson (ed.), *Metabolism of Nucleotides, Nucleosides, and Nucleobases in Microorganisms*. Academic Press, London.
- Neuhard, J. and R. A. Kelln.** 1996. Biosynthesis and conversion of pyrimidines, p. 580-599. *In* F. Neidhardt and R. Curtiss (eds.), *Escherichia coli and Salmonella*. American Society for Microbiology, Washington D.C.
- Nyunoya, H. and C. J. Lusty.** 1983. The *carB* gene of *Escherichia coli*: a duplicated gene coding for the large subunit of carbamoyl-phosphate synthetase. *Proc.Natl.Acad.Sci.U.S.A.* **80**:4629-4633.
- O'Donovan, G. A. and J. Neuhard.** 1970. Pyrimidine metabolism in microorganisms. *Bacteriol.Rev.* **34**:278-343.
- Ogawa, J., S. Takeda, S. X. Xie, H. Hatanaka, T. Ashikari, T. Amachi, and S. Shimizu.** 2001. Purification, characterization, and gene cloning of purine nucleosidase from *Ochrobactrum anthropi*. *Appl.Environ.Microbiol.* **67**:1783-1787.
- Ohtsuki, K., M. Yokoyama, T. Koike, and N. Ishida.** 1984. Nucleoside diphosphate kinase in *Escherichia coli*: its polypeptide structure and reaction intermediate. *Biochem.Int.* **8**:715-723.
- Parkin, D. W.** 1996. Purine-specific nucleoside N-ribohydrolase from *Trypanosoma brucei* *brucei*. Purification, specificity, and kinetic mechanism. *J.Biol.Chem.* **271**:21713-21719.

- Parkin, D. W., B. A. Horenstein, D. R. Abdulah, B. Estupinan, and V. L. Schramm.** 1991. Nucleoside hydrolase from *Crithidia fasciculata*. Metabolic role, purification, specificity, and kinetic mechanism. *J.Biol.Chem.* **266**:20658-20665.
- Parkin, D. W., G. Limberg, P. C. Tyler, R. H. Furneaux, X. Y. Chen, and V. L. Schramm.** 1997. Isozyme-specific transition state inhibitors for the trypanosomal nucleoside hydrolases. *Biochemistry* **36**:3528-3534.
- Py, B., C. F. Higgins, H. M. Krisch, and A. J. Carpousis .** 1996. A DEAD-box RNA helicase in the *Escherichia coli* RNA degradosome. *Nature* **381**:169-172.
- Rasmussen, U. B., B. Mygind, and P. Nygaard.** 1986. Purification and some properties of uracil phosphoribosyltransferase from *Escherichia coli* K12. *Biochim.Biophys.Acta* **881**:268-275.
- Regnier, P. and C. M. Arraiano.** 2000. Degradation of mRNA in bacteria: emergence of ubiquitous features. *Bioessays* **22**:235-244.
- Roland, K. L., F. E. Powell, and C. L. Turnbough, Jr.** 1985. Role of translation and attenuation in the control of *pyrBI* operon expression in *Escherichia coli* K-12. *J.Bacteriol.* **163**:991-999.
- Roof, W. D., K. F. Foltermann, and J. R. Wild.** 1982. The organization and regulation of the *pyrBI* operon in *E. coli* includes a rho-independent attenuator sequence. *Mol.Gen.Genet.* **187**:391-400.

- Rubio, V. and J. Cervera.** 1995. The carbamoyl-phosphate synthase family and carbamate kinase: structure- function studies. *Biochem.Soc.Trans.* **23**:879-883.
- Sakai, T., T. Watanabe, and I. Chibata.** 1971. Metabolism of pyrimidine nucleotides in a microorganism. 3. Enzymatic production of ribose-5-phosphate from uridine-5'-monophosphate by *Pseudomonas oleovorans*. *Appl.Microbiol.* **22**:1085-1090.
- Sander, E. G. and M. J. Heeb.** 1971. Purification and properties of dihydroorotase from *Escherichia coli* B. *Biochim.Biophys.Acta* **227**:442-452.
- Schramm, V. L.** 1997. Enzymatic N-riboside scission in RNA and RNA precursors. *Curr.Opin.Chem.Biol.* **1**:323-331.
- Schurr, M. J., J. F. Vickrey, A. P. Kumar, A. L. Campbell, R. Cunin, R. C. Benjamin, M. S. Shanley, and G. A. O'Donovan.** 1995. Aspartate transcarbamoylase genes of *Pseudomonas putida*: requirement for an inactive dihydroorotase for assembly into the dodecameric holoenzyme. *J.Bacteriol.* **177**:1751-1759.
- Seymour, K. K., S. D. Lyons, L. Phillips, K. H. Rieckmann, and R. I. Christopherson.** 1994. Cytotoxic effects of inhibitors of de novo pyrimidine biosynthesis upon *Plasmodium falciparum*. *Biochemistry* **33**:5268-5274.
- Shepherdson, M. and D. McPhail.** 1993. Purification of aspartate transcarbamoylase from *Pseudomonas syringae*. *FEMS Microbiol.Lett.* **114**:201-205.

- Shi, W., V. L. Schramm, and S. C. Almo.** 1999. Nucleoside hydrolase from *Leishmania major*. Cloning, expression, catalytic properties, transition state inhibitors, and the 2.5-Å crystal structure. *J.Biol.Chem.* **274**:21114-21120.
- Smallshaw, J. E. and R. A. Kelln.** 1992. Cloning, nucleotide sequence, and expression of the *Escherichia coli* K-12 *pyrH* encoding UMP kinase. *Genetics (Life Sciences)* **11**:65.
- Sorensen, K. I., K. E. Baker, R. A. Kelln, and J. Neuhard.** 1993. Nucleotide pool-sensitive selection of the transcriptional start site *in vivo* at the *Salmonella typhimurium pyrC* and *pyrD* promoters. *J.Bacteriol.* **175**:4137-4144.
- Stevens, R. C., Y. M. Chook, C. Y. Cho, W. N. Lipscomb, and E. R. Kantrowitz.** 1991a. *Escherichia coli* aspartate carbamoyltransferase: the probing of crystal structure analysis via site-specific mutagenesis. *Protein Eng.* **4**:391-408.
- Stevens, R. C., K. M. Reinisch, and W. N. Lipscomb.** 1991b. Molecular structure of *Bacillus subtilis* aspartate transcarbamoylase at 3.0 Å resolution. *Proc.Natl.Acad.Sci.U.S.A.* **88**:6087-6091.
- Takagi, Y. and B. L. Horecker.** 1957. Purification and properties of a bacterial riboside hydrolase. *J.Biol.Chem.* **225**:77-86.
- Terada, M., M. Tatibana, and O. Hayaishi.** 1967. Purification and properties of nucleoside hydrolase from *Pseudomonas fluorescens*. *J.Biol.Chem.* **242**:5578-5585.
- Theisen, M., R. A. Kelln, and J. Neuhard.** 1987. Cloning and characterization of the *pyrF* operon of *Salmonella typhimurium*. *Eur.J.Biochem.* **164**:613-619.

- Thoden, J. B., H. M. Holden, G. Wesenberg, F. M. Raushel, and I. Rayment.** 1997. Structure of carbamoyl phosphate synthetase: a journey of 96 Å from substrate to product. *Biochemistry* **36**:6305-6316.
- Thoden, J. B., G. N. Phillips, Jr., T. M. Neal, F. M. Raushel, and H. M. Holden.** 2001. Molecular structure of dihydroorotase: a paradigm for catalysis through the use of a binuclear metal center. *Biochemistry* **40**:6989-6997.
- Valentin-Hansen, P.** 1978. Uridine-cytidine kinase from *Escherichia coli*. *Methods Enzymol.* **51**:308-314.
- Van de Castele, M., C. Legrain, L. Desmarez, P. G. Chen, A. Pierard, and N. Glansdorff.** 1997. Molecular physiology of carbamoylation under extreme conditions: what can we learn from extreme thermophilic microorganisms? *Comp.Biochem.Physiol.A.Physiol.* **118**:463-473.
- Versees, W., K. Decanniere, R. Pelle, J. Depoorter, E. Brosens, D. W. Parkin, and J. Steyaert.** 2001. Structure and function of a novel purine specific nucleoside hydrolase from *Trypanosoma vivax*. *J.Mol.Biol.* **307**:1363-1379.
- Vial, T. C., K. E. Baker, and R. A. Kelln.** 1993. Dual control by purines and pyrimidines of the expression of the *pyrD* gene of *Salmonella typhimurium*. *FEMS Microbiol.Lett.* **111**:309-314.
- Vickrey, J. F., G. Herve, and D. R. Evans.** 2002. *Pseudomonas aeruginosa* aspartate transcarbamoylase. Characterization of its catalytic and regulatory properties. *J.Biol.Chem.* **277**:24490-24498.

von der, S. W., P. M. Anderson, and J. J. Villafranca. 1985. Mechanistic investigations of *Escherichia coli* cytidine-5'-triphosphate synthetase. Detection of an intermediate by positional isotope exchange experiments. *J.Biol.Chem.* **260**:14993-14997.

Washabaugh, M. W. and K. D. Collins. 1984. Dihydroorotase from *Escherichia coli*. Purification and characterization. *J.Biol.Chem.* **259**:3293-3298.

Washabaugh, M. W. and K. D. Collins. 1986. Dihydroorotase from *Escherichia coli*. Sulfhydryl group-metal ion interactions. *J.Biol.Chem.* **261**:5920-5929.

Wild, J. R., S. J. Loughrey-Chen, and T. S. Corder. 1989. In the presence of CTP, UTP becomes an allosteric inhibitor of aspartate transcarbamoylase. *Proc.Natl.Acad.Sci.U.S.A.* **86**:46-50.

Xi, X. G., C. De Staercke, F. Van Vliet, F. Triniolles, A. Jacobs, P. P. Stas, M. M. Ladjimi, V. Simon, R. Cunin, and G. Herve. 1994. The activation of *Escherichia coli* aspartate transcarbamylase by ATP. Specific involvement of helix H2' at the hydrophobic interface between the two domains of the regulatory chains. *J.Mol.Biol.* **242**:139-149.

CHAPTER 2

CLONING AND CHARACTERIZATION OF THREE ISOGENIC NUCLEOSIDE HYDROLASES FROM *Escherichia coli* K-12

Introduction

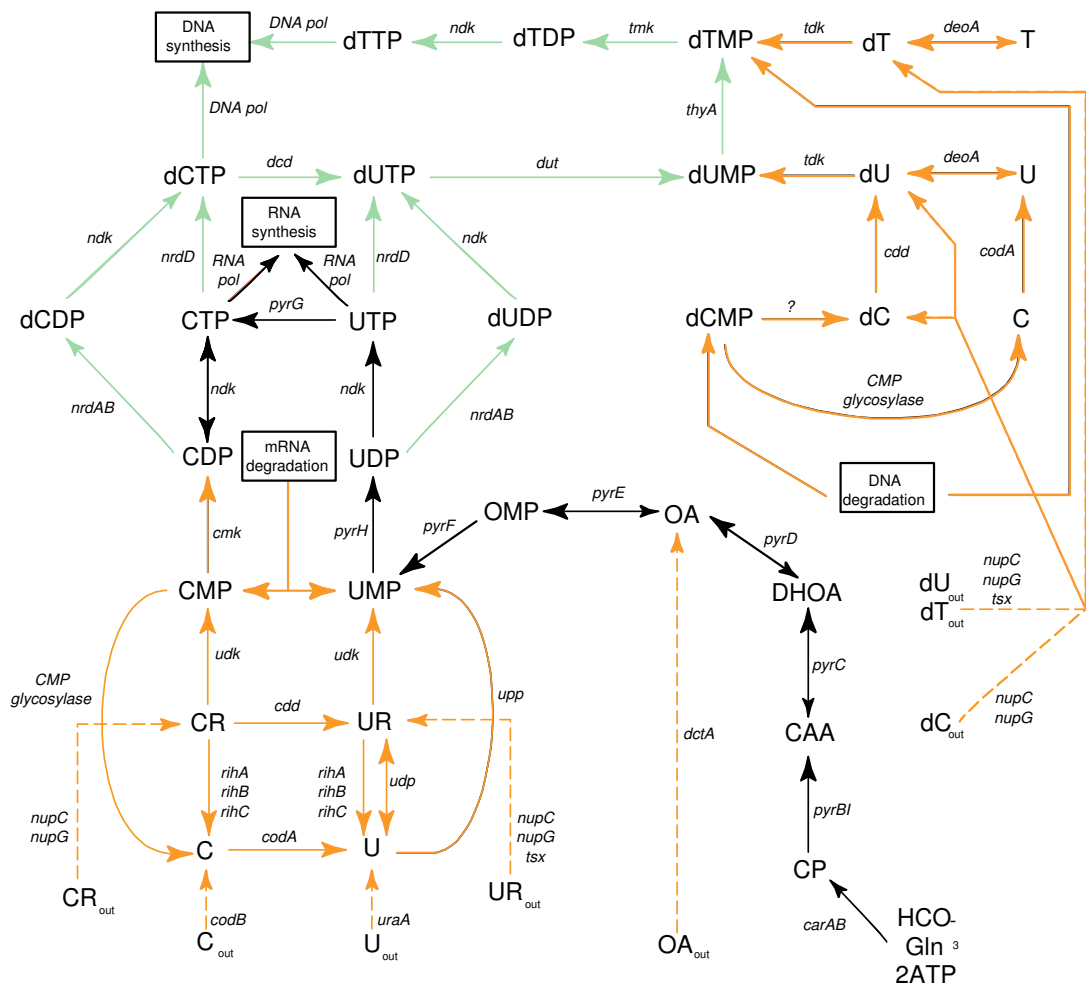
The salvage of nucleosides and bases is a ubiquitous series of reactions that is present, at least in part, in all organisms. In *Escherichia coli*, many enzymes have been implicated in the recycling of purines and pyrimidine bases and nucleosides. As shown in Figure 2.1, *E. coli* can utilize bases and nucleosides by various routes (Neuhard and Kelln, 1996).

Nucleosides can be catabolized by either a phosphorylytic or a hydrolytic cleavage at the β -N-glycosyl bond (Figure 2.2). These reactions are catalyzed by nucleoside phosphorylases and nucleoside hydrolases, respectively. A pyrimidine-specific nucleoside hydrolase activity had previously been reported for *E. coli* (Beck, 1995; O'Donovan and Shanley, 1995), *Salmonella typhimurium* (Beck et al., 1996), and several pseudomonads (West, 1988; Terada et al., 1967; Sakai and Omata, 1976). A recent comprehensive study (Beck, 1995) reported nucleoside hydrolase activity in all bacterial samples tested. Furthermore, degradative activity towards uridine, as evidenced by 5-fluorouridine sensitivity, had been noted in uridine phosphorylase-deficient *E. coli* strains (Neuhard, 1983). Mutants in this activity had not been isolated previously, leading to the hypothesis that 5-fluorouridine was cleaved by thymidine phosphorylase in low concentrations (Neuhard, 1983).

The nucleoside hydrolases and the catalytically-related monophosphate glycosylases (such as CMP glycosylase) are able to hydrolyze either nucleosides or nucleoside

monophosphates at the β -N-glycosyl bond, leaving a pentose sugar (ribose, deoxyribose, or ribose-5-phosphate) and a base (Figure 2.2; Neuhard and Kelln, 1996). Either the pentose or the base can be reutilized to form more nucleoside triphosphates or be broken down for carbon, nitrogen, or energy (Vogels and Van der Drift, 1976). Previously, cloned activities for nucleoside hydrolases have been reported for the parasitic protozoans *Crithidia fasciculata* (Parkin et al., 1991) and *Trypanosoma brucei brucei* (Pellé et al., 1998). All display significant activity towards purine nucleosides, with some activity for pyrimidine nucleosides. However, none displayed activity towards nucleoside monophosphates (NMPs), indicating that any activity that would hydrolyze the β -N-glycosyl bond would likely be catalyzed by another enzyme.

In this section, I focus on nucleoside hydrolysis in *E. coli*. Three homologues of nucleoside hydrolases have been found in *E. coli* (ORFs *yeiK*, *ybeK*, and *yaaF*) using the complete genome sequence (Blattner et al., 1997). All three *E. coli* genes have been cloned from the *E. coli* chromosome. Cloned genes have been expressed in order to determine their specificities. The deduced amino acid sequence is compared to the crystallized nucleoside hydrolases from *C. fasciculata* and *L. major* in order to determine potential catalytic residues and protein-substrate contacts. The proposed primary structure for the *ybeK*-encoded nucleoside hydrolase (YbeK-NH) is used in a comparative modeling simulation to determine the possible mechanisms of pyrimidine specificity and the potential structure of the active site.



Pyrimidine <i>de novo</i> pathway	Pyrimidine Salvage Pathways
<i>carAB</i> - carbamoyl-phosphate synthetase	<i>uraA</i> - uracil permease
<i>pyrBI</i> - aspartate transcarbamoylase	<i>upp</i> - uracil phosphoribosyltransferase
<i>pyrD</i> - dihydroorotase	<i>udp</i> - uridine phosphorylase
<i>pyrC</i> - dihydroorotate dehydrogenase	<i>rih</i> - nucleoside hydrolase
<i>pyrE</i> - orotate phosphoribosyltransferase	<i>udk</i> - uridine kinase
<i>pyrF</i> - OMP decarboxylase	<i>codB</i> - cytosine permease
<i>pyrH</i> - UMP (uridylyate) kinase	<i>codA</i> - cytosine deaminase
<i>ndk</i> - nucleoside diphosphate kinase	CMP glycosylase (gene not known)
<i>pyrG</i> - CTP synthetase	<i>cmk</i> - CMP (cytidylate) kinase
	<i>cdd</i> - cytidine deaminase
	<i>nupC, nupG, tsx</i> - nucleoside permeases
	<i>dctA</i> - dicarboxylate transport
dCTP and dTTP Biosynthesis	<i>deoA</i> - thymidine phosphorylase
<i>nrdAB</i> - aerobic ribonucleotide reductase	<i>tmk</i> - dTMP (thymidylate) kinase
<i>nrdD</i> - anaerobic ribonucleotide reductase	<i>tdk</i> - thymidine kinase
<i>ndk</i> - nucleoside diphosphate kinase	
<i>dcd</i> - dCTP deaminase	
<i>dut</i> - dUPTase	
<i>thyA</i> - thymidylate synthase	
<i>tmk</i> - thymidylate kinase	

Figure 2. 1 – Pyrimidine salvage pathway reactions in *E. coli* K-12. Orange arrows (↑) – salvage reactions, black arrows (↑) - *de novo* reactions to CTP formation, green arrows (↑), reactions leading to formation of DNA precursors dCTP and dTTP, dashed arrows – imported compounds.

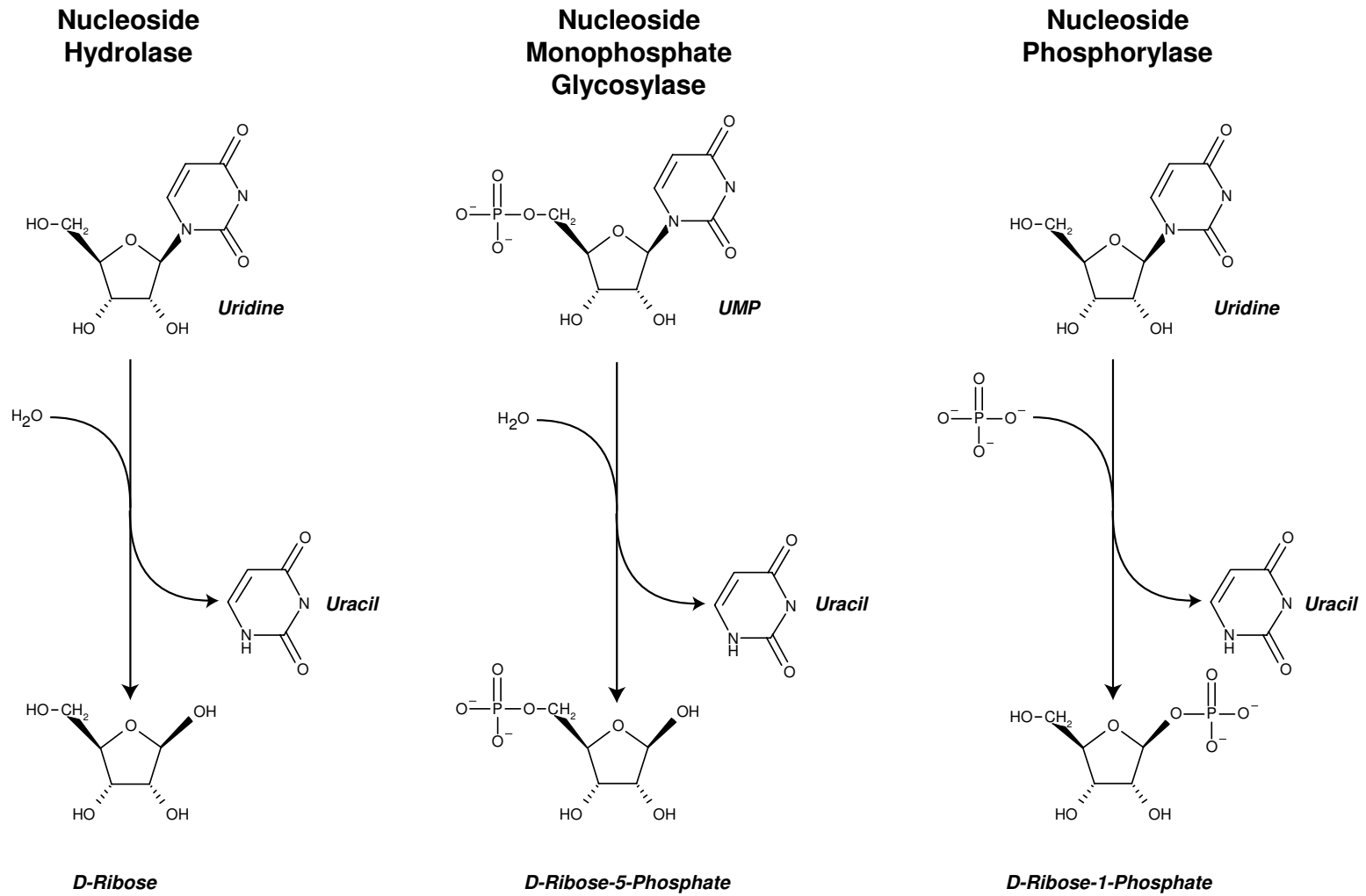


Figure 2. 2 – Hydrolytic and phosphorylytic breakdown of uridine and UMP.

Materials and Methods

Abbreviations and common names used

A list of abbreviations is shown in Table 2.1.

Chemicals and Supplies

All chemicals used, except the following, were purchased from Sigma-Aldrich. Agarose, Lennox-based LB medium, and Tris (free base) were purchased from Fisher Scientific. A DNA band prep kit was used for extracting DNA from agarose gels (Prep-a-Gene™, BioRad Corp., Hercules, CA, www.biorad.com). *Pfu* polymerase, used in all PCR amplifications, was purchased from Stratagene Corp. (La Jolla, CA, www.stratagene.com). The plasmid pZeRO2.1 was obtained from Dr. John Knesek (Texas Woman's University, Denton, TX) and originated from Invitrogen Corp. (Carlsbad, CA, www.invitrogen.com). All automated sequencing was performed by Lone Star Labs, Inc (San Antonio, TX). Primers used for PCR amplification were purchased from Integrated DNA Technologies, Inc. (Coralville, IA), or Biosynthesis, Inc. (Lewisville, TX)

Bacterial strains and media

The *E. coli* strains and plasmids listed in Table 2.2 were used in this study. All strains were grown in LB medium. Media were solidified with 1.5% agar when needed. Media were also supplied with the following additional components, where applicable: IPTG (1mM), kanamycin (50 µg/ml), and ampicillin (100 µg/ml).

Table 2.1 – List of abbreviations

<u>Abbreviation</u>	<u>Full Name</u>
A	Adenine
AR	Adenosine
ATP	adenosine 5'-triphosphate
bp	base pair
C	Cytosine
CAA	N-carbamoyl aspartate (carbamoyl aspartic acid)
CDP	cytidine 5'-diphosphate
CMP	cytidine 5'-monophosphate
CR	Cytidine
CTAB	cetyltrimethylammonium bromide
CTP	cytidine 5'-triphosphate
dC	2'-deoxycytidine
dCDP	2'-deoxycytidine 5'-diphosphate
dCMP	2'-deoxycytidine 5'-monophosphate
dCTP	2'-deoxycytidine 5'-triphosphate
ddH₂O	distilled deionized water
DHOA	dihydroorotate (dihydroorotic acid)
DNA	deoxyribonucleic acid

<u>Abbreviation</u>	<u>Full Name</u>
dT	2'-deoxythymidine
dTDP	2'-deoxythymidine 5'-diphosphate
dTMP	2'-deoxythymidine 5'-monophosphate
DTT	Dithiothreitol
dTTP	deoxythymidine 5'-triphosphate
dU	deoxyuridine
dUMP	deoxyuridine 5'-triphosphate
dUTP	deoxyuridine 5'-triphosphate
EDTA	ethylenediaminetetraacetic acid
G	Guanine
Gln	Glutamine
GR	Guanosine
HCO₃⁻	bicarbonate
HEPES	N-2-hydroxyethylpiperazine-N'-2-ethansulfonic acid
Hx	hypoxanthine
HxR	Inosine
IAGNH	inosine-adenosine-guanosine preferring nucleoside hydrolase
IPTG	isopropyl-B-D-galactoside
IUNH	inosine-uridine preferring nucleoside hydrolase

<u>Abbreviation</u>	<u>Full Name</u>
kb	kilobase pairs
kDa	Kilodalton
LB	Luria-Bertani media, composed of 10g tryptone, 5g yeast extract, 5 g NaCl
NDP	Nucleoside 5'-diphosphate
NH	Nucleoside hydrolase
NMP	Nucleoside 5'-monophosphate
NTP	Nucleoside 5'-triphosphate
OA	Orotate (orotic acid)
OMP	Orotidine 5'-monophosphate
PCR	Polymerase chain reaction
<i>Pfu</i>	<i>Pyrococcus furiosus</i>
RNA	ribonucleic acid
SDS	sodium dodecylsulfate
T	Thymine
TE	10 mM Tris-HCl-1 mM EDTA, pH 8.0
Tris	tris(hydroxymethyl)aminomethane
TSS	Transformation and Storage Solution
U	Uracil
UDP	uridine 5'-diphosphate

<u>Abbreviation</u>	<u>Full Name</u>
UMP	uridine 5'-monophosphate
UR	Uridine
UTP	uridine 5'-triphosphate

Table 2.2 – List of strains, plasmids, and primers

<i>E. coli</i> Strains		Source
K12	wild type	ECGS*
TOP10F'	F' { <i>lacIq Tn10</i> (TetR)} <i>mcrA</i> .(<i>mrr-hsdRMS-mcrBC</i>) Φ 80 <i>lacZ</i> Δ M15 <i>lacX74 deoR recA1 araD139 (ara-leu)7697 galU galK rpsL</i> (Str ^R) <i>endA1 nupG</i>	Invitrogen
Plasmids		
pZeRO2.1	KanR cloning vector with <i>lacZ-ccdA</i> fusion	Invitrogen J. Knesek
pCJF2	pZeRO2.1 with <i>yaaF</i> PCR fragment in <i>EcoRV</i> site in orientation with the P _{<i>lac</i>} promoter	This study
pCJF2r	pZeRO2.1 with <i>yaaF</i> PCR fragment in <i>EcoRV</i> site in opposite orientation from P _{<i>lac</i>} promoter	This study
pCJF3	pZeRO2.1 with <i>ybeK</i> PCR fragment in <i>EcoRV</i> site in orientation with the P _{<i>lac</i>} promoter	This study
pCJF3r	pZeRO2.1 with <i>ybeK</i> PCR fragment in <i>EcoRV</i> site in opposite orientation from P _{<i>lac</i>} promoter	This study
pCJF4r	pZeRO2.1 with <i>yeiK</i> PCR fragment in <i>EcoRV</i> site in opposite orientation from P _{<i>lac</i>} promoter	This study
pZeRO2.1 Δ	Isolated pZeRO2.1 derivative with ~100 bp deletion in multiple cloning site	This study
Primers		
<i>yaaF</i> For	CTCCGGATATTCTGGTGCGAG	This study
<i>yaaF</i> Rev	TTTTTCAGAGTAACCAGCGCA	This study
<i>ybeK</i> For	GACGCTTTCCTTCGATGATCC	This study
<i>ybeK</i> Rev	ATTTGGAATTAATTGCGCGG	This study
<i>yeiK</i> For	GTATCGGCTGAAACATCCGT	This study
<i>yeiK</i> Rev	CGCTGTACGCCATCACTTTA	This study

* *E. coli* Genetic Stock Center

Chromosomal DNA Isolation

A modified method using CTAB (Ausubel, 2001) was used to isolate chromosomal DNA and to remove carbohydrates which interfered with PCR. Briefly, a 5 ml LB culture of the bacterium of interest was grown to saturation in LB medium, Lennox mix (this was normally an overnight culture). 1.5 ml of the overnight culture was harvested in a table-top centrifuge (10,000 x *g* for 30 seconds). The pellet was resuspended in 567 μ l TE buffer by repeated pipetting and vortexing. 30 μ l of 10% SDS and 3 μ l of proteinase K stock solution (10 mg/ml) were added to the mix by inverting several times, and the samples were incubated at 65°C for 10 minutes. NaCl (using a 5 M stock solution) was added to a final concentration of 0.7 M (the added volume varied slightly per experiment, normally due to differences in growth and strains). 0.1 volume of CTAB/NaCl solution (20% CTAB in 150 mM NaCl) was then added by inversion. Extraction was performed using an equal volume of chloroform/isoamyl alcohol (24:1), avoiding vortexing due to potential shearing of DNA. A clarification spin at 10,000 rpm for 5 minutes was used to separate phases (a white interface indicates the removal of polysaccharide). The top layer was removed with a clipped-off blue pipette tip and transferred to a new tube. The extraction using CTAB/NaCl was repeated before extracting twice using an equal volume of phenol/chloroform/isoamyl alcohol (25:24:1, using equilibrated phenol at pH 8.0). After a clarification spin, the supernatant was removed to a new tube, in which the DNA was precipitated using 0.6 vol of isopropanol. The pellet was washed with 70% ethanol to remove salts. The pellet was dried *in vacuo* and resuspended in 50-500 μ l of TE (pH 8.0). Typically, the concentration of DNA isolated ranged from 100-1000 ng/ μ l.

Cloning and sequence determination

An outline of the procedure is shown in Figure 2.3. Primers were constructed that flanked the coding region of *ybeK* and *yaaF* from the complete *E. coli* genome sequence (Table 1.1). The program Prophet 5.0™ (BBN Systems and Technologies, Inc., Cambridge, MA) was used to pick optimal primer pairs based upon several constraints, including distance (300 base pairs 5' and 3' of each gene), T_m of approximately 60°C, GC content of 50%, and a 3' end GC clamp to enhance primer binding to the template. PCR amplifications using the high fidelity enzyme *Pfu* polymerase were performed using the following parameters: 95°C chromosomal DNA melting (1 minute), 60°C annealing (45 sec), 72°C extension (3 minutes, 45 seconds for the *E. coli* genes) for 16 cycles; then 14 cycles utilizing the previous parameters with a 1°C lower annealing temperature and 20 seconds longer extension time. The PCR was allowed to proceed after all 30 cycles with a 10 minute cleanup step at 72°C, after which it was analyzed on a 0.8 % agarose gel (Figure 2.5). Discrete bands were obtained, as shown in Figure 2.5. These were loaded on a preparative gel using wider lanes and the same conditions for running as above, loading the remaining PCR reaction into the individual wells.

Electrophoresed PCR products were removed from the individually prepared gel slices using the Prep-a-Gene kit. All steps were carried out at room temperature unless otherwise described. After agarose gels were electrophoresed to resolve the individual bands (1-1.5 hours), each gel was carefully cut to isolate the individual bands, preventing cross-contamination with other PCR products or the molecular weight markers. Isolated gel fragments were added to Eppendorf tubes and spun down to determine an approximate volume, using a ratio of 1 g/ml (the slices were normally less than 0.5 ml). The Prep-a-Gene™ binding buffer (6 M sodium perchlorate, 50 mM Tris-HCl, 10 mM EDTA, pH 8.0) was added next (3 volumes of the

E. coli yaaF gene region

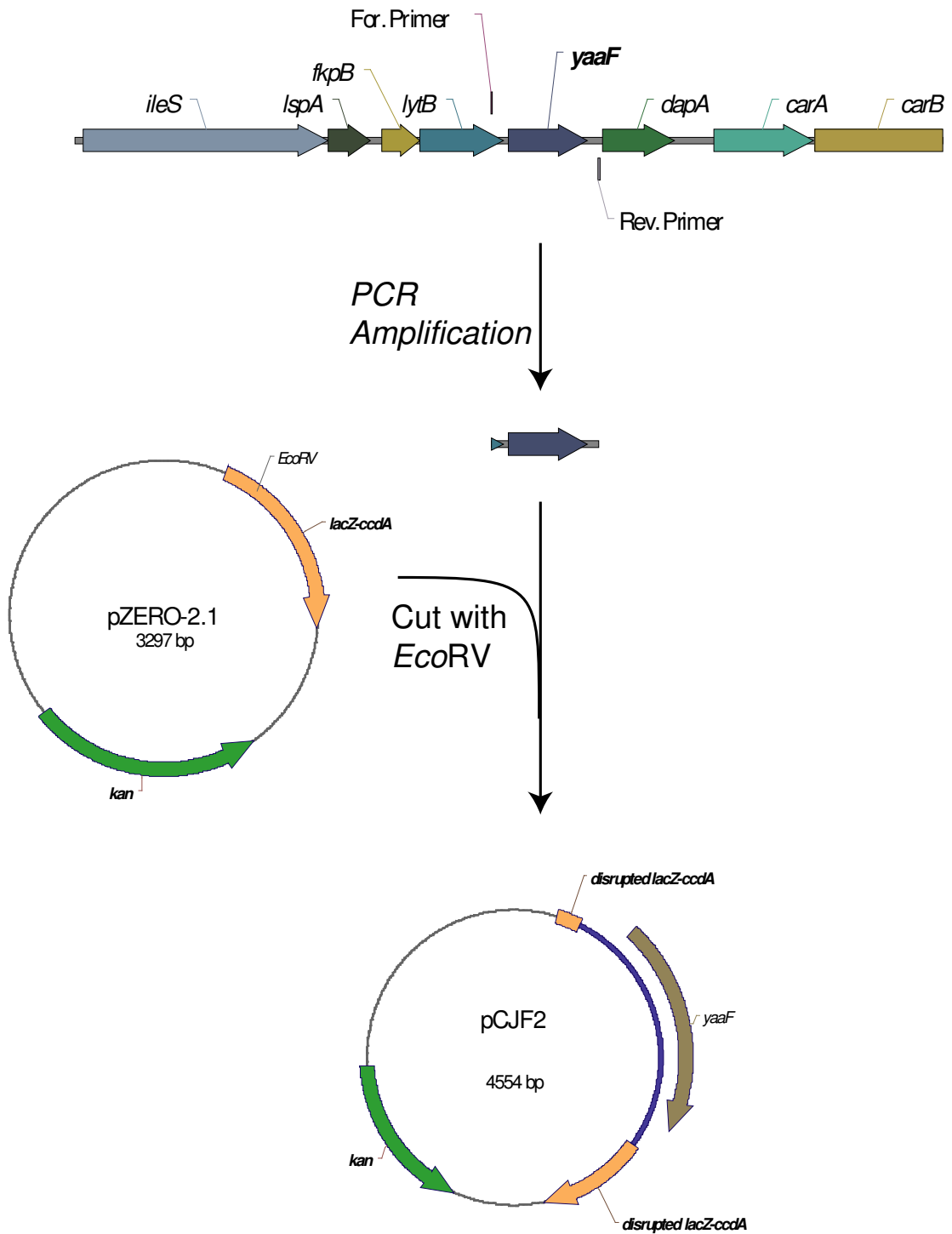


Figure 2.3 – Outline of cloning procedure.

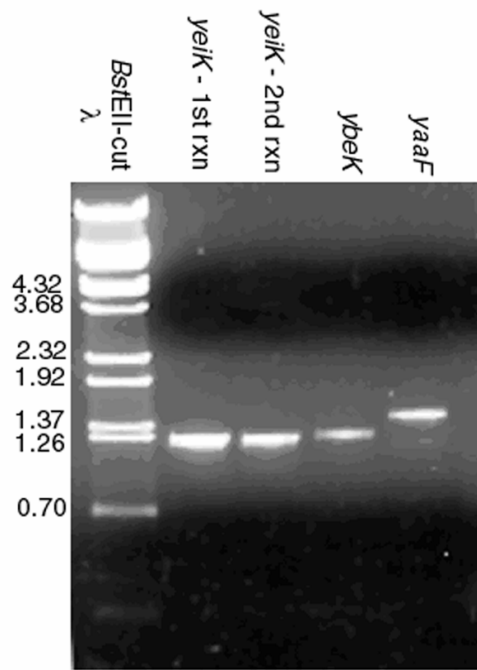


Figure 2.4 – PCR reaction products.

original gel slice). The gel slices were incubated at 65°C for 10 minutes or until the gel slice dissolved. 5 µl of Prep-a-Gene™ DNA binding matrix (diatomaceous earth in 1x TE) were added and the solution was incubated at room temperature, with gentle agitation, for 5-10 minutes. The matrix, with the bound DNA, was collected by centrifugation, after which the pellet was washed twice with 125 µl of Prep-a-Gene™ Wash Buffer (50% ethanol, 400 mM NaCl, 20 mM Tris-HCl, 2 mM EDTA pH 8.0, at room temperature). After aspiration of the remaining ethanol, the matrix pellet was dried *in vacuo* for 3 minutes. Elution of the bound DNA was accomplished by addition of 10 µl of Prep-a-Gene Elution Buffer (TE, pH 7.5) for 15 minutes at 37°C. After collection, the supernatant was removed, and an additional back-elution of the matrix was performed with 10 µl of Elution Buffer. A clarifying step was performed in which remaining matrix was removed by centrifugation. The DNA in the supernatant was ethanol-precipitated and dried *in vacuo*.

The three *E. coli* PCR products were blunt-end ligated directly into the *EcoRV* site of pZeRO2.1 (Invitrogen); the procedure used is outlined in Figure 2.3. All ligations were transformed into *E. coli* strain TOP10F', made competent using either the TSS protocol (Chung et al., 1989) or Hanahan's method (Hanahan et al., 1991). Transformants were plated onto LB agar containing 50 µg kanamycin per ml and 1 mM IPTG in order to screen for clones. Resulting plasmids were screened for inserts, and positive clones were end-sequenced to confirm the insert. Once confirmed, the plasmids were amplified using a midi-prep column purification system (Qiagen). The bulked plasmids were sequenced (Lone Star Labs, Inc.). Plasmid, pZeRO2.1Δ, which has a non-inducible *ccdB* gene from a small deletion (~100 bp) in the multiple cloning site, was used as a negative control during induction studies due to the background of the native *E. coli* NHs.

Nucleoside hydrolase enzyme assay

Cultures of *E. coli* TOP10F' cells containing each cloned gene were in 2 liters of LB broth with 50 µg kanamycin per ml. At an OD₆₀₀ of 0.6 (mid-log phase), IPTG was added to a final concentration of 125 µM. Induction of the cloned genes was allowed to proceed for 6 hours. Cells were pelleted at 10,000 x g, resuspended in breaking buffer (50 mM HEPES pH 7.3, 0.1 mM DTT, 100 µM EDTA, 100 µM CaCl₂) at a concentration of 1g/ml, based on the wet weight of the cells. Cells were sonicated twice (2 minutes apiece) using a Branson Cell Disrupter 200 with a duty cycle setting of 0.2-0.3 at 50% pulse rate. Cell debris was pelleted at 25,000 x g, and the cell-free extract was removed to a new tube and assayed directly. Nucleoside hydrolase activity was detected using a scaled-down version of the reducing sugar assay (Parkin et al., 1991), in a final volume of 100 µl. Final reaction mixtures contained 10 µl of enzyme, 50 mM HEPES pH 7.3, and 5 mM nucleoside (except guanosine, which was 2 mM final). Reactions were initiated with the addition of 10 µl of cell extract and allowed to proceed for 20 minutes. A background blank to determine native NH activity in *E. coli* was run for each sample by using 10 µl of cell extract in 50 mM HEPES, pH 7.3 (100 µl total). Reactions were stopped by the addition of 100 µl of 0.1 M ZnSO₄, equilibrated using 100 µl of 0.1 M NaOH, and centrifuged at 14,000 x g for 5 minutes to remove precipitated proteins. Samples of 75 µl from each reaction supernatant were added (in duplicate) to a 96-well microtiter plate using a micropipettor, after which 150 µl of a 1:1 mix of color mix A (4% Na₂CO₃, 1.6% glycine, 0.0045% CuSO₄•5H₂O) and B(0.12% neocuproine) was added. Color development was accomplished by covering the microtiter plate with plastic wrap and developing in a 65°C water bath for 10 minutes (addition of tape to cover the microtiter plate wells was avoided due to

reaction of the color mix to the polysaccharide from the tape). Reactions were read on a microtiter plate reader (BioTek Corp., Winooski, VT) using a filter set at 450nm. Enzyme activity was determined by comparison against a D-ribose standard curve (0.01-0.16 μ moles of D-ribose dissolved in the reaction buffer above and added to the same microtiter plates before color development). New standard curves were generated with each set of assays due to some variability in color development per set of reaction. A typical reducing sugar standard curve is shown in Figure 2.5. Protein concentrations were determined by the method of Bradford (Bradford, 1976) using lysozyme as a standard (an example is shown in Figure 2.6).

Software used

ClustalX 1.81 was used for constructing a multiple sequence alignment using the default parameters (Jeanmougin et al., 1998). Alscript v. 2.0 (Barton, 1993) was used for detailing the multiple alignment. Other sequences used in the alignment were : *Crithidia fasciculata* IUNH (GenPept #AAC47119), *Leishmania major* IUNH (CAC24663), *Mycobacterium tuberculosis* IUNH (CAA15778), and *Saccharomyces cerevisiae* URH1 (Q04179). The crystal structures for the *C. fasciculata* IUNH (Degano et al., 1996) and *L. major* IUNH (Shi et al., 1999) were obtained from the Protein Databank server (www.rcsb.org/pdb/; Berman et al., 2000). Analysis of the three *E. coli* nucleoside hydrolase-encoding open reading frames was accomplished by using the EMBOSS suite of programs (Rice et al., 2000) on the Human Genome Mapping Project server (Medical Research Council, Hinxton, UK, www.hgmp.mrc.ac.uk) .

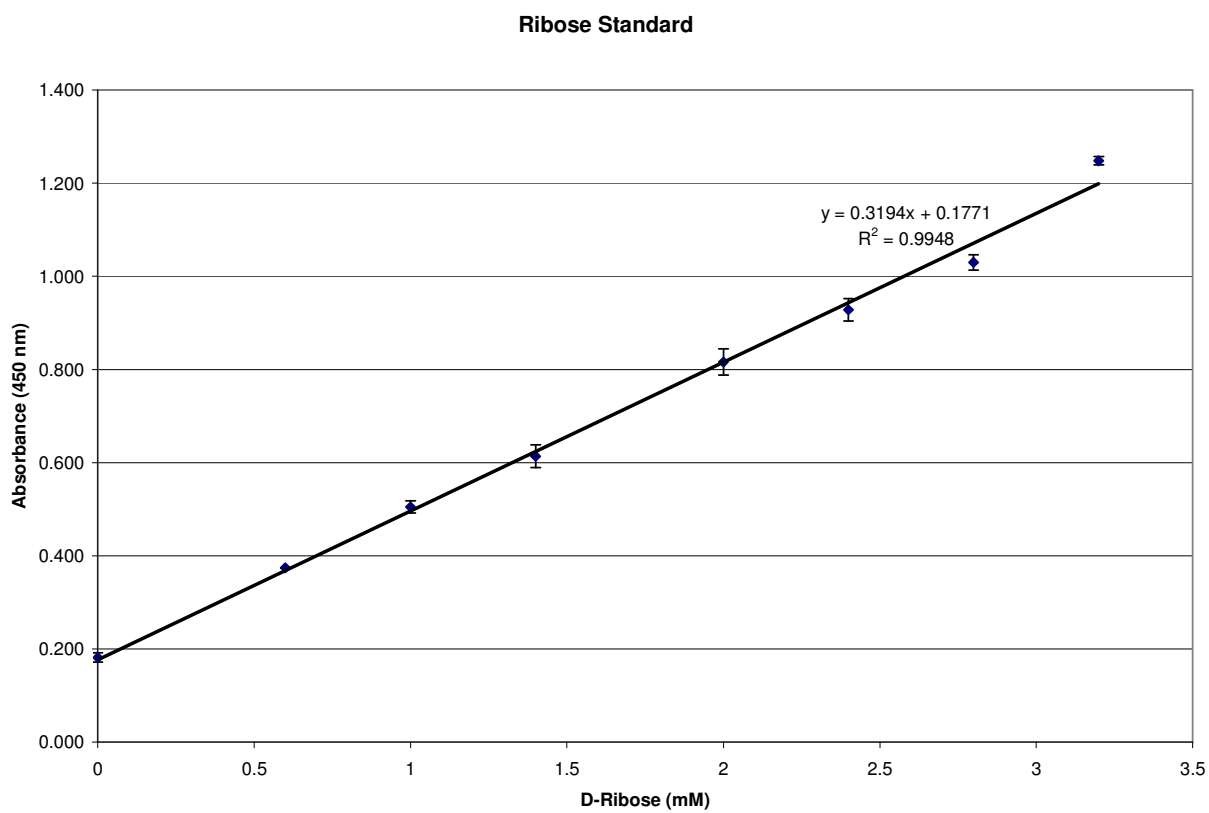


Figure 2.5 – Standard determination for the reducing sugar assay. Normal standard assays use eight different concentrations including a blank for checking background absorbance.

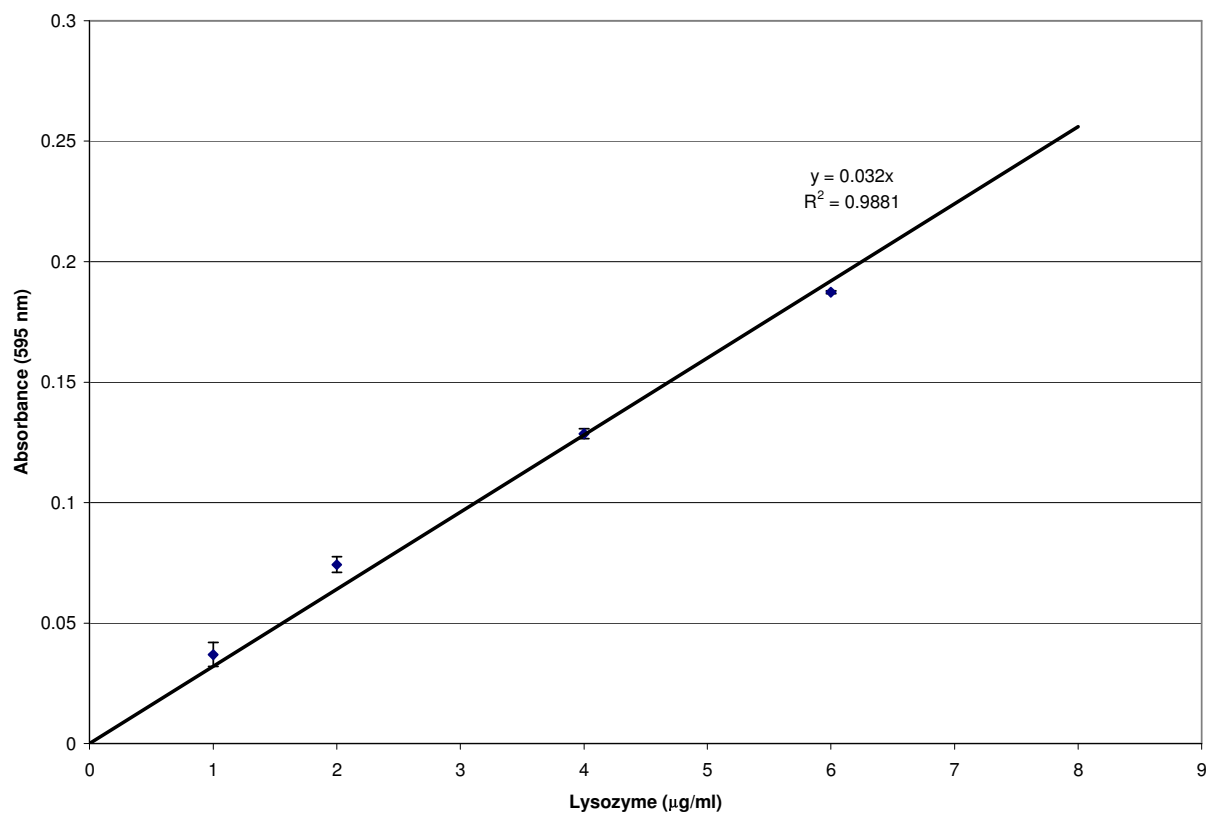


Figure 2.6 – Bradford protein concentration assay, using lysozyme as a standard.

The GC content, codon adaptation index, and codon usage bias were calculated using the program CodonW (Sharp and Matassi, 1994). Potential transcription factor binding sites were located using the matrix searching program MatInspector 3.5 (© Genomatix Software, München, Germany; Werner, 2000), utilizing a remodeled data set for the known transcription factors from *E. coli* (McGuire et al., 2000). Analysis of the promoter region of the three genes for potential promoters was accomplished using the *E. coli* matrices and MatInspector 3.5; alternately, the web server at the *Drosophila* Genome Web Site (www.fruitfly.org/seq_tools/promoter.html) was used with the prokaryotic setting. Potential secondary structures, indicating the presence of terminators, were located in the sequence using the program RNAstructure 3.71 (© David Mathews, Michael Zuker, and Douglas Turner; Mathews et al., 1999) and were visualized using the program RNADraw (Matzura and Wennborg, 1996). The current list of finished and unfinished microbial genomes was searched at NCBI (www.ncbi.nlm.nih.gov/cgi-bin/Entrez/genom_table.cgi) using the program TBLASTN (© National Center for Biotechnology Information, Washington, D.C.; Altschul et al., 1997). Structural modeling was accomplished using the SWISS-MODEL server (Guex and Peitsch, 1997). Analysis of the YbeK-generated structure was accomplished using the Visual Molecular Dynamics (VMD) suite (© Board of Trustees of the University of Illinois, Urbana, IL; Humphrey et al., 1996).

Results and Discussion

Cloning and expression of *ybeK*, *ybeK*, and *yaaF*

The PCR reaction products for the three hydrolase genes were shown in Figure 2.4. All fragments isolated were of the approximate size predicted from sequence analysis. This was confirmed by sequencing the inserts after cloning into the vector pZeRO2.1. Using pZeRO2.1 as

a cloning vector improved efficiency of cloning due to the lethality of the *ccdA* gene (a toxin for DNA gyrase). The resulting constructs were: pCJF2 (*yaaF*), pCJF3 (*ybeK*), and pCJF4r (*yeiK*) (Figure 2.7). The cloning efficiency was about 8 positive clones per 10 colonies with the exception of the *yeiK* gene, with a lower cloning efficiency (~20%) and only in the reverse orientation. This is likely to be due to a fusion of the N-terminus of the gene downstream of *yeiK* to the C-terminus of *ccdA*, thus reactivating the lethal CcdA protein. This has been confirmed by an *in silico* cloning experiment using the sequence given (Figure 2.8) and gives some indirect evidence that the downstream gene (*yeiJ*) is likely to be translated into a viable protein. The other genes were also cloned in the reverse direction but were not used further.

Induction and expression of the cloned nucleoside hydrolase genes

All gene products were induced in *E. coli* TOP10F' during log phase growth, using a control TOP10F' strain containing plasmid with no insert and a deletion in the multiple cloning site. The results are shown in Figure 2.9. A preliminary report of these results was given previously (Fields et al., 2000). An increase in the presence of D-ribose is seen in the induced clones versus the control. YaaF has activity for uridine, cytidine, adenosine, and inosine, and some activity for guanosine.

YbeK, in contrast, has specificity for uridine and cytidine, with little or no activity for the purine nucleosides. The YeiK enzyme, which only cloned in reverse, was not induced. However, an increase of activity is noted for the pyrimidine nucleosides, and a slight increase is noted for some purine nucleotides (Fields et al., 2000). A later study has confirmed these results and has also indicated that the *yeiK* gene product is a pyrimidine-preferring nucleoside hydrolase (Petersen and Moller, 2001).

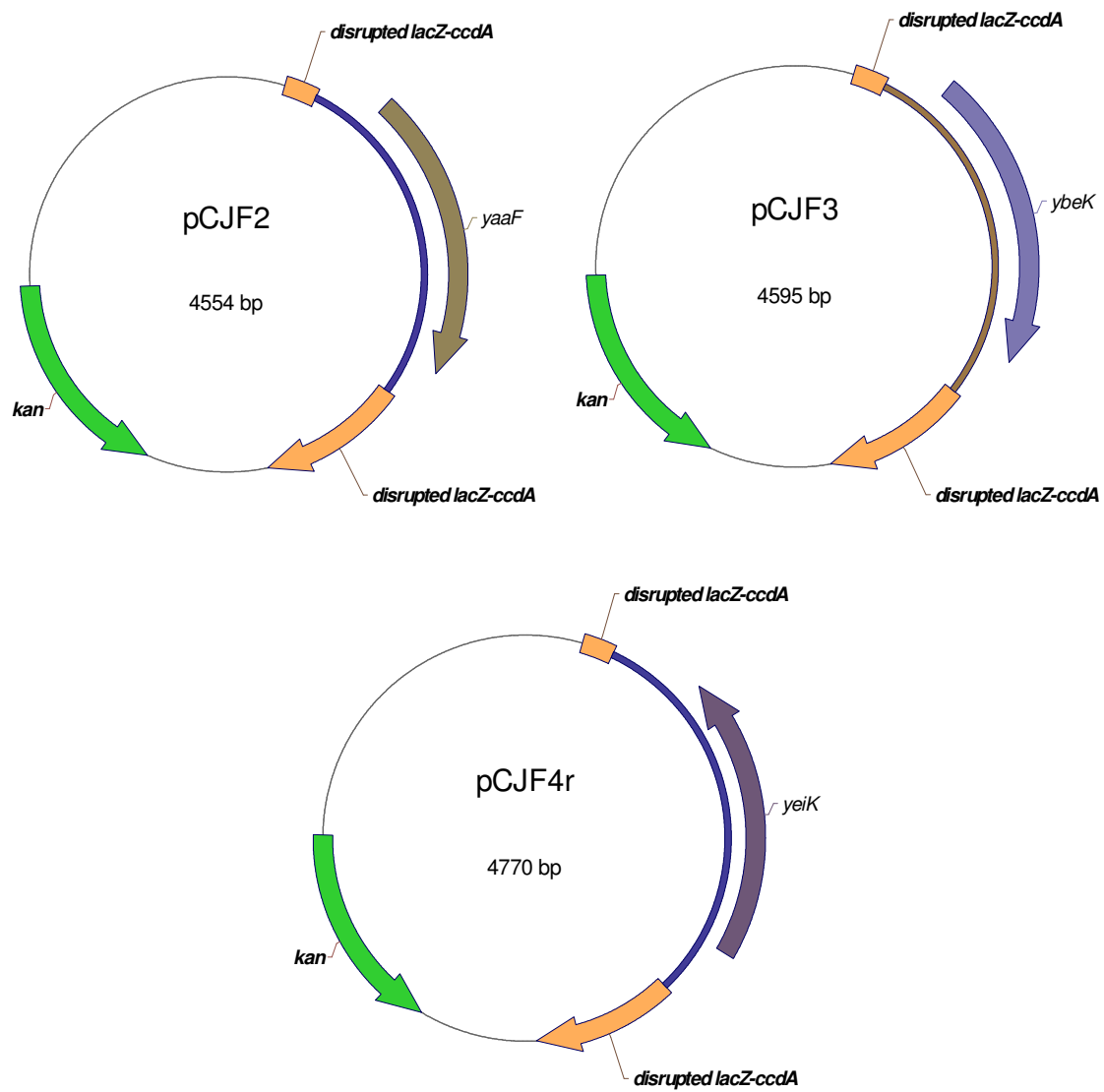


Figure 2. 7 – Plasmid constructs pCJF2, pCJF3, pCJF4r

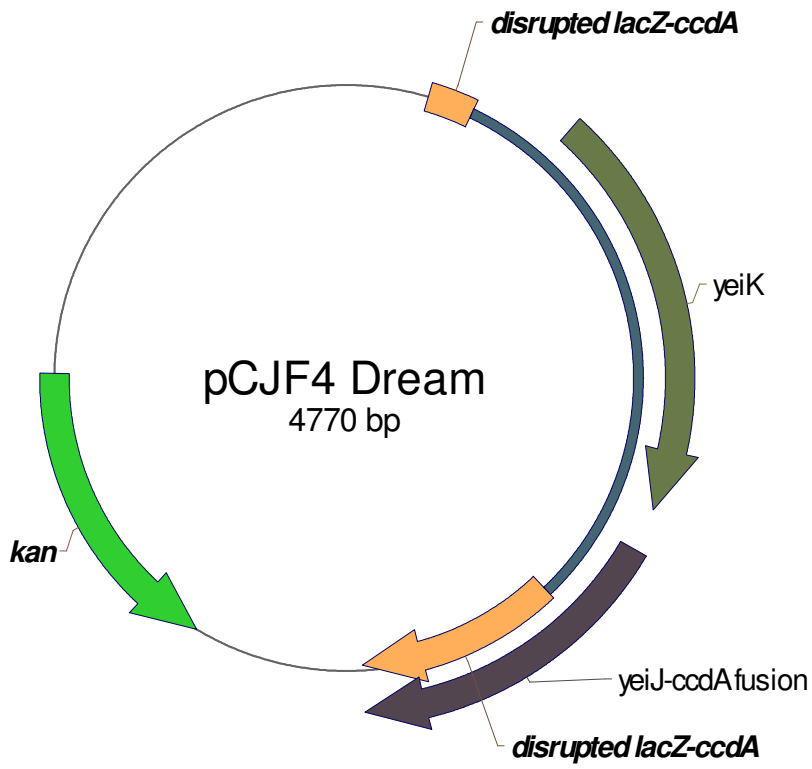


Figure 2.8 – Hypothetical plasmid construct of *yeiK* gene in orientation with the promoter

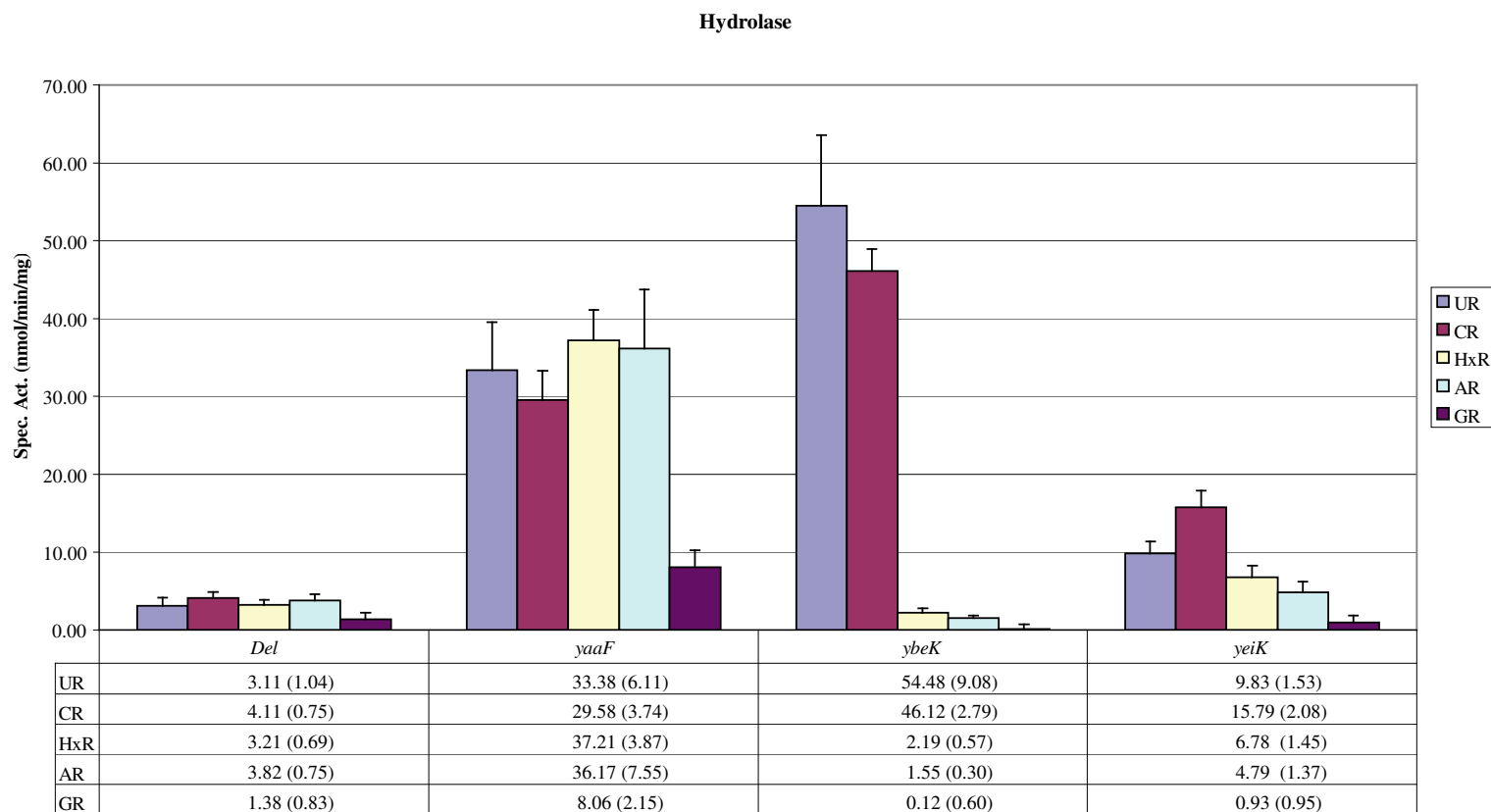


Figure 2.9 – Specific activity of induced nucleoside hydrolase clones from plasmids pCJF2, pCJF3, pCJF4r

Multiple alignment and analysis of the translated nucleoside hydrolase genes

A sequence comparison was made using the currently known nucleoside hydrolases and their homologues. The alignment (Figure 2.10) reveals that most residues necessary for catalysis are conserved throughout all the sequences, including those known to bind Ca^{++} and the ribose moiety hydroxyl groups (Degano et al., 1996). Notably, all three enzymes have a higher degree of similarity to the *Crithidia fasciculata* nucleoside hydrolase than to the recently characterized *T. vivax* IAGNH (Versees et al., 2001). Accordingly, this latter crystal structure was not used in comparative studies. It is proposed that the catalytic mechanism will be quite similar to that seen for the IUNH's (Degano et al., 1996; Shi et al., 1999).

Structural Analysis

Comparison of the gene product is shown in Table 2.3. YaaF and YbeK share the closest similarity and likely arose from a more recent common ancestor, while YeiK represents a more ancient homologue. This is unusual, as YeiK and YbeK share substrate specificity. However, the fluid nature of substrate specificity is not unusual for this family of enzymes, as is noted by the low similarity of the *S. cerevisiae* URH1 (uridine-preferring nucleoside hydrolase) to all of the structures. As no residues are currently known that specifically hydrogen bond the nucleic acid moiety of the nucleoside in the characterized NH active sites (Degano et al., 1996; Shi et al., 1999; Versees et al., 2001), it is likely that several varying factors may contribute to pyrimidine preference, such as unique hydrogen-bond interactions in the pyrimidine-specific NHs that is not present in the others. The purine base for the *T. vivax* IAGNH also relies on a unique base-stacking interaction to prevent pyrimidine bases from entering (Versees et al., 2001).

Figure 2.10 – Multiple alignment of nucleoside hydrolase homologues. The Ca⁺⁺-binding residues are designated by green up arrows (▲) under the alignment; residues known to bind the 2'- and 3' hydroxyls are shown as blue down arrows (▼) above the alignment. His-241 (*C. fasciculata* primary sequence numbering) is shown with a red circle (●). Secondary structural elements for each *E. coli* gene shown were predicted by the PHD server (Rost et al., 1994). Structural elements from the two IUNHs were obtained from the Protein Structure Database (Berman et al., 2000).

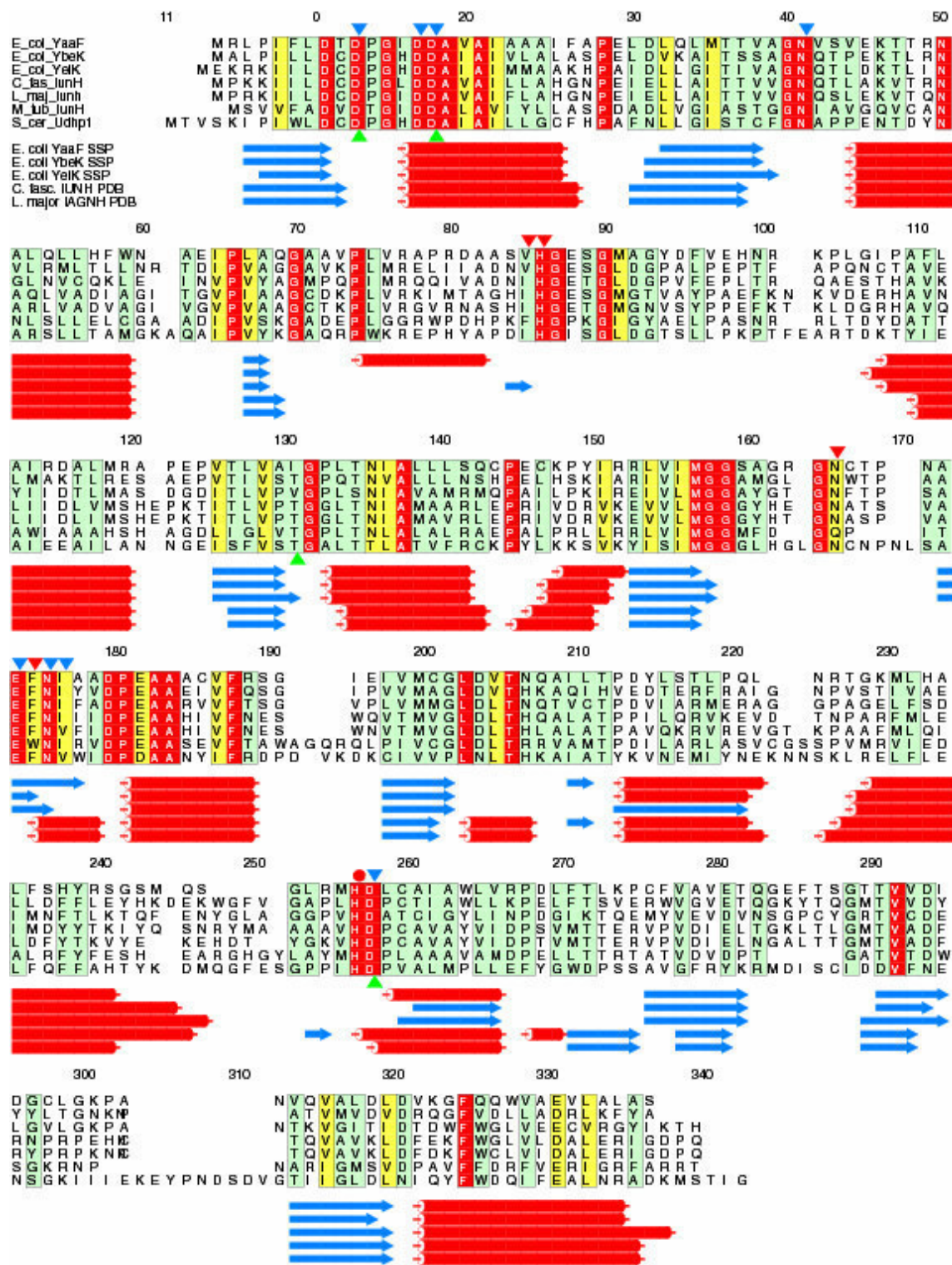


Table 2.3 – Statistical analysis of *E. coli* NHs.

Numbers below the diagonal: # residues identical

residues similar

residues with gaps

Numbers above the diagonal: % identity

% similarity

% gapped

	YaaF	YbeK	YeiK	<i>C. fasciculata</i> IUNH	<i>L. major</i> IUNH	<i>M. tuberculosis</i>	<i>S. cerevisiae</i>
YaaF		43% 60% 2%	36% 54% 2%	34% 53% 3%	35% 54% 3%	29% 48% 8%	25% 44% 10%
YbeK	136 188 7		39% 60% 1%	34% 54% 1%	34% 55% 2%	30% 48% 7%	28% 46% 9%
YeiK	115 171 9	123 189 6		37% 59% 1%	39% 59% 2%	26% 49% 6%	27% 45% 7%
<i>C. fasciculata</i> IUNH	110 169 11	110 173 6	120 187 4		75% 84% 0%	27% 50% 6%	25% 44% 7%
<i>L. major</i> IUNH	113 173 12	108 177 9	126 188 7	239 268 3		26% 46% 6%	26% 44% 8%
<i>M. tuberculosis</i>	93 154 28	99 155 23	86 158 21	90 162 21	84 150 20		22% 42% 9%
<i>S. cerevisiae</i>	85 150 36	97 158 31	93 156 27	86 153 27	91 152 28	77 145 34	

Therefore, the pyrimidine-specific NHs from *E. coli*, YbeK and YeiK, likely represent a potential new class of pyrimidine-preferring nucleoside hydrolase. To investigate this and determine if the active site residues would possibly have the same conformation, a structural comparison was utilized to examine the substrate binding pocket and determine the relative positions in comparison to the *C. fasciculata* IUNH.

Structure-based modeling using the YbeK gene product revealed that the position of several key residues is conserved when threaded into the structure for the *C. fasciculata* IUNH (Figure 2.11). The binding pocket was slightly enlarged when compared to the *Crithidia* IUNH (Figure 2.12). This enlargement in the active site is anomalous, as one would expect steric hindrance in the active site that would prevent purines from binding. However, since this is a simple modeling approach, several drawbacks should be noted. Water molecules and other compounds present in the original structure are not present in the model; therefore some molecular spacing may be off in the site. The use of a threaded structure, in effect, creates a predisposed notion of what the active site may resemble when the true catalytic mechanism or substrate binding may be quite different, as found for the trypanosomal IAGNHs (Versees et al., 2001).

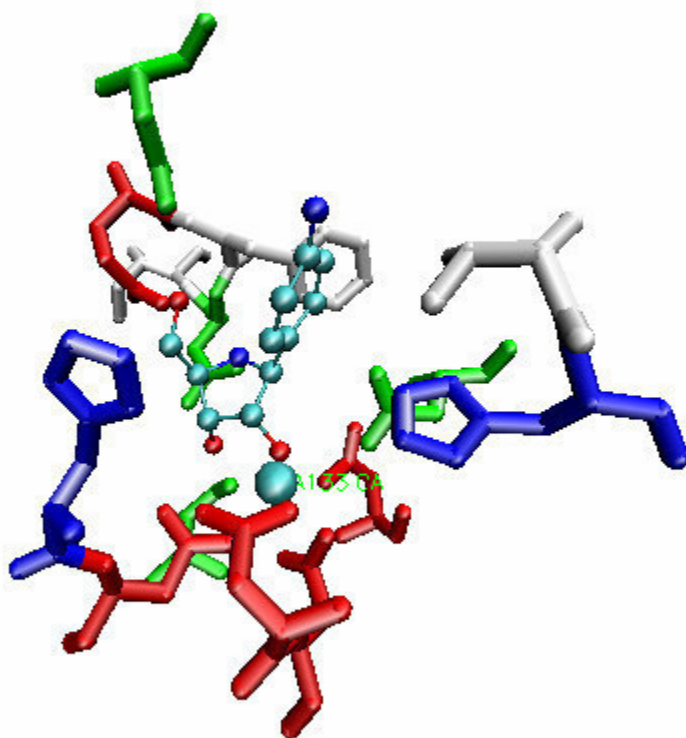


Figure 2.11 – Proposed catalytic site of *E. coli* YbeK nucleoside hydrolase. Aspartate residues are in red, histidine residues are blue, threonine and asparagine residues are in green, and aliphatic residues and hydrophobic residues are in white. The molecule in the middle is a transition state inhibitor (phenyl-imino-ribitol, or PIR) and the grey sphere directly below is the coordinated calcium ion.

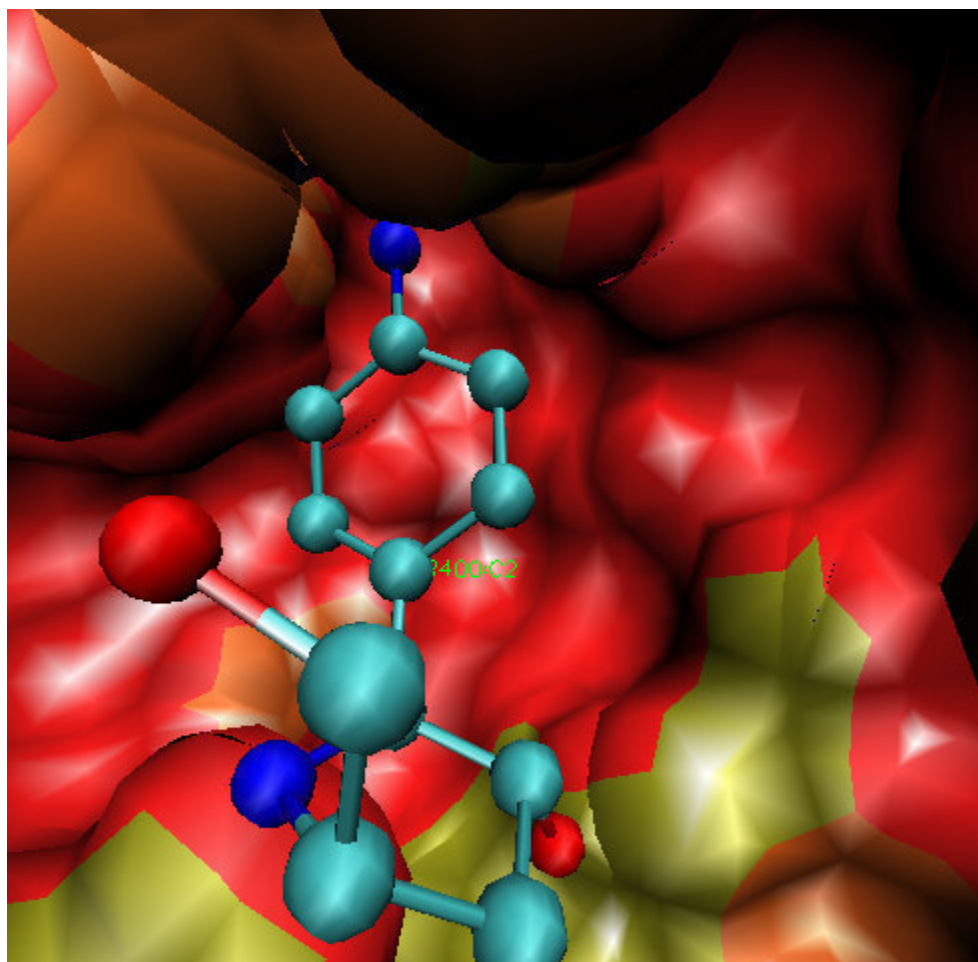


Figure 2.12 – Surface layering of the *E. coli* YbeK active site. The surface of the NH and PIR are colored by charge (reds hues = acidic, blue hues = basic, gold hues = neutral). The iminophenyl group of the substrate inhibitor PIR is shown in the background in the potential binding cleft. No apparent structures are present that would occlude purines.

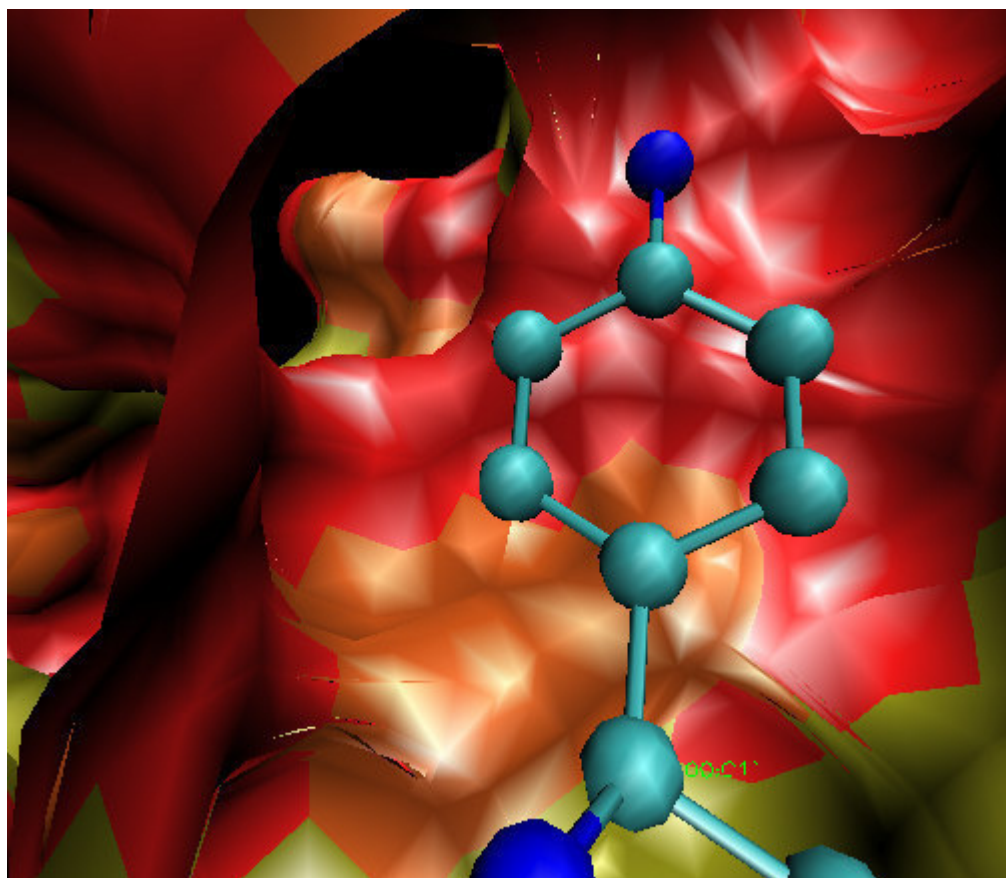


Figure 2.13 – *C. fasciculata* binding site. The large area present around the iminophenyl group, which would allow for both purines and pyrimidines to bind.

Analysis of the genes and promoter regions

Analysis of *yaaF* revealed a large region upstream of the gene that is likely to contain a promoter. When this region was scanned for possible σ^{70} sites, several potential candidate promoters emerged. One was later confirmed by Petersen and Moller as the true promoter (Petersen and Moller, 2001) and is shown in Fig 2.14. Due to its genetic isolation from other genes, with a separation upstream of 65 bp from the gene *lytB* and downstream of *dapB* by 166 bp from the gene, it is believed the *yaaF* gene expressed as a simple monocistronic message (Fig 2.14a). A structure resembling a rho-independent terminator is also found upstream (Figure 2.14b), which likely acts as the transcriptional terminator for the *lytB* gene. No potential DNA binding sites were located using the current dataset of *E. coli* transcription factor binding sites. However, a putative σ^{70} consensus was located in this region (Fields et al., 2000) which has now been confirmed as the true promoter (Petersen and Moller, 2001).

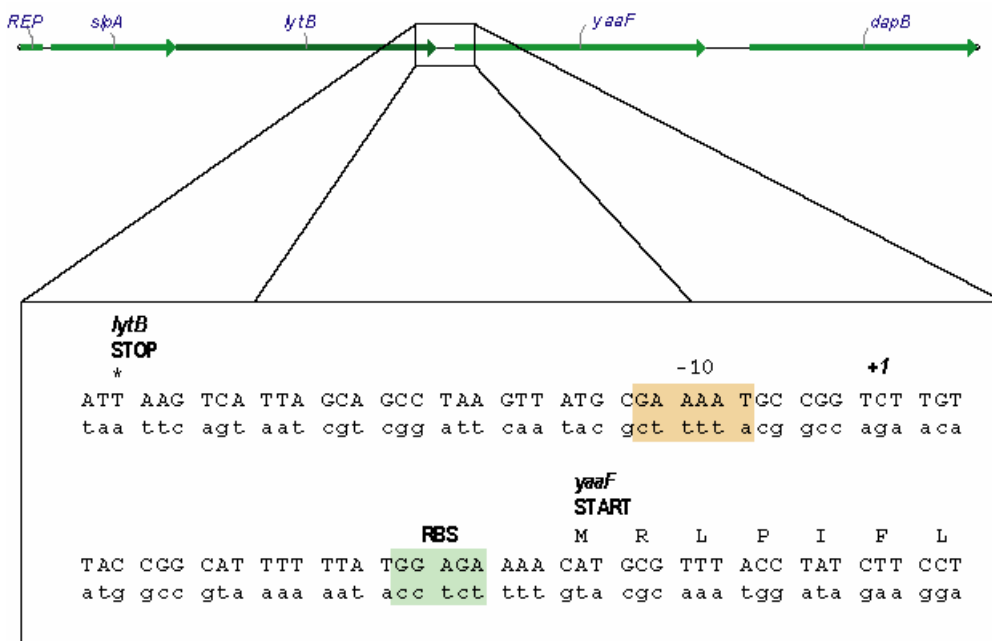
The *ybeK* gene also appears isolated, being separated upstream from the gene *glgL* by 117 bp and downstream from *ybeW* by 83 bp. A single σ^{70} -dependent promoter has been found for this gene and has been confirmed (Petersen and Moller, 2001). A likely CRP-binding site was located upstream of the start using MatInspector (Fig 2.15a), while a potential rho-independent terminator has also been located in the downstream region of the gene (Figure 2.15b). However, no catabolite repression has been associated with this gene (Petersen and Moller, 2001); it is possible that this site may still represent a CRP-binding site that is activated or repressed in specific conditions and should be characterized further.

Escherichia coli and the closely related genus *Salmonella* differ with respect to the presence of the gene *yeiK*. This gene is actually part of a larger cluster of genes found in three *E. coli* strains and several species of *Shigella*. This gene cluster has not been found in other

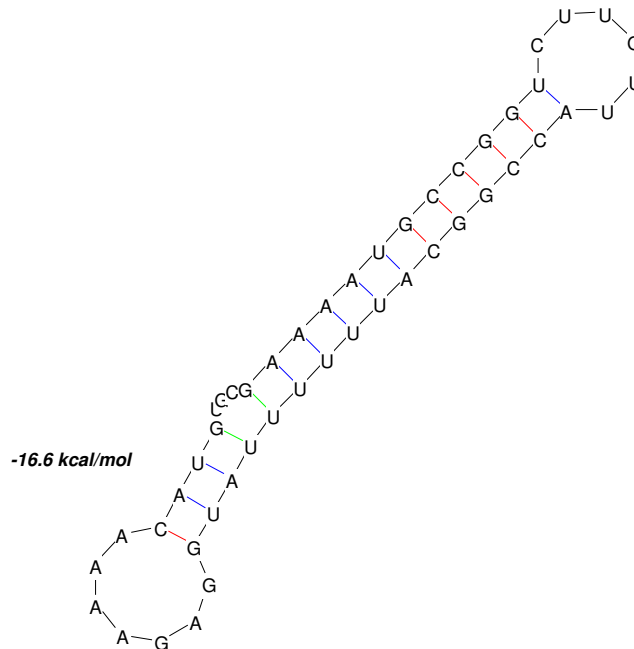
enterics, however, and may be a recent introduction in the *E. coli* genome. This cluster also includes two putative nucleoside transport proteins (*yeiM* and *yeiJ*) and a cAMP-dependent transcriptional activator related to CAP (*yeiL*), which has been recently characterized (Beck, 1995). The intergenic region between the divergently transcribed *yeiK* and *yeiL* have potential DeoR, CytR, CRP, and ArcA binding sites (Figure 2.16a; alignments in Figure 2.17). DeoR and CytR are known to play a role in the regulation of other nucleoside salvage enzymes, including all three nucleoside phosphorylases (Neuhard and Kelln, 1996). An alignment of the potential transcription factor binding sites is shown in Figure 2.16. The *E. coli* catabolite repression protein (CRP) is also needed for proper CytR gene regulation. Notably, the CRP binding site is located next to the potential CytR site; this is normally seen CytR sites (Rasmussen et al., 1996). Also, a potential Rho-independent terminator is located between *yeiK* and *yeiJ*, which encodes a potential nucleoside permease (Figure 2.16b). As the dissociation energy is quite high for this structure, it likely forms to terminate *yeiK* transcription. The gene *yeiJ*, therefore, may only be expressed in conditions which allow read-through of the terminator (antitermination). This possibility is currently being explored (C. Petersen, personal communication).

As shown for Table 2.4, the GC content and the codon adaptation index varies quite considerably for each gene. The *yaaF* gene has a much higher percentage of G+C (56.5%) than the average *E. coli* genes (~50.1%). Furthermore, the codon adaptation index (CAI), which is close to 3, indicates that this gene should be expressed at low levels, as experimentally shown. The *ybeK* and *yeiK* genes both are expected to be moderately expressed (CAI above 3.5).

Figure 2.14 – Genetic organization of *yaaF*.

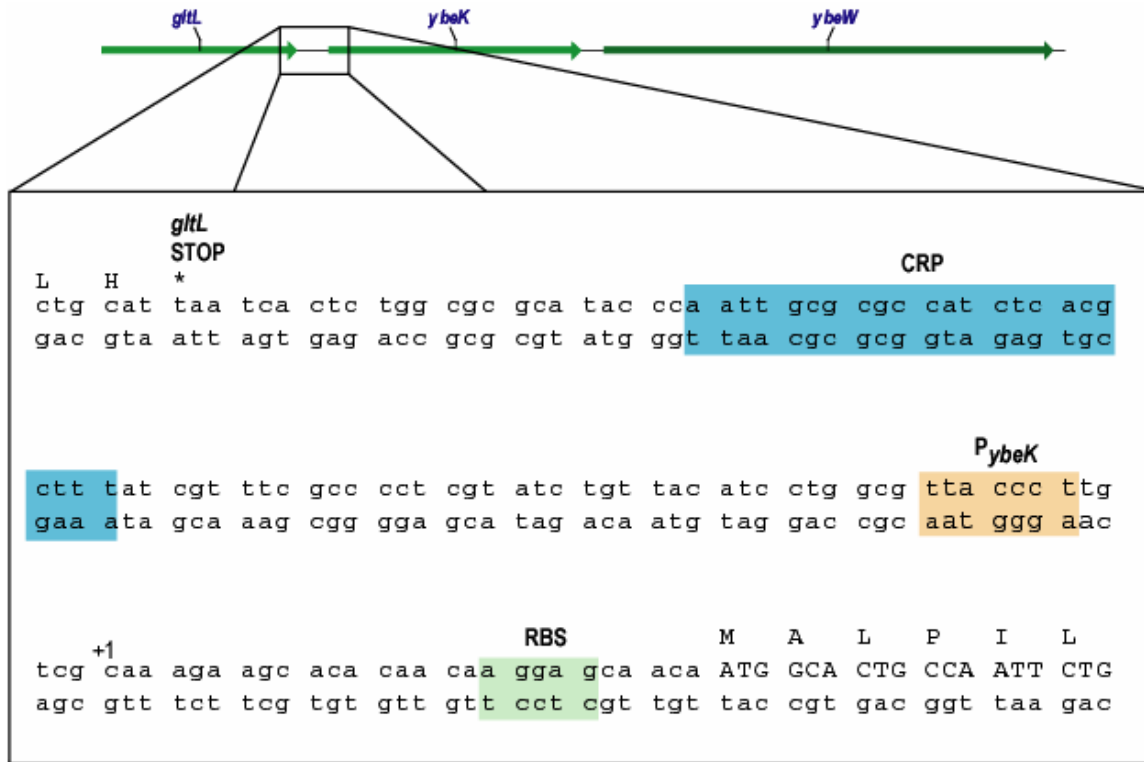


a) Upstream region of *yaaF*. The promoter, transcriptional start site, and ribosomal binding site are designated.

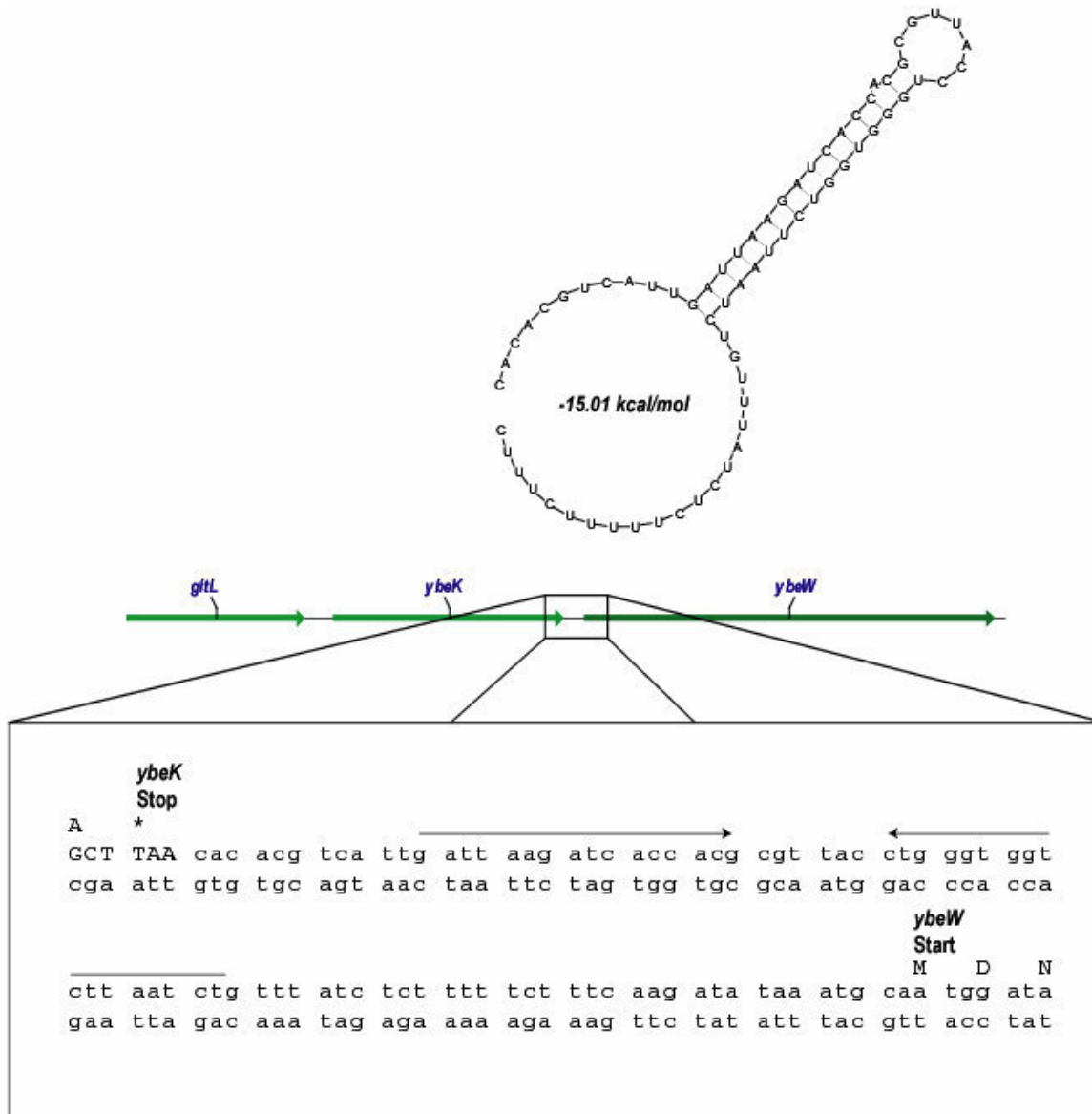


b) Putative rho-independent terminator 5' of *yaaF*.

Figure 2.15 – Genetic organization of *ybeK*.

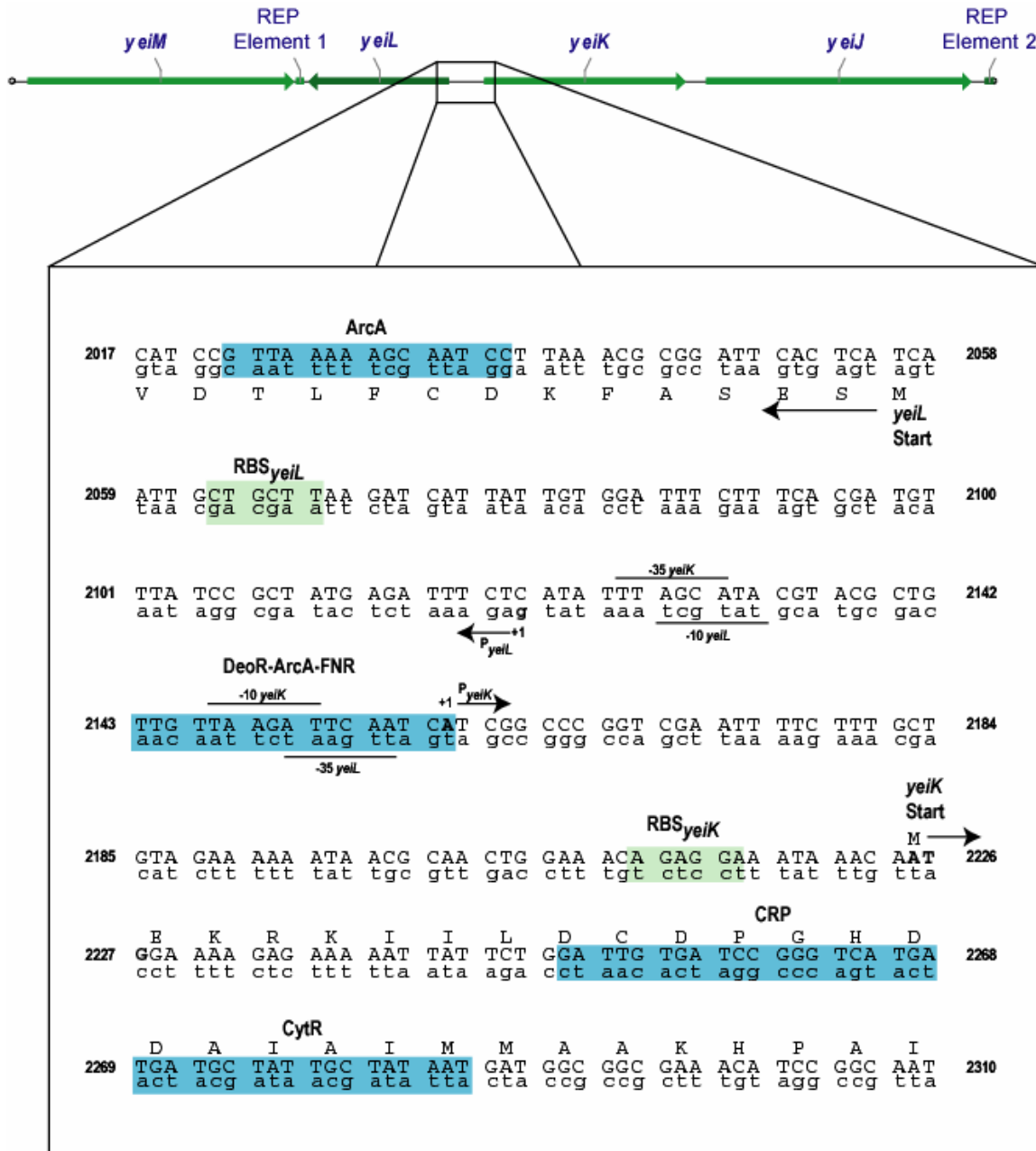


a) 5' upstream region of *ybeK*. The CRP is shown as a green box. The promoter and transcriptional start site, and ribosomal binding site are designated.

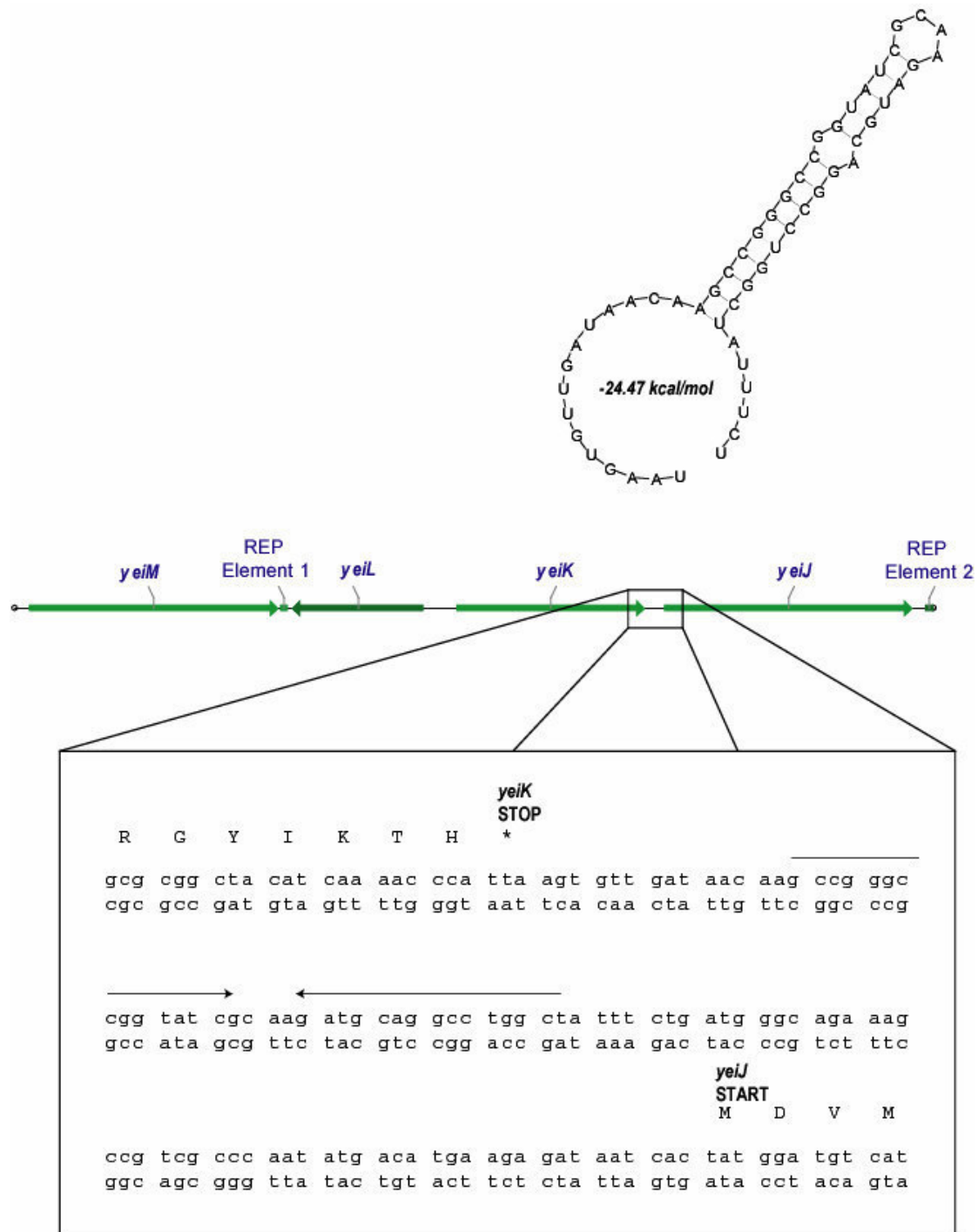


b) 3' downstream region of *ybeK*. The rho-independent transcriptional terminator 3' of the stop codon of *ybeK* is shown above the sequence.

Figure 2.16 – Genetic organization of *yeiK*.



a) Promoter region of *yeiK*. The potential CRP, ArcA, CytR, DeoR, and FNR binding sites are shown. The promoters, transcriptional start sites, and ribosomal binding sites for both *yeiL* and *yeiK* are designated.



b) Downstream terminator region of *yeiK*. Rho-independent transcriptional terminator 3' of the stop codon of *yeiK*.

Table 2.4 – Analysis of *E. coli* open reading frames

Gene	CAI	CBI	Fop	Nc	GC3s	GC
<i>ybeK</i>	0.377	0.257	0.557	46.47	0.487	51.0%
<i>yeiK</i>	0.36	0.266	0.569	50.53	0.562	52.2%
<i>yaaF</i>	0.302	0.163	0.5	52.2	0.586	56.5%

Figure 2.17 – Alignment of potential transcription factor binding sites.

a) CRP

```

yeiK      : GAT TGTGATCCGGGTCATGATG
ybeK      : AAT TGC GCGCCATCTCACGCTT
aldB      : ATT CGTGATAGCTGTCGTAAAG
ansB      : TTT TGT TACCTGCCTCTAACTT
araB1     : AAG TGTGACGCCGTGCAAATAA
araB2     : TGCC GTGATTATAGACACTTTT
cdd 1     : ATT TCGGATGCGTCGCGCATTT
cdd 2     : TAA TGA GATT CAGAT CACATAT
crp_1     : TAA TGTGACGTCCTTTGCATAC
crp_2     : GAAGG CCGACCTGGGT CATGCTG
cya       : AGG TGT TAAAT TGAT CACGTTT
cytR 1    : CGA TGC GAGCGGATCGAAAAA
cytR 2    : AAA TCA ATATTCATCACACTT
dadAX 1   : AGA TGTGAGCCAGCTCACCATA
dadAX     : AGA TGTGATTAGATTATTATTC
deoP2 1   : AAT TGTGATGTTATCGAAGTG
deoP2_2   : TTA TTTGA ACCAGATCGCATTA
fur       : AAA TGT AAGCTGTGCCACGTTT
gal       : AAG TGTGACATGGAATAAATTA
glpACB (glp : TTG TTTGATTTTCGCGCATATTC
glpACB (glp : AAACGTGATTTTCATGCGTCATT
glpACB (glp : ATG TGTGCGGAATTCACATTT
glpD      : TAA TGT TATACATATCACTCTA
glpFK 1   : TTT TATGACGAGGCACACACAT
glpFK 2   : AAG TTCGATATTTCTCGTTTTT
gut       : TTT TCGGATCAAAAATAACACTT
ilvB     : AAACGTGATCAACCCCTCAATT
lac 1     : TAA TGTGAGTTAGCTCACTCAT
lac 2     : AAT TGTGAGCGGATAACAATTT
malEpKp1  : TTG TGTGATCTCTGTTACAGAA
malEpKp2  : TAA TGTGGAGATGCGCACATAA
malEpKp3  : TTT TGC AAGCAACATCACGAAA
malEpKp4  : GACCTCGGTTTAGTTTACAGAA
malT     : AAT TGTGACACAGTGCAAAATTC
melR     : AACCGTGCTCCCACCTCGCAGTC
mtl       : TCT TGTGATT CAGATCACAAAG
nag       : TTT TGTGAGTTTTGTCCACAAA
nupG2    : AAA TGT TATCCACATCACAAAT
nupG1    : TTA TTTGCCACAGGTAACAAAA
ompA     : ATGCC T GACGGAGTT CACACTT
ompR     : TAACGTGATCATATCAACAGAA
ptsH A   : TTT TGTGGCTTGCTTCAAACCTT
ptsH B   : TTT TATGATTTGGTTCAATTCT
rhaS     : AAT TGTGAACATCATCACGTTTC
rot 1    : TTT TGTGATCTGTTTAAATGTT
rot 2    : AGAGGTGATTTTGTACACGGAA
tdcA     : ATT TGTGAGTGGTCGCACATAT
tnaL     : GAT TGTGATTCGATTCACATTT
tsx 2    : GTG TGTAAAACGTGAACGCAATC
tsx 1    : AAC TGTGAACGAAACATATTT
uxuAB    : TCT TGTGATGTGGTTAACCAAT
          tgtga      c
    
```

b) ArcA

```

yeiL1     : GTTAAAA GCAATCC
yeiK-L    : GTTAAGATTCAATCA
icd       : GTTAATGTTTGTAA
aldA      : GTTAATTTACATCAA
sodA      : GTTAATTTAATGATA
lctP      : GTTAACTAATGTTA
glcC      : GTTAACTCAATGTTA
cydA1     : GTTAATTTAATATA
cydA1_2   : GTTAACTAATGTTA
cydA2     : GTTAATCATGTTTCA
cydA3     : GTTAATAAAAACCTCA
pflA2     : GTTAATTTAAAAGGA
traY      : GTTAAGTAAATGTTA
lpdA      : GTTAACAATTTTTTAA
gltA/sdhC2 : GTTAATTGTAATGAT
gltA/sdhC2 : GTTCA CA AATCATT
          GTTaa a a
    
```

C) DeoR

```

yeiK-yeiL : TGT TAAGAT TCAATCA
deoC-1    : TGT TAGAAT TCTAACA
deoC-2    : TGT TAGAAT ACTAACA
deoC-OE   : TGT GAAAAT TTTATCA
          TGTtA aATtctA CA
    
```

D) CytR

```

yeiK      : T GAT GCT ATT GCT AT AAT
cdd-1     : T G T T C A C G C G T T G C A T A
cytR      : T C A T G A A A A T T C T G T A A C
deoP-1    : T G A T G C A A A C T T G T A A G T
tsx       : T G A T A G A A C T G T G A A A C G
udp       : T T A T G C A A C G C A T T T G C G
          T a T aa a
    
```

Conclusions

Three genes for nucleoside hydrolases have been identified in *E. coli* and confirmed by enzyme analysis. Two of the genes (*ybeK* and *yeiK*) encode pyrimidine-preferring nucleoside hydrolases, while the third gene (*yaaF*) encodes a relatively nonspecific nucleoside hydrolase. A recent report (Petersen and Moller, 2001), which confirmed these results, has also shown that the NHs encoded by these genes do not cleave deoxyribonucleosides. Furthermore, deletion of these genes does not cause a detectable phenotype in normally growing *E. coli* cells. It is not currently understood why *E. coli* contains three nucleoside hydrolases for activity, especially knowing that one (YaaF) is capable of cleaving both purine and pyrimidine nucleosides. However, several potential hints now exist as to how at least two of the genes may be controlled which could explain their physiological relevance. Petersen and Moller (Petersen and Moller, 2001) reported that the *yaaF* gene appears to be catabolite-repressed when grown using glucose as a carbon source, regardless of the absence of a CRP-like binding site in the promoter region of the gene. This is corroborated by analysis using a luciferase-based DNA microarray (Van Dyk et al., 2001), which indicates that *yaaF* expression increased approximately 8-fold in conditions in which nalidixic acid was added. This suggests that the *yaaF* gene product may be regulated by a novel mechanism involving DNA supercoiling. Also using a DNA microarray, another study (DeLisa et al., 2001) has identified approximately 242 *E. coli* genes which are induced or repressed in the presence of autoinducer 2 (AI-2), currently an uncharacterized molecule important for *E. coli* quorum sensing. The *yeiK* gene, encoding a pyrimidine-preferring NH, was one of the most induced genes, with a 25.4-fold increase in expression. This could be directly related to the intergenic region, described above, which *yeiL* and *yeiK* share. A recent study (Anjum et al., 2000) has indicated that the *yeiL* gene, upstream of *yeiK* and which encodes a

CRP/FNR homologue, is regulated by a mechanism that involves aerobic and anaerobic control. The present study has located several more potential binding sites in this region, including several for integration host factor (IHF), the leucine response protein (Lrp), and the anaerobic regulator FNR (Figure 2.16a). It is worth noting that the DeoR, ArcA, and FNR sites all overlap the -10 and -35 regions of *yeiL* and *yeiK* and that ArcA and FNR are both involved in the regulation of genes involved in anaerobic cell growth (Gunsalus and Park, 1994). Furthermore, the finding (Anjum et al., 2000) that the *yeiL* gene seems to be activated in a stage during cell death in nitrogen-starved conditions is likely to involve some cell clustering due to higher cell densities; this could explain the induction seen for the quorum-sensing molecule AI-2 (Van Dyk et al., 2001).

The location of potential regulatory sites upstream of the *yeiK* gene is important. However, the work of Petersen and Moller (2001) found that *cytR* and *deoR* mutants did not induce or repress the expression of a *yeiK-lacZ* fusion on a plasmid. However, their experiments did not include examination of the upstream gene *yeiL* (the potential catabolite repressor, discussed above), and that the presence of multiple transcription factor binding sites in this intergenic region indicate the regulation of this gene cluster is much more complex and may rely on varying several conditions (cell growth, presence of AI-2, presence of repressing catabolites, and presence of nucleosides).

The presence of multiple nucleoside hydrolases in the *E. coli* genome easily explains why mutants for these activities have never been recovered. Multiple separate yet simultaneous mutations would need to occur in distal areas of the genome. It could also explain the lack of a mutant for the CMP glycosylase activity, which would cleave the N- β -glycosyl bond in a manner similar to these hydrolases (Figure 2.2). However, the work by Petersen and Moller (Petersen

and Moller, 2001) indicates that the three nucleoside hydrolase genes are unable to hydrolyze nucleoside monophosphates, and the knowledge about the structure of three nucleoside hydrolases (Degano et al., 1996; Shi et al., 1999; Versees et al., 2001) has led to the postulation that monophosphorylated nucleotides may not act as substrates. Although the presence of nucleoside hydrolase activity in *E. coli* is now indisputable, the physiological purpose for the presence of three nucleoside hydrolases remains a mystery.

References

- Altschul, S. F., T. L. Madden, A. A. Schaffer, J. Zhang, Z. Zhang, W. Miller, and D. J. Lipman.** 1997. Gapped BLAST and PSI-BLAST: a new generation of protein database search programs. *Nucleic Acids Res.* **25**:3389-3402.
- Anjum, M. F., J. Green, and J. R. Guest.** 2000. YeiL, the third member of the CRP-FNR family in *Escherichia coli*. *Microbiology* **146 Pt 12**:3157-3170.
- Ausubel, F. M.** 2001. *Current protocols in molecular biology*. Wiley, New York.
- Barton, G. J.** 1993. ALSCRIPT: a tool to format multiple sequence alignments. *Protein Eng.* **6**:37-40.
- Beck, D. E.** 1995. *Pyrimidine salvage enzymes in microorganisms : labyrinths of enzymatic diversity*. Ph.D. dissertation. The University of North Texas.
- Beck, D. E., Jordan, B. G., and O'Donovan, G. A.** 1996. HPLC analysis of the pyrimidine salvage enzymes, uridine hydrolase and uridine phosphorylase, in enterics. *In Abstracts of the 96th General Meeting of the American Society for Microbiology*.
- Berman, H. M., J. Westbrook, Z. Feng, G. Gilliland, T. N. Bhat, H. Weissig, I. N. Shindyalov, and P. E. Bourne.** 2000. The Protein Data Bank. *Nucleic Acids Res.* **28**:235-242.
- Blattner, F. R., G. Plunkett, III, C. A. Bloch, N. T. Perna, V. Burland, M. Riley, J. Collado-Vides, J. D. Glasner, C. K. Rode, G. F. Mayhew, J. Gregor, N. W. Davis, H. A.**

- Kirkpatrick, M. A. Goeden, D. J. Rose, B. Mau, and Y. Shao.** 1997. The complete genome sequence of *Escherichia coli* K-12. *Science* **277**:1453-1474.
- Bradford, M. M.** 1976. A rapid and sensitive method for the quantitation of microgram quantities of protein utilizing the principle of protein-dye binding. *Anal.Biochem.* **72**:248-254.
- Chung, C. T., S. L. Niemela, and R. H. Miller.** 1989. One-step preparation of competent *Escherichia coli*: transformation and storage of bacterial cells in the same solution. *Proc.Natl.Acad.Sci.U.S.A.* **86**:2172-2175.
- Degano, M., D. N. Gopaul, G. Scapin, V. L. Schramm, and J. C. Sacchettini.** 1996. Three-dimensional structure of the inosine-uridine nucleoside N- ribohydrolase from *Crithidia fasciculata*. *Biochemistry* **35**:5971-5981.
- DeLisa, M. P., C. F. Wu, L. Wang, J. J. Valdes, and W. E. Bentley.** 2001. DNA microarray-based identification of genes controlled by autoinducer 2-stimulated quorum sensing in *Escherichia coli*. *J.Bacteriol.* **183**:5239-5247.
- Fields, C. J., Beck, D. E., and O'Donovan, G. A.** 2000. Nucleoside hydrolases in *Escherichia coli* and *Pseudomonas aeruginosa*. In Abstracts of the 100th Annual Meeting of the American Society for Microbiology.
- Guex, N. and M. C. Peitsch.** 1997. SWISS-MODEL and the Swiss-PdbViewer: an environment for comparative protein modeling. *Electrophoresis* **18**:2714-2723.

- Gunsalus, R. P. and S. J. Park.** 1994. Aerobic-anaerobic gene regulation in *Escherichia coli*: control by the ArcAB and Fnr regulons. Res.Microbiol. **145**:437-450.
- Hanahan, D., J. Jessee, and F. R. Bloom.** 1991. Plasmid transformation of *Escherichia coli* and other bacteria. Methods Enzymol. **204**:63-113.
- Humphrey, W., A. Dalke, and K. Schulten.** 1996. VMD: visual molecular dynamics. J Mol.Graph. **14**:33-38.
- Jeanmougin, F., J. D. Thompson, M. Gouy, D. G. Higgins, and T. J. Gibson.** 1998. Multiple sequence alignment with Clustal X. Trends Biochem.Sci. **23**:403-405.
- Mathews, D. H., J. Sabina, M. Zuker, and D. H. Turner.** 1999. Expanded sequence dependence of thermodynamic parameters improves prediction of RNA secondary structure. J.Mol.Biol. **288**:911-940.
- Matzura, O. and A. Wennborg.** 1996. RNAdraw: an integrated program for RNA secondary structure calculation and analysis under 32-bit Microsoft Windows™. Comput.Appl.Biosci. **12**:247-249.
- McGuire, A. M., J. D. Hughes, and G. M. Church.** 2000. Conservation of DNA regulatory motifs and discovery of new motifs in microbial genomes. Genome Res. **10**:744-757.
- Neuhard, J.** 1983. Utilization of preformed pyrimidine bases and nucleosides, p. 95-148. In A. Munch-Peterson (ed.), Metabolism of Nucleotides, Nucleosides, and Nucleobases in Microorganisms. Academic Press, London.

- Neuhard, J. and R. A. Kelln.** 1996. Biosynthesis and conversion of pyrimidines, p. 580-599. *In* F. Neidhardt and R. Curtiss (eds.), *Escherichia coli* and *Salmonella*. American Society for Microbiology, Washington D.C.
- O'Donovan, G. A. and M. S. Shanley.** 1995. Pyrimidine metabolism in *Pseudomonas*. *Paths Pyr.:An Int'l Nwsltr.* **3**:49-59.
- Parkin, D. W., B. A. Horenstein, D. R. Abdulah, B. Estupinan, and V. L. Schramm.** 1991. Nucleoside hydrolase from *Crithidia fasciculata*. Metabolic role, purification, specificity, and kinetic mechanism. *J.Biol.Chem.* **266**:20658-20665.
- Pellé, R., V. L. Schramm, and D. W. Parkin.** 1998. Molecular cloning and expression of a purine-specific N-ribohydrolase from *Trypanosoma brucei brucei*. Sequence, expression, and molecular analysis. *J.Biol.Chem.* **273**:2118-2126.
- Petersen, C. and L. B. Moller.** 2001. The RihA, RihB, and RihC ribonucleoside hydrolases of *Escherichia coli*. Substrate specificity, gene expression, and regulation. *J.Biol.Chem.* **276**:884-894.
- Rasmussen, P. B., B. Holst, and P. Valentin-Hansen.** 1996. Dual-function regulators: the cAMP receptor protein and the CytR regulator can act either to repress or to activate transcription depending on the context. *Proc.Natl.Acad.Sci.U.S.A.* **93**:10151-10155.
- Rice, P., I. Longden, and A. Bleasby.** 2000. EMBOSS: the European Molecular Biology Open Software Suite. *Trends Genet.* **16**:276-277.

- Rost, B., C. Sander, and R. Schneider.** 1994. PHD - an automatic mail server for protein secondary structure prediction. *Comput.Appl.Biosci.* **10**:53-60.
- Sakai, T. and S. Omata.** 1976. Distribution of enzymes related to cytidine degradation in bacteria. *Agric.Biol.Chem.* **40**:1893-1895.
- Sharp, P. M. and G. Matassi.** 1994. Codon usage and genome evolution. *Curr.Opin.Genet.Dev.* **4**:851-860.
- Shi, W., V. L. Schramm, and S. C. Almo.** 1999. Nucleoside hydrolase from *Leishmania major*. Cloning, expression, catalytic properties, transition state inhibitors, and the 2.5-Å crystal structure. *J.Biol.Chem.* **274**:21114-21120.
- Terada, M., M. Tatibana, and O. Hayaishi.** 1967. Purification and properties of nucleoside hydrolase from *Pseudomonas fluorescens*. *J.Biol.Chem.* **242**:5578-5585.
- Van Dyk, T. K., E. J. DeRose, and G. E. Gonye.** 2001. LuxArray, a high-density, genomewide transcription analysis of *Escherichia coli* using bioluminescent reporter strains. *J.Bacteriol.* **183**:5496-5505.
- Versees, W., K. Decanniere, R. Pelle, J. Depoorter, E. Brosens, D. W. Parkin, and J. Steyaert.** 2001. Structure and function of a novel purine specific nucleoside hydrolase from *Trypanosoma vivax*. *J.Mol.Biol.* **307**:1363-1379.
- Vogels, G. D. and C. Van der Drift.** 1976. Degradation of purines and pyrimidines by microorganisms. *Bacteriol.Rev.* **40**:403-468.

Werner, T. 2000. Computer-assisted analysis of transcription control regions. Matinspector and other programs. *Methods Mol.Biol.* **132**:337-349.

West, T. P. 1988. Metabolism of pyrimidine bases and nucleosides by *Pseudomonas fluorescens* biotype F. *Microbios* **56**:27-36.

CHAPTER 3

CLONING AND CHARACTERIZATION OF *nuh* ENCODING NUCLEOSIDE HYDROLASE IN *Pseudomonas aeruginosa* PAO1 AND *Pseudomonas fluorescens* Pf0-1

Introduction

The enzyme nucleoside hydrolase (NH) is involved in the initial steps of nucleoside catabolism by catalyzing the hydrolytic cleavage of the β -N-glycosyl bond (Chapter 2, Fig. 2.2) to release a free base and ribose. These compounds can be further converted into carbon and nitrogen sources for the organism. NHs are classified based upon the specificity of the enzyme for purine or pyrimidine ribonucleosides, although some rare NHs are able to catalyze the reaction with deoxyribonucleosides (Cui et al., 2001). The gene encoding NH was first cloned and sequenced from parasitic protozoa (Parkin et al., 1991, Gopaul et al., 1996). More recently, several NHs have been characterized from bacteria, including *E. coli* (Lee, 1991; Beck, 1995; Petersen and Moller, 2001) and *Ochrobactrum anthropi* (Ogawa et al., 2001). All of the characterized NHs so far have mixed substrate specificities, either utilizing only purines, only pyrimidines, or a mix of purines and pyrimidines.

The pyrimidine salvage pathway differs substantially between *E. coli* and *Pseudomonas* (Figure 3.1). Most of the key *E. coli* salvage enzymes are not present, including all nucleoside phosphorylases, nucleoside kinases, and cytidine deaminase (West and Chu, 1986; West, 1988; Beck, 1995; West, 1996); one exception recently found (Beck, 1995) is the presence of uridine phosphorylase activity in *Pseudomonas putida* PRS1. Despite the lack of many salvage enzymes, some nucleoside and base conversions still occur. Significant among these is the

presence of a single nucleoside hydrolase. This enzyme has been characterized previously in *Pseudomonas aeruginosa* (Lee, 1991; Beck, 1995; West, 1996) and *P. fluorescens* (Terada et al., 1967; West, 1988).

In this chapter, I discuss the cloning and characterization of the NHs from *P. aeruginosa* PAO1 and *P. fluorescens* Pf0-1. Although the primary amino acid sequences are 84% similar and encode nonspecific nucleoside hydrolases, the *nuh* gene for each organism differs in its genetic organization and enzyme induction. Here, I show that NHs for both *Pseudomonas* species are localized in the periplasmic space. I also examine possible physiological explanations for the presence of a periplasmic nucleoside hydrolase.

Materials and Methods

Abbreviations used

Abbreviations are listed in Table 3.1.

Bacterial strains and media

Bacterial strains, plasmids, and primers are listed in Table 3.2. *P. aeruginosa* and *P. fluorescens* were grown in 50 ml batch cultures for all experiments determining substrate specificity, enzyme induction, and cellular localization. Cells were grown in a modified basal salts medium (PC, containing 67 mM KH_2PO_4 , 42 mM NaOH, 2 mM $\text{MgSO}_4 \cdot 7\text{H}_2\text{O}$, 180 μM $\text{FeSO}_4 \cdot 7\text{H}_2\text{O}$, and 100 μM $\text{CaCl}_2 \cdot 2\text{H}_2\text{O}$; the last three components were added after autoclaving from a 200x stock solution in 2% hydrochloric acid, referred to as R-salts) (Kunz et al., 1998). The medium contained 20 mM of a carbon source (glucose, succinate, or ribose, where specified) and 20 mM $(\text{NH}_4)_2\text{SO}_4$. PNC medium is PC medium with the ammonium sulfate

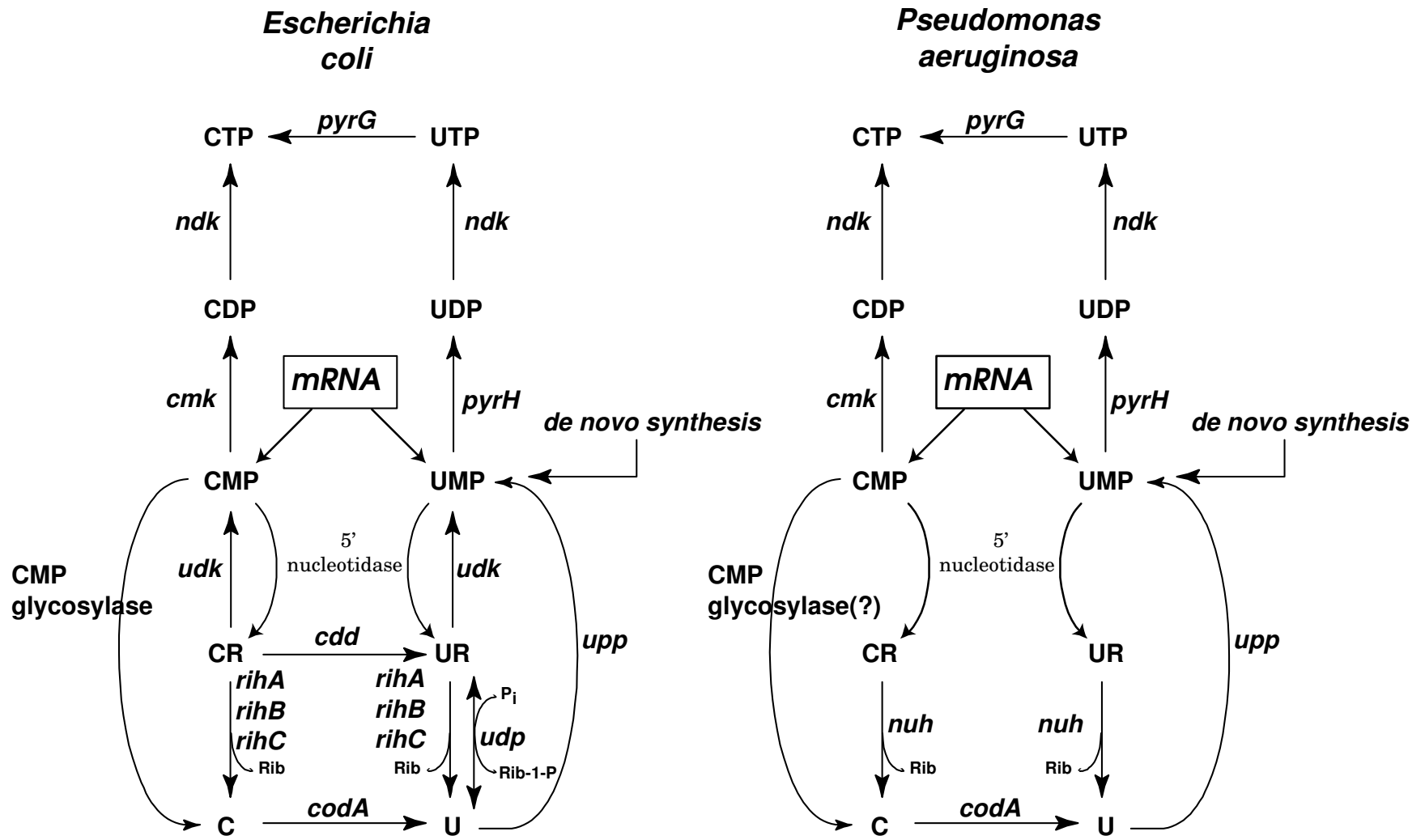


Figure 3.1 – Pyrimidine salvage circuits of *E. coli* and *Pseudomonas aeruginosa*.

Table 3.1 – List of abbreviations.

<u>Abbreviation</u>	<u>Full Name</u>
A	Adenine
AR	Adenosine
ATP	adenosine 5'-triphosphate
bp	base pair
C	Cytosine
CAA	N-carbamoyl aspartate (carbamoyl aspartic acid)
CDP	cytidine 5'-diphosphate
CMP	cytidine 5'-monophosphate
CR	Cytidine
CTAB	cetyltrimethylammonium bromide
CTP	cytidine 5'-triphosphate
dC	2'-deoxycytidine
dCDP	2'-deoxycytidine 5'-diphosphate
dCMP	2'-deoxycytidine 5'-monophosphate
dCTP	2'-deoxycytidine 5'-triphosphate
ddH₂O	distilled deionized water
DHOA	dihydroorotate (dihydroorotic acid)
DNA	deoxyribonucleic acid

<u>Abbreviation</u>	<u>Full Name</u>
dT	2'-deoxythymidine
dTDP	2'-deoxythymidine 5'-diphosphate
dTMP	2'-deoxythymidine 5'-monophosphate
DTT	Dithiothreitol
dTTP	deoxythymidine 5'-triphosphate
dU	deoxyuridine
dUMP	deoxyuridine 5'-triphosphate
dUTP	deoxyuridine 5'-triphosphate
EDTA	ethylenediaminetetraacetic acid
G	Guanine
Gln	Glutamine
GR	Guanosine
HCO₃⁻	bicarbonate
HEPES	N-2-hydroxyethylpiperazine-N'-2-ethansulfonic acid
Hx	hypoxanthine
HxR	Inosine
IAGNH	inosine-adenosine-guanosine preferring nucleoside hydrolase
IPTG	isopropyl-B-D-galactoside
IUNH	inosine-uridine preferring nucleoside hydrolase

<u>Abbreviation</u>	<u>Full Name</u>
kb	kilobase pairs
kDa	Kilodalton
LB	Luria-Bertani media, composed of 10g tryptone, 5g yeast extract, 5 g NaCl
MES	2-(N-morpholino)-ethanesulfonic acid
NDP	Nucleoside 5'-diphosphate
NH	Nucleoside hydrolase
NMP	Nucleoside 5'-monophosphate
NTP	Nucleoside 5'-triphosphate
OA	Orotate (orotic acid)
OMP	Orotidine 5'-monophosphate
PCR	Polymerase chain reaction
<i>Pfu</i>	<i>Pyrococcus furiosus</i>
RNA	ribonucleic acid
SDS	sodium dodecylsulfate
T	Thymine
TE	10 mM Tris-HCl-1 mM EDTA, pH 8.0
Tris	tris(hydroxymethyl)aminomethane
TSS	Transformation and Storage Solution
U	Uracil

<u>Abbreviation</u>	<u>Full Name</u>
UDP	uridine 5'-diphosphate
UMP	uridine 5'-monophosphate
UR	Uridine
UTP	uridine 5'-triphosphate

Table 3.2: Strains, plasmids, and primers

<i>E. coli</i> Strains		
TOP10F'	F' <i>{lacIq Tn10 (TetR)} mcrA .(mrr-hsdRMS-mcrBC) Φ80lacZΔM15 lacX74 deoR recA1 araD139 (ara-leu)7697 galU galK rpsL (Str^R) endA1 nupG</i>	Invitrogen
<i>Pseudomonas</i> Strains		
<i>P. aeruginosa</i> PAO1	Wild-type	PSGS*
<i>P. fluorescens</i> Pf0-1	Wild-type, environmental isolate	Casaz et al., 2001
Plasmids		
pZeRO2.1	KanR cloning vector with <i>lacZ-ccdA</i> fusion	Invitrogen
pCJF5	pZeRO2.1 with <i>P. aeruginosa nuh</i> PCR fragment in <i>HindIII/SpeI</i> site in orientation with the <i>P_{lac}</i> promoter	This study
pCJF7	pZeRO2.1 with <i>P. fluorescens nuh</i> PCR fragment in <i>HindIII/XbaI</i> site in orientation with the <i>P_{lac}</i> promoter	This study
Primers		
<i>Panuh</i> -for	CCCCCAAGCTTCCAGGCCCTGTACCTGCAAC	
<i>Panuh</i> -rev	GGACTAGTGCGGAAACTCTATCTGGCCG	
<i>Pfnuh</i> -for	CCCAAGCTTGCAAAACCGAGGACGAGG	
<i>Pfnuh</i> -rev	GCTCTAGAAAATATAAGCAATCCCGCCC	

**Pseudomonas* Genetic Stock Center

added to a final concentration of 20 mM before autoclaving. All samples grown for experiments were performed in triplicate.

Enzyme repression and induction experiments used the following conditions. For detection of catabolite repression or ribose regulation, cells were grown in PNC medium containing 20 mM of glucose, ribose, or succinate, where appropriate. For determination of enzyme induction using free nucleic acids and nucleosides, cells were grown in PNC medium containing 20 mM glucose, 20 mM $(\text{NH}_4)_2\text{SO}_4$, and 1 mM of the compound of interest (nucleoside or base). Guanine induction was not tested as it posed problems due to its low solubility and high acidity after addition to solution. All samples were grown to 100 Klett Units (KU) using a #54 green filter.

Starvation experiments were conducted as follows. For glucose starvation, cells were grown in PNC to 100 Klett units in a 50 ml Klett flask. The cells were aseptically pelleted at 12,000 x g, and resuspended in 50 ml of PC medium containing 20 mM $(\text{NH}_4)_2\text{SO}_4$ and 0.1 mM glucose. The cells were allowed to grow for a 24 hour period after which they were harvested, sonicated, and assayed as detailed below. For nitrogen starvation, cells were initially grown and harvested as described above for glucose starvation. The cells were resuspended in PC medium containing 20 mM glucose and 0.1 mM $(\text{NH}_4)_2\text{SO}_4$. The cells were allowed to grow for 24 hours, after which they were harvested, as above, and sonicated.

Determination of cellular localization

For the determination of enzyme localization, cells were grown in Tris-buffered medium (T medium, consisting of 50 mM Tris-HCl pH 7.3, with 1x final concentration of R-salts) (Harold, 1963). The following were added for growth: 0.3 mM potassium phosphate buffer (pH

7.0), 20 mM glucose, 1 mM uridine, and 20 mM (NH₄)₂SO₄ (final concentration). This medium was chosen in order to facilitate detection of alkaline phosphatase and phospholipase C, both periplasmic enzyme markers (Poole and Hancock, 1984). Cells were grown to 100 Klett units and processed as follows. Cells were pelleted at 12,000 x g and the resulting supernatant was saved for future assays (this fraction was designated SM, for “spent medium”). Pelleted cells were treated using 2 ml of a modified sphaeroblasting solution (0.2 M CaCl₂, 50 mM Tris-HCl, pH 8.0) in order to release the periplasmic contents (Poole and Hancock, 1984). After gently resuspending the pellet, the resulting mix was added to a shaker bath at 30 °C. After 15 minutes, the cells were added to a 4°C ice bucket for an additional 15 minutes. This cycling step was repeated twice between 30°C and 4°C (15 minutes at each temperature) in order to heat-shock proteins in the outer membrane. After pelleting the cells, the supernatant was saved and designated fraction P1. The pelleted cells were resuspended in 2 ml sphaeroblasting solution and the above extraction procedure was repeated once more. The resulting supernatant was designated fraction P2. Cells were pelleted, resuspended in 50 mM Tris-HCl (pH 7.5) with 10 µM CaCl₂, and sonicated. The resulting cell suspension was centrifuged at 10000 x g for 15 minutes, the supernatant was removed and designated CX, for “cell extract,” and the pellet was resuspended in 50 mM Tris-HCl (pH 7.5), 0.1% Triton X-100. This final fraction was designated CM, for “cell membrane.” All samples were prepared at least three times for assay.

Cloning and sequence determination

Pseudomonas aeruginosa PAO1 and *P. fluorescens* Pf0-1 DNA were prepared exactly as detailed in Chapter 2. A strategy similar to that used for cloning the *E. coli* NH genes was

utilized in order to clone the two *Pseudomonas nuh* genes. However, some slight modifications were included in order to force-directionally ligate the genes into the multiple cloning site.

Primers were designed by using the program Prophet™ (ver. 5.0, BBN Systems and Technologies, Inc., Cambridge, MA) to pick five pairs of optimal primers, using the same conditions set forth to pick the primers for *E. coli*, ($T_m=60^\circ\text{C}$, G+C=50%, GC-clamp at 3' end). However, a larger region (500 bp 5' and 3' of the ORF) was amplified in order incorporate any potential promoter region. The primers used for amplifying the *P. aeruginosa* and *P. fluorescens nuh* gene are listed in Table 3.1. Extensions incorporating restriction sites were included in the 5' end of the optimal forward (*Hind*III) and reverse (*Spe*I) primers calculated by Prophet 5.0™. *Pseudomonas aeruginosa nuh* was amplified by PCR using the following parameters: 95°C chromosomal DNA melting (1 minute), 60°C annealing (45 sec), 72°C extension (4 minutes, 15 seconds) for 16 cycles; then 14 cycles utilizing the previous parameters with a 1°C lower annealing temperature and 20 seconds longer extension time. The PCR was allowed to proceed after all 30 cycles with a 10 minute cleanup step at 72°C , after which it was analyzed on a 1% agarose gel. *P. aeruginosa nuh* amplified PCR products (Figure 3.2) and pZeRO2.1 were digested using *Hind*III and *Spe*I and electrophoresed using 1x TAE in a 0.8% gel for 1.5 hours. The resulting bands were purified as described before (Chapter 2) and cloned into *Hind*III/*Spe*I-cut pZeRO2.1 (Fig 3.3). Transformants in TOP10F' were selected based on conditions described in Chapter 2.

The primers for the *nuh* gene of *P. fluorescens* were designed with a similar strategy in mind (Table 3.1). The forward and reverse primers were extended to include cut sites for *Hind*III (Pfnuh-for) and *Xba*I (Pfnuh-rev). The *P. fluorescens nuh* gene was amplified similarly but using the following changes in conditions: 95°C chromosomal DNA melting (1 minute),

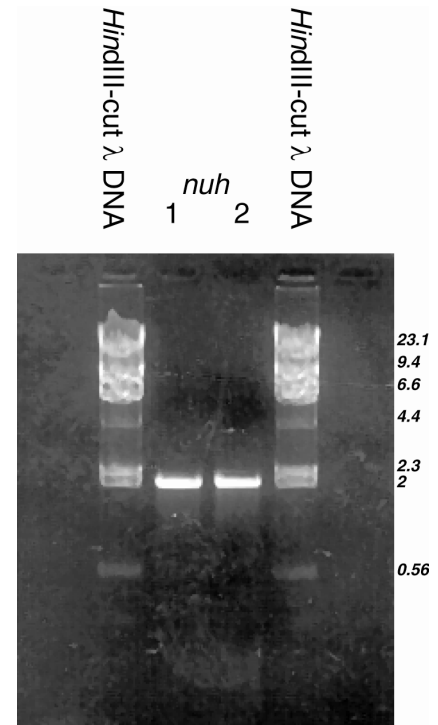


Figure 3.2 - *Pseudomonas aeruginosa* PAO1 PCR reactions.

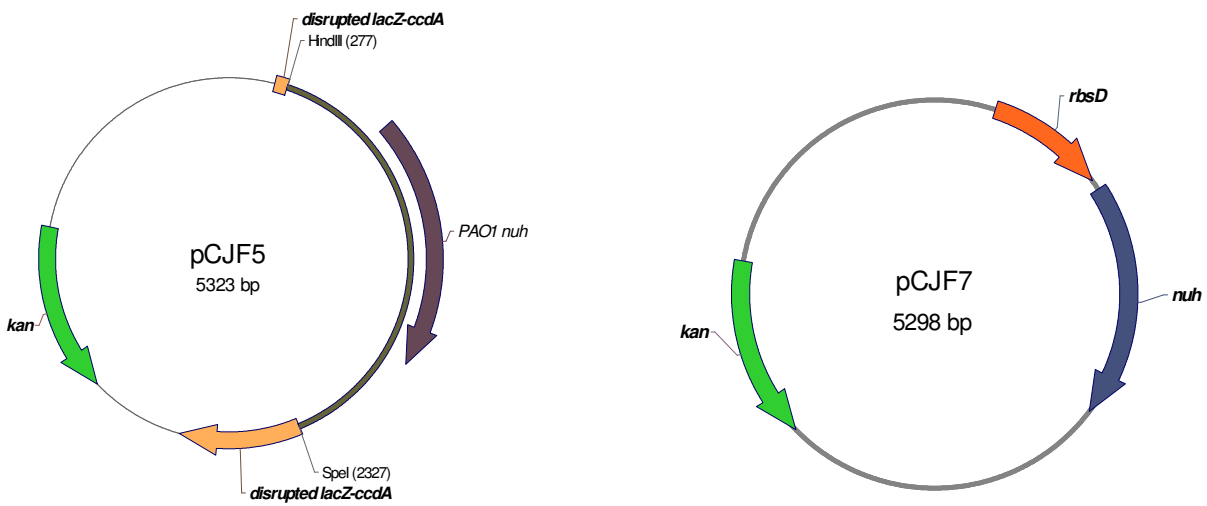


Figure 3.3 – Plasmid maps

59°C annealing (45 seconds), 72°C extension (4 minutes, 30 seconds) for 16 cycles; then 14 cycles utilizing the previous parameters with a 2°C lower annealing temperature and 15 seconds longer extension time. The PCR was allowed to proceed after all 30 cycles with a 10 minute cleanup step at 72°C, after which it was analyzed on a 1% agarose gel. The resulting PCR product was digested, gel-purified using the technique described above and in Chapter 2, and ligated into *HindIII/XbaI*-cut pZeRO2.1 (Figure 3.3). The rest of the transformation procedure is as described previously (Chapter 2).

Nucleoside hydrolase enzyme assay

Each *Pseudomonas nuh* gene was transformed into *E. coli* strain TOP10F'. The transformants were grown in 2 L of LB broth with 50 µg kanamycin per ml. At an OD₆₀₀ of 0.6, IPTG was added to a final concentration of 125 µM. Induction of the cloned genes was allowed to proceed for 6 hours. Cells were pelleted at 10,000 x g, resuspended in breaking buffer (50 mM HEPES pH 7.3, 0.1 mM DTT, 0.1 mM EDTA) at a concentration of one gram wet weight of cells per ml and sonicated twice (2 minutes apiece) using a Branson Cell Disrupter™ 200 (with a duty cycle setting of 0.2-0.3 at 50% (pulse). Cell debris was pelleted at 25,000 x g, and the cell-free extract was removed to a new tube and assayed directly. Nucleoside hydrolase activity was detected using a modification of the reducing sugar assay (Parkin et al., 1991) using a final volume of 100 µl. Final reaction conditions were 50 mM HEPES (pH 7.5), 5 mM nucleoside (except guanosine, which was 2 mM final). Reactions were initiated with the addition of 10 µl of cell extract and allowed to proceed for 20 minutes. A background blank was run for each clone by using 10 µl of cell extract in 50 mM HEPES, pH 7.3 (100 µl total). Reactions were stopped by the addition of 100 µl of 0.1 M ZnSO₄, equilibrated using 100 µl of 0.1 M NaOH, and

centrifuged at 14,000 x g for 5 minutes to remove precipitated proteins. 75 µl of each reaction supernatant were added in duplicate to a 96-well microtiter plate, after which 150 µl of a 1:1 mix of color mix A (4% Na₂CO₃, 1.6% glycine, 0.0045% CuSO₄•5H₂O) and B (0.12% 2,9-dimethyl-1,10-phenanthroline) was added. The microtiter plate was covered with plastic wrap and developed in a 65°C water bath for 10 minutes. Enzyme activity was determined by comparison against a D-ribose standard curve (0.01-0.16 µmoles, Figure 2.6). Protein concentrations were determined using lysozyme as a standard (Bradford, 1976).

Cells grown in minimal medium in studies on gene induction and enzyme localization were assayed as above with the following exceptions. The nucleoside hydrolase assay was conducted using 50 mM Tris-HCl pH 7.5, 10 µM CaCl₂, and 5 mM uridine in a final volume of 200 µl. The nucleoside used (uridine) was not varied per assay to maintain similar conditions throughout. Protein concentrations for enzyme induction and enzyme localization were determined using the DC™ assay (BioRad Corp., Hercules, CA; www.biorad.com) using bovine γ-globulin as a standard. An example of a DC™ assay standard curve is shown in Figure 3.4.

Aspartate transcarbamoylase assay

The enzyme aspartate transcarbamoylase (ATCase) was assayed using a modified version of the standard protocol (Prescott and Jones, 1969). In brief, three microliters of the cell-free extract for each sample was added, in triplicate, to wells in a microtiter plate. 4 µl of a tribuffer stock (1 M MES, 0.51 M N-ethylmorpholine, 0.51 M diethanolamine, pH 8; Leger and Herve, 1988) was added to each well containing the sample, and the volume was increased to 80 µl with ddH₂O. 10 µl of 200 mM L-aspartate (potassium salt) was added with a multichannel pipettor. The plate was equilibrated by gently placing on a submerged platform in a 30°C water bath and

allowed to incubate for 3 minutes. Standards (0-0.016 μmol DL-carbamoyl aspartate) were also added to empty wells in triplicate. The reaction was initiated by addition of 10 μl of 100 mM carbamoyl phosphate using a multichannel pipettor, allowing 10 second increments per row. Appropriate blanks, in which water was added instead of carbamoylphosphate, were prepared for each sample. The microtiter plate with samples was then incubated in a 37°C water bath for 20 minutes after the entire plate was covered using plate-sealing tape. The assay was stopped by the addition of the color mix, which is one part color mix A (0.8% w/v 2,3 butanedione monoxime in 5% v/v acetic acid) to two parts color mix B (1% antipyrine in 50% sulfuric acid), and the microtiter plate was covered and incubated at 65°C in the presence of light for 2.5 hours. Specific activity was calculated for each sample using the loaded standards by comparing the absorbance of the standards and the samples at an absorbance of 450 nm. An example of the carbamoyl aspartate standard curve generated is shown in Figure 3.5.

Alkaline phosphatase assay

Alkaline phosphatase was assayed using a modification of a standard protocol (Hancock, 1999) with *p*-nitrophenylphosphate (pNPP) as substrate. In brief, 10 μl sample of cell extract was added to a microtiter plate in triplicate. 40 μl of ddH₂O and 50 μl of 100 mM Tris-HCl pH 7.5 were added. The microtiter plate was placed in the preprogrammed microtiter plate reader at room temperature; at this point, 100 μl of pNPP stock solution (0.5 mg/ml pNPP in 50 mM Tris-HCl, pH 7.5) was quickly added to each well. The wells in the plate were continuously read at 405 nm to monitor the increase of *p*-nitrophenol over time. The reaction was allowed to proceed for 10 minutes. The reaction rate was determined from the linear region of the *p*-nitrophenol absorbance curve. After 10 minutes, the measurement was stopped. The plate was allowed to

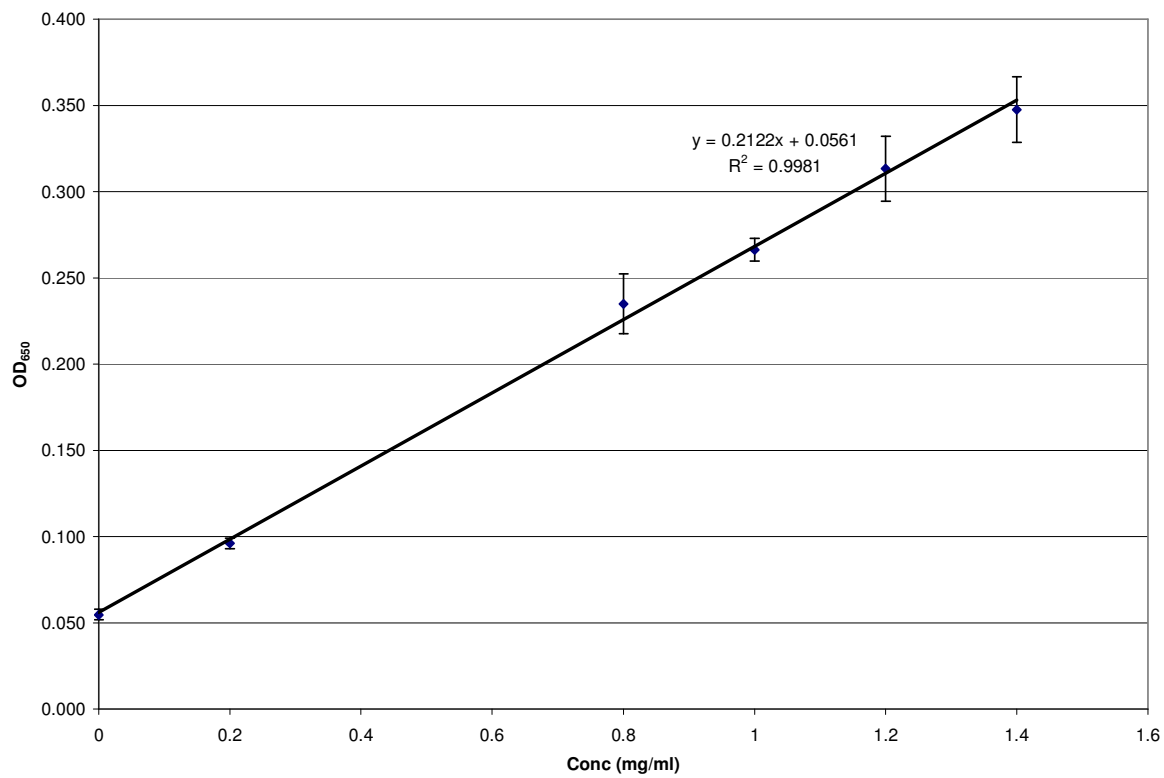


Figure 3.4 – Standards determined using the DC microtiter plate assay. Assays were performed in triplicate.

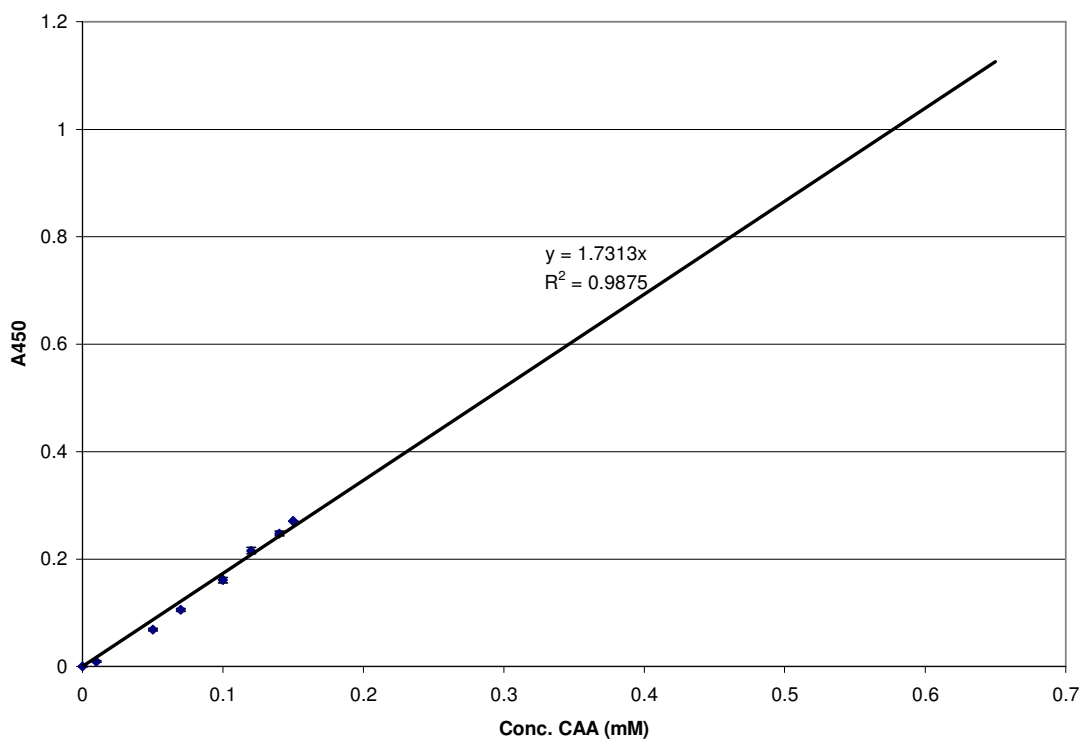


Figure 3.5 – Standards used for the determination of carbamoyl aspartate concentration. Assays were performed in triplicate.

remain in the plate reader for 30 minutes-1 hour or until absorbance reached a plateau, and a second absorbance reading was made to determine the extinction coefficient (0.38 μ moles hydrolyzed per one unit of absorbance at 405 nm). Alkaline phosphatase specific activity was calculated using the rate of hydrolysis for the sample (measured as mOD/min), multiplying by the extinction coefficient, and dividing by the protein concentration as determined by the DC assay.

Phospholipase C assay

Phospholipase C was assayed in a similar manner as for alkaline phosphatase. The assays were set up in a similar manner and volume as above; the stock solution used in this case consisted of 3 mg nitrophenylphosphorylcholine (pNPC) per ml in 0.25 M Tris-HCl pH 7.5 and 60% (v/v) glycerol. The absorbance was monitored at 405 nm. Extinction coefficients and specific activity were calculated in a similar manner as above (in this case, 0.24 μ moles formed per absorbance unit).

Software used

Sequence and primer analysis was performed using PROPHET™ (as stated above) and the EMBOSS package (Rice et al., 2000). The CloneIt server (Lindenbaum, 1998) was used to determine the optimal restriction sites for cloning the *nuh* gene from *P. aeruginosa* and *P. fluorescens*.

Matrix searches were performed using the program MatInspector (ver. 2.2, © Genomatix Software, München, Germany; Werner, 2000); the matrices were created from the sequences for all known transcription factor binding sites in *E. coli* (McGuire et al., 2000) and the few from

Pseudomonas aeruginosa PAO1 (Anderson, 1977; Charlier et al., 1988; Mohr et al., 1992; Miczak et al., 1996).

Protein localization prediction was determined using the PSORT server (Nakai and Horton, 1999) and the SignalP server (ver. 2.0; Nielsen et al., 1999). Multiple alignment of NH amino acid sequences and protein signal regions was performed using the program ClustalX (ver. 1.81; Thompson et al., 1997), using a gap penalty of 8 and a gap extension penalty of 0.1. Sequence post-processing was carried out using the Alscript packages (ver. 2.0; Barton, 1993) at the Human Genome Mapping Project Resource Center (or HGMP, funded by the Medical Research Council in the UK; www.hgmp.mrc.ac.uk). Sequences used in the alignment are: *Pseudomonas fluorescens* Pf0-1 (Joint Genome Institute), *P. putida* KT2440 (TIGR), *P. fluorescens* SBW25 (Sanger Institute), *P. syringae* (TIGR), *P. aeruginosa* (AAG03533), *Ralstonia solanoceareum* (CAD16255), *Crithidia fasciculata* (Q27546), *Leishmania major* (CAC24663), *Saccharomyces cerevisiae* (AAG44107), *Schizosaccharomyces pombe* (CAB91168), *Escherichia coli* YbeK (AAC73752), *E. coli* YeiK (AAA60514), *E. coli* YaaF (AAB40852). Alignment coloring (as seen in Figure 3.15a and b) was performed using the program GeneDoc (ver. 2.6.002; Nicholas and Nicholas, 2001).

Protein structure threading was accomplished using the Swiss-Model web server (Guex and Peitsch, 1997) using the *C. fasciculata* IUNH as a model. The protein model acquired was compared to the predicted secondary structure determined by the PHD server (Rost et al., 1994) for determining the accuracy of the multiple alignment.

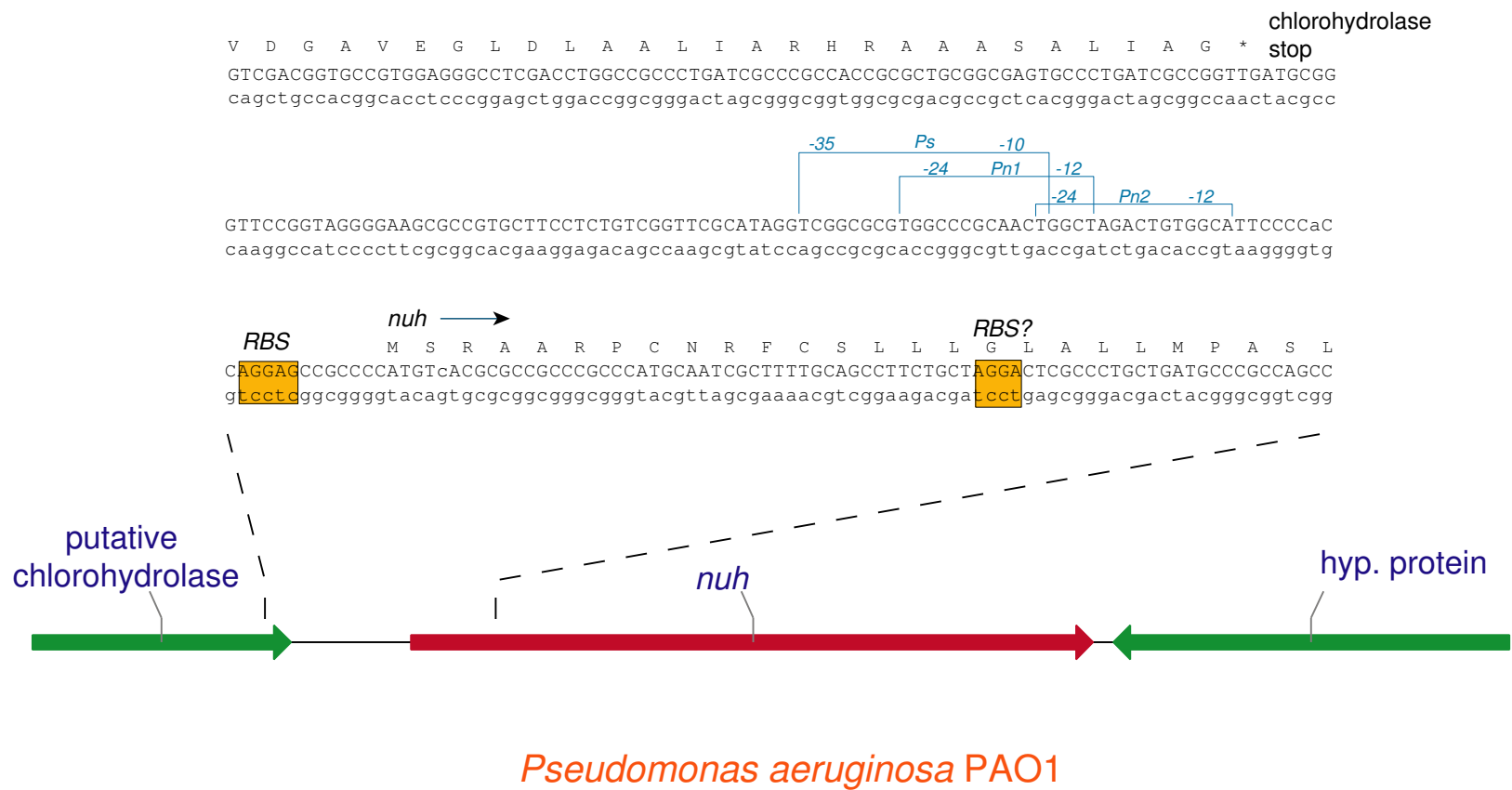
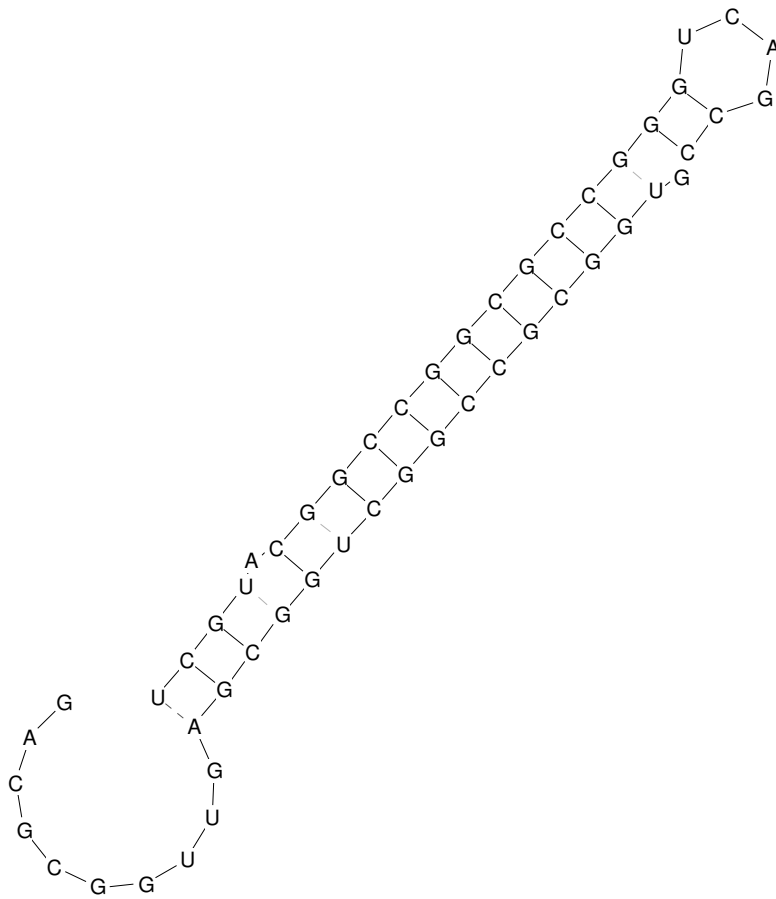


Figure 3.6 – Genetic organization of the *P. aeruginosa nuh* gene

Figure 3.7 – Potential terminator located 3' of the *nuh* gene. $\Delta G = -27.28$ kcal/mol.



Results and Discussion

Analysis of *nuh* genes in *Pseudomonas aeruginosa* and *Pseudomonas fluorescens*

The genetic organization for the *nuh* genes, as revealed by the genome sequence of *Pseudomonas aeruginosa*, is shown in Figure 3.6. During investigation into the cellular localization of the *Pseudomonas* NH, it became apparent that the *P. aeruginosa* NH was exported outside of the cytoplasm into the periplasmic space. This prompted a reanalysis of the upstream region of the gene and located two sequencing mistakes. During the annotation phase of the *P. aeruginosa* genome project, an initial start codon was placed at the far 3' end of the fragment (shown in Figure 3.6 next to the second potential RBS). This was due to the presence of a potential ribosomal-binding site, the coincident length of the ORF when compared to the *E. coli* ORFs (detailed in Chapter 2), and the lack of a second start upstream. When the final sequence was analyzed, a base change in the upstream sequence changed one codon from a TGA to a TCA and extended the sequence to the immediately preceding start codon, which has a functional ribosomal binding site. This change has since been corrected with the *Pseudomonas* genome project organizers (Fiona Brinkman and Bob Hancock, personal communication). A second correction further upstream was also made that did not affect the coding sequence. The sequence of the cloned *nuh* gene from pCJF5 also confirmed these changes.

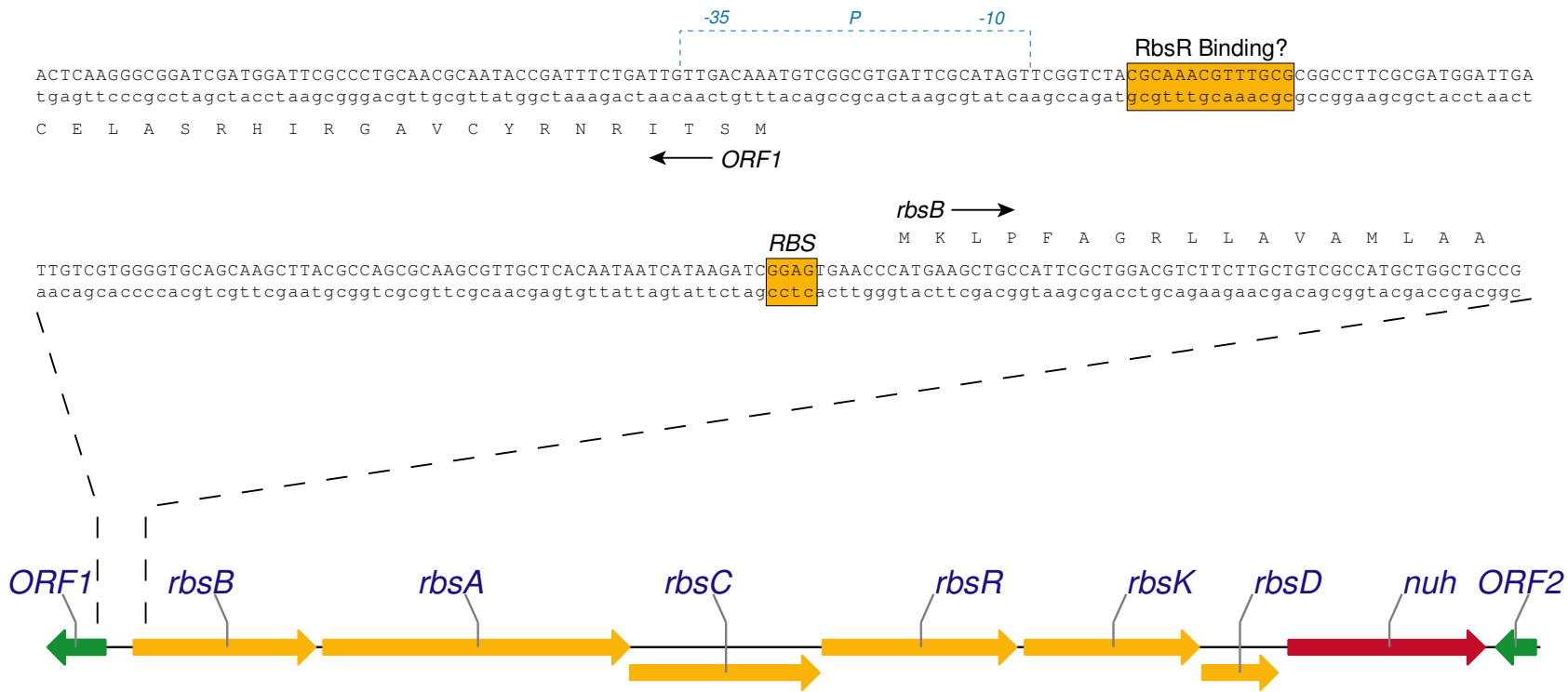
The PAO1 *nuh* gene is relatively isolated from the upstream gene (PA0142, encoding a putative chlorohydrolase) and the downstream gene (PA0144, encoding an unknown protein). A putative transcriptional terminator structure is located between *nuh* and PA0144 (Figure 3.4). Using the program MatInspector™, two potential σ^{54} promoter elements (Farinha et al., 1993; Merrick, 1993) were located approximately 30 bp upstream of the translational start. An alignment against known σ^{54} promoters is shown in Figure 3.8. As the upstream untranslated

```

PA01_NUH_P : TGGCCGGCAACTGGGT
PA01_NUH_P : TGGCTAGACTTGTGGC
ABNIFH      : TGGCAGGGGGATGCA
ACFIXABC    : TGGTAGGACACTTGGT
ACNIFH      : TGGCAGCACCTTGGT
ADAZU       : AGGCAATGTGCCTGGG
AEHOXS      : TGGCGGACATCTGGG
AVFIXABCX   : TGGTAGGGCTGTGCA
AVIGLNA     : TGGCATGAAACTTGGT
AVIMONFE    : TGGCAGAGACGCTGCA
AVINIFA     : TGGCAGAGACGCTGCA
AVINIFBQ    : CGGCAAGGGTATGGT
AVINIFF     : TGGCTGTCTTCTTGGT
AVINIFH2A   : TGGCAGGGCCCTGGT
AVINIFREG   : TGGTGTGCAGGTGGC
AVINIFUSV   : TGGTGTGCAGGTGGC
AVNIFE      : TGGTAGGCACTTGGC
AVNIFL      : CGGCAAGGATTTGGT
BSLEVANOP   : TGGCAGATCCTTGGC
ECCELY      : TGGCGGGGTGTGCA
ECHEVOP     : TGGCAGAAAAATGGT
ECHYP       : TGGCAGAAATTTGGT
ECOFDHF     : TGGCATAAAGATGCA
ECOGLNA     : TGGCAGAGATTTGGT
ECOHISPUR2  : TGGCATAGACCTGCA
ENTNIFHAA   : TGGTAGAAACACTGCA
HSNIFABX    : GGGCATGAAGTTTGGT
KPLNA       : TGGCAGAGATTTGGT
KPNIFAB     : TGGTAGAGATTTGGC
KPNIFF      : TGGCAGAGCTTGGC
KPNIFH01    : TGGTAGTTCCCTGCA
KPNIFJ      : TGGCAGGGCTGTGGT
KPNIFXUS    : TGGTAGCGCAATGGT
KPNIFZM     : TGGCCGGAATTTGCA
KPNNACP     : TGGCAGCAAAATGCA
KPNNIFEPR   : TGGCAGCGGAATGCA
KPNNIFL     : GGGCGGACGGTTGCA
KPNNIFLA    : GGGCGGACGGTTGCA
MLCGSA      : TGGCAGTTAATCGGG
MXAHA       : TGGCAGGCCATCTGGT
PAAZU       : CGGCAATCTGTGGT
PANIRAX     : TGGCAGCGAGGTGGT
PRNIFDK     : TGGCATGCTCGTTGCA
PSEALGC_a1  : CGGCAACGCACITGGC
PSEHRPL     : TGGCAGGTTATGCA
PSEPHHYD    : TGGCAGAGCCGTGGT
PSEXYLA     : TGGCATGGCGGTGGT
PVGLNABC    : TGGCATGGTTTGGCA
RCANIFPRA   : TGGCAGATGGCTGGT
RCNIF       : TGGCAGGCTTCTGGT
RCNIFAB     : TGGCAGGTTCTTGGT
RHBGLNB     : TGGCATAGACCTGGT
RHBNIFB     : CGGCAATGCAAGTTGGT
RHMDCABD    : TGGCAGCATGTGGT
RHMFIXA     : TGGCAGGAATGATGCA
RHMFIXABCX  : TGGCAGGACTTTGGC
RHMNIFAX    : TGGCATGGCTTTGGG
RHMNIFB     : TGGCATAGCTGTGGT
RHMNIFDK    : TGGCATGCTGGTTGCA
RHMNIFDKZ   : TGGCATGCCGGTTGCA
RHMNIFH1X   : TGGCAGGGTTTCAA
RHMNIFKH3   : TGGCAGGCTTTCAA
RLDCTA      : TGGCAGGGGATGGG
RLFIXZ      : TGGCTGCCTCTATGCC
RLGLNA      : TGGCAGATATCTGCA
RLNIFAB     : TGGCATCGCTCTTGGT
RRGLNBA     : TGGCAGAGGCGTGGT
RRNIFJ      : TGGCAGACGCGACGG
RSPNIFHD    : TGGCAGGCTGGGTGCA
S52478      : TGGCAGAAAGTTGGT
STYARGTR    : TGGCATAGACCTGCA
STYDHUA     : TGGCAGATAGTGGCA
STYGLNAA    : TGGCAGAGATTTGGT
TFENIFHDK   : TGGCAGGGCCCTGCA
tGGca      tGc

```

Figure 3.8 – Alignment of the putative P1 and P2 of *P. aeruginosa nuh* to other known σ^{54} promoters.



Pseudomonas fluorescens Pf0-1

Figure 3.9 – Genetic organization of the *P. fluorescens nuh* gene

region would be rather short, it is expected that the PAO1 NH message may be degraded relatively quickly due to the lack of a 5' hairpin structure (Regnier and Arraiano, 2000). The low activity later noted for the PAO1 NH may be related to this. A weak match was also found for σ^S , the stationary phase sigma factor. This could explain the low constitutive nature of expression of *nuh* in *P. aeruginosa*, as σ^S and σ^{70} have some overlapping binding specificities (Nguyen and Burgess, 1997).

The *P. fluorescens nuh*, unlike that of *P. aeruginosa*, is located in a different region of the chromosome and appears to be the distal gene in a large operon (Figure 3.9) encoding genes involved in D-ribose catabolism (Iida et al., 1984; Lopilato et al., 1984). The genes for this operon are arranged in a different order from that seen for *E. coli* (*rbsBACRKD* for *Pseudomonas fluorescens*, *rbsDACBKR* in *E. coli*) (Lopilato et al., 1984). This operon also includes the gene for the ribose repressor (RbsR; Mauzy and Hermodson, 1992), suggesting that *nuh* expression may be regulated by one of its products. In the upstream, region of the ribose operons in several different pseudomonads, conserved regions have been located which denote the positions of the promoter region and potential RbsR-binding site (Figure 3.10). The roles of ribose and nitrogen in regulating the *Pseudomonas nuh* genes were investigated further.

Enzyme specificity and regulation of NH expression

A prior analysis of the substrate specificity of the NHs from *Pseudomonas* has shown it to be somewhat nonspecific (Lee, 1991). This was investigated using the induction system for the cloned *P. aeruginosa* NH. The results are shown in Figure 3.11 and confirm the lack of specificity.

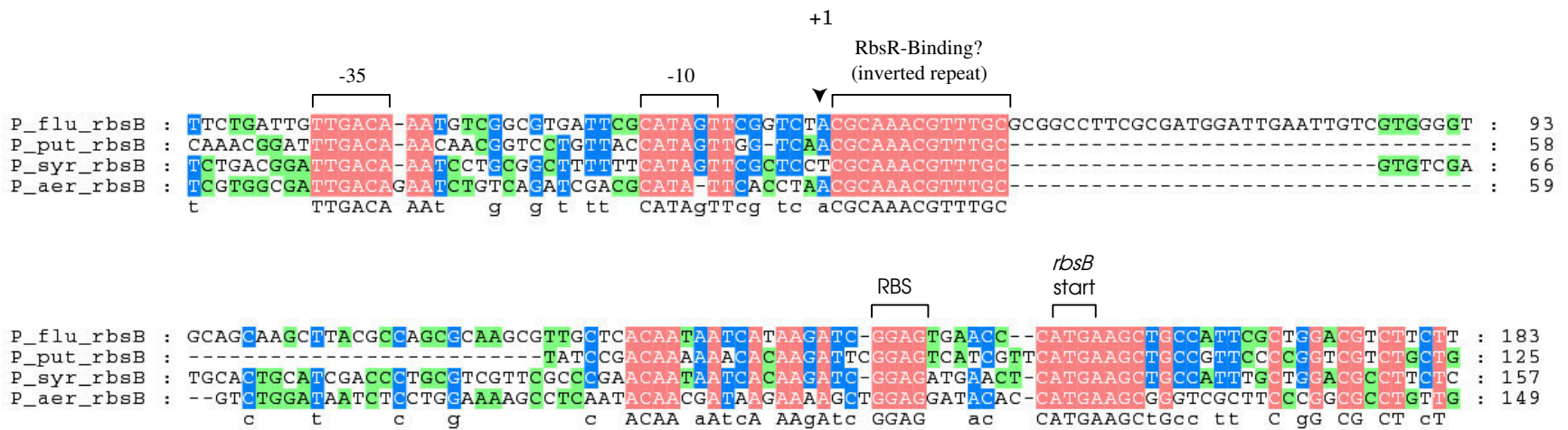


Figure 3.10 – Alignment of upstream of *Pseudomonas rbs* operons, revealing the operator binding site and the promoter (indicated as marked).

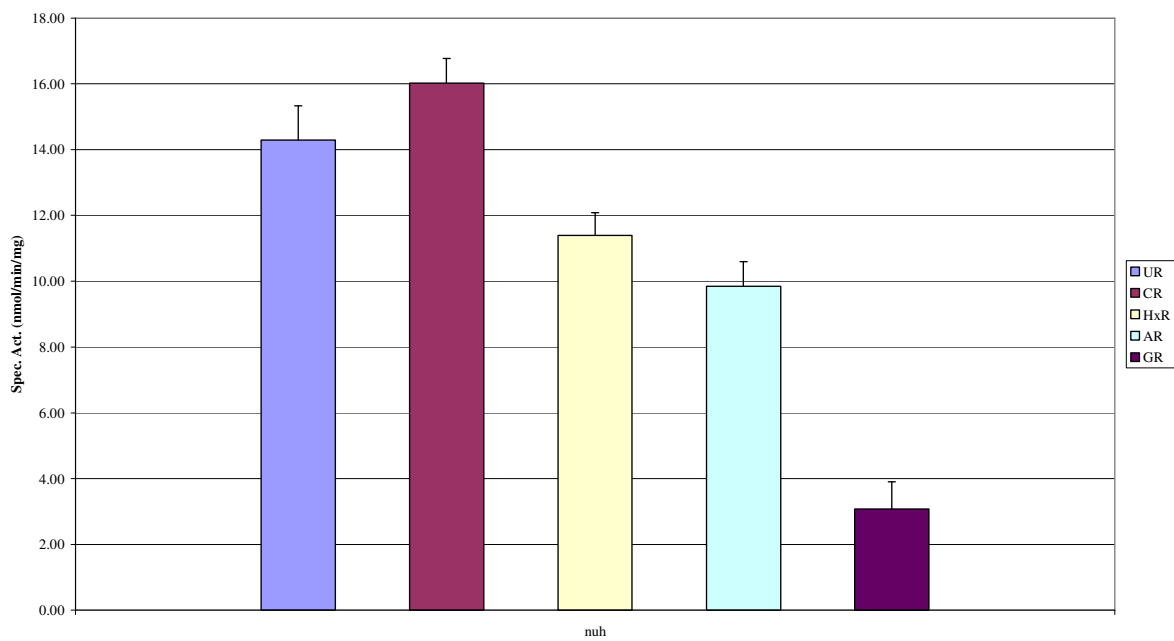


Figure 3.11 – Nucleoside specificity of *P. aeruginosa* NH

Figure 3.12 – Regulation under different conditions of growth of *P. aeruginosa* NH expression.

Experimental conditions are as described in Materials and Methods.

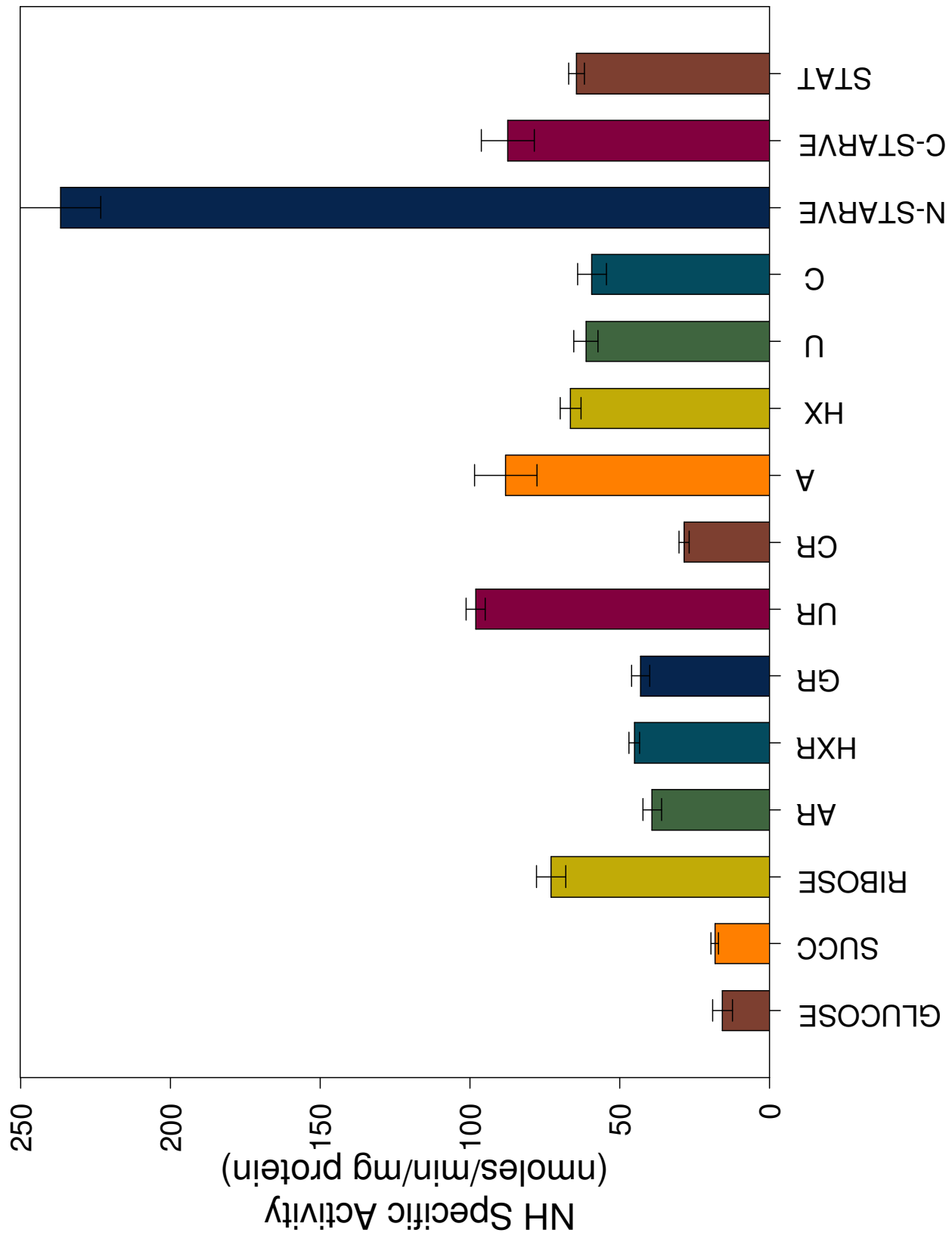
Abbreviations: Carbon sources: GLUCOSE = 20 mM glucose; SUCC = 20 mM succinate;

RIBOSE = 20 mM ribose.

Nucleosides and bases (1 mM of each) : AR (adenosine); GR (guanosine); HxR (inosine); UR (uridine); CR (cytidine); A (adenine); Hx (hypoxanthine); U (uracil); C (cytosine).

Starvation experiments: N-STARVE (nitrogen starvation); C-STARVE (carbon starvation);

STAT (stationary phase of growth).



The *nuh* genes from *P. aeruginosa* PAO1 and *P. fluorescens* Pf0-1 are present in each genome within entirely different genetic contexts. The PAO1 *nuh* (Figure 3.6) is monocistronic and may be regulated by σ^{54} . Experiments were performed to determine if the gene was regulated under these conditions or if other factors play a role. The wild-type *P. aeruginosa* PAO1 strain was grown under various conditions, as described in Materials and Methods. The results are shown in Figure 3.12. A noticeable increase in NH was observed when the cells were starved for nitrogen for 24 hours, with *nuh* expression being induced 15-fold, thus confirming the role of a nitrogen- regulated factor such as σ^{54} . Expression of *nuh* under carbon starvation was similar to that for stationary phase (5.5-fold vs. 4-fold); both may be due to the action of σ^S , which regulates during stationary phase and under starvation conditions (Hengge-Aronis, 1999). A weak match to a σ^S promoter is found overlapping the two σ^{54} promoters and may represent a third promoter site (Figure 3.9; Nguyen and Burgess, 1997). A significant increase in NH activity was also seen for the carbon source ribose. The source for this is currently unknown, as no potential binding sites for RbsR or other transcription factors were located upstream. This does not rule out the direct action of a regulatory factor other than RbsR or an indirect effect from RbsR. Another potential factor is the long generation time that *P. aeruginosa* has when utilizing ribose as a carbon source (26.4 hours). The addition of succinate does not catabolite-repress the protein's expression (MacGregor et al., 1996). Uridine is the strongest nucleoside inducer (6-fold) and is likely to represent the real inducer, as other nucleosides tested (adenosine, guanosine, inosine, and cytidine) only increased expression 2-3 fold, a factor that may be due to induction from the breakdown product ribose. Also, the bases increased *nuh* expression quite significantly (range of 3.5 to 5.5-fold), with adenine being the highest. Addition of adenine is known to deplete PRPP pools in *E. coli* through allosteric inhibition of PRPP synthetase and

regulation of the encoding gene *prs* (J. Neuhard, personal communication). The effect that adenine has may represent some connection with PRPP metabolism. This could also result from a positive feedback loop indicating the presence of pyrimidines and purines, both being a rich source of nitrogen for the cell (Chu and West, 1990; Kim and West, 1991). Regulation of *nuh* from PAO1 likely represents some form of mixed-mode regulation, perhaps via the actions of alternative sigma factors and possible regulatory proteins.

The expression of the *P. fluorescens nuh* represents a much more straightforward and yet more extreme induction (Figure 3.13). Under conditions where glucose is a carbon source, the specific activity is very low, less than half seen for *P. aeruginosa* grown in the same conditions. However, upon addition of ribose, NH activity is induced approximately 67-fold. Ribose thus represents the true inducer as the nucleosides (which carry the ribose moiety) induced enzyme activity while the bases (lacking the ribose group) showed little to no significant increase in NH activity. Another factor is that the generation time for growth on ribose is approximately 130 minutes, much shorter than for *P. aeruginosa*. A noticeable drop in activity is also seen under starvation conditions but is not present in the stationary phase culture; this could be due to complete loss of NH activity under stressed conditions. In these conditions, NH activity could be wasteful. The aspartate transcarbamoylase of *Bacillus* is degraded under conditions of carbon or nitrogen starvation in the cell (Hu and Switzer, 1995). It is possible that this represents a similar mechanism.

A summary of the data is shown in Table 3.3.

Figure 3.13 – Regulation under different conditions of growth of *P. fluorescens* NH expression.

Experimental conditions are as described in Materials and Methods.

Abbreviations : Carbon sources: GLUCOSE = 20 mM glucose; SUCC = 20 mM succinate;

RIBOSE = 20 mM ribose.

Nucleosides and bases (1 mM of each) : AR (adenosine); GR (guanosine); HxR (inosine); UR (uridine); CR (cytidine); A (adenine); Hx (hypoxanthine); U (uracil); C (cytosine).

Starvation experiments : N-STARVE (nitrogen starvation); C-STARVE (carbon starvation);

STAT (stationary phase of growth).

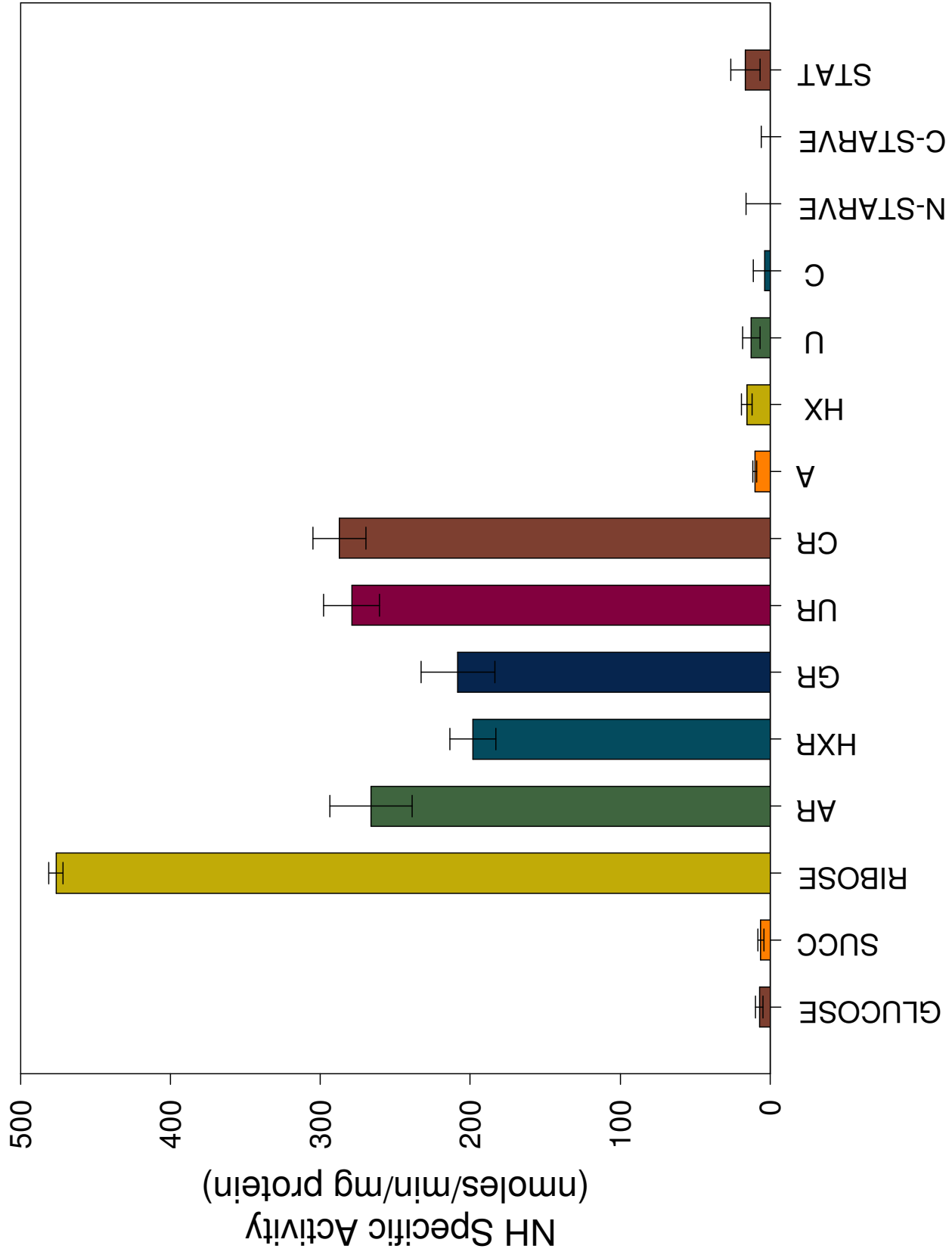


Table 3.3: Summary of enzyme induction studies

	<i>P. aeruginosa</i>			<i>P. fluorescens</i>		
	Spec. Activity	Std. Dev	Fold-Difference	Spec. Activity	Std. Dev	Fold-Difference
Glucose	15.71	3.30	1.00	7.13	2.55	1.00
Succinate	18.23	1.29	1.16	6.04	2.22	0.85
Ribose	72.95	4.89	4.64	476.35	4.73	66.77
Adenosine	39.21	3.06	2.50	266.22	27.34	37.32
Inosine	45.10	1.75	2.87	198.24	15.33	27.79
Guanosine	43.08	3.01	2.74	208.19	24.66	29.18
Uridine	98.06	3.22	6.24	279.11	18.49	39.12
Cytidine	28.54	1.64	1.82	287.22	17.57	40.26
Adenine	88.07	10.45	5.61	10.03	1.41	1.41
Hypoxanthine	66.44	3.53	4.23	15.42	3.53	2.16
Uracil	61.33	4.05	3.90	12.48	5.77	1.75
Cytosine	59.29	4.76	3.77	3.54	7.40	0.50
Nit. Starvation	236.74	13.47	15.07	0.02	21.61	0.00
Carb. Starvation	87.32	8.84	5.56	0.05	31.23	0.00
Stationary phase	64.45	2.64	4.10	16.45	9.82	2.31

Multiple alignment and analysis of the N-terminal signaling peptide

The multiple alignment of the known *Pseudomonas* nucleoside hydrolase sequences is shown in Figure 3.14. The N-terminal extension of all *Pseudomonas* nucleoside hydrolase is approximately 10-15 amino acids longer than the other nucleoside hydrolases, with the exception of the *R. solanocearum* putative NH, which is also believed to be exported outside the cell (as predicted by the programs PSORT and SignalP). The *Ochrobactrum anthropi* purine-specific nucleosidase (Ogawa et al., 2001) also is thought to represent an exported NH; this has never been experimentally determined, however. Residues known to bind the Ca^{++} (required for enzyme activity) and the ribose moiety are all present (Figure 3.14, Degano et al., 1996; Degano et al., 1998; Shi et al., 1999), indicating that the *Pseudomonas* nucleoside hydrolases are likely to have a catalytic mechanism similar to that of the nonspecific IUNH from *Crithidia fasciculata* (Degano et al., 1996).

SignalP analysis graphs for the *P. aeruginosa* and *P. fluorescens* NHs are shown in Figure 3.15. The alignment of the signal sequences, shading for the amino acid properties, is shown in Figure 3.15a. The consensus SecA-dependent signal motifs are present, with a basic N-terminus, followed by a hydrophobic cluster of residues and the cleavage site (Nielsen et al., 1999). The proposed cleavage region is relatively conserved in all the sequences (Figure 3.15a and b) and is thus likely to represent the true cleavage site.

Cellular localization studies of *Pseudomonas* NHs

The above information predicts that NHs from *Pseudomonas* may be exported. However, it cannot predict whether the enzymes will be excreted into the extracellular milieu or retained in the periplasmic space. To determine this, cells were grown and fractionated into the extracellular

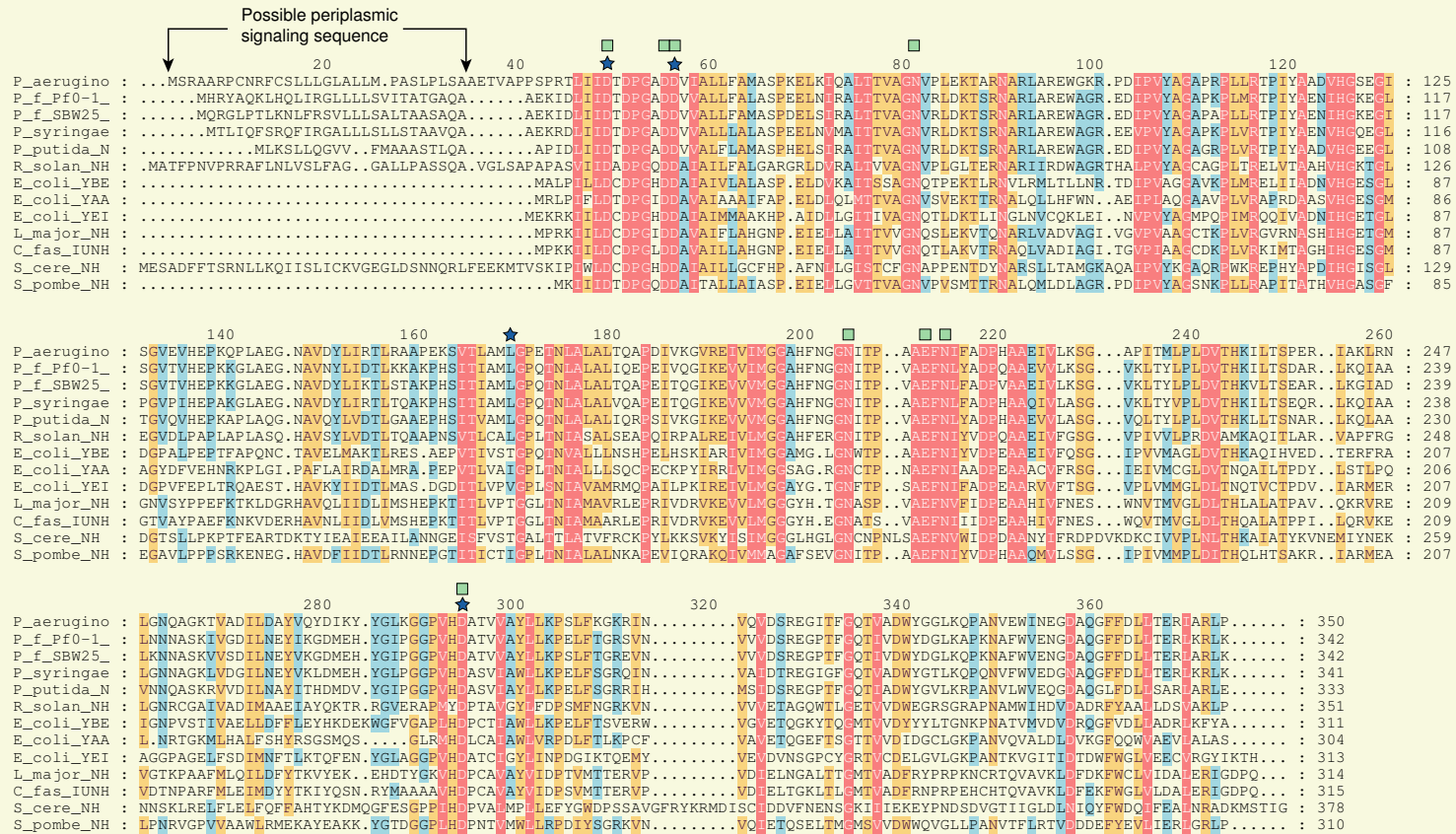


Figure 3.14 – Multiple alignment of nucleoside hydrolases. Stars (★) indicate residues involved in Ca⁺⁺-binding, boxes (■) represent residues known to bind hydroxyls on the nucleoside ribosyl group.

component (spent medium, SM), periplasmic fractions (P1 and P2), cytoplasmic fraction (cell-free extract, CX), and cell membrane fraction. Markers for the cytoplasmic space (aspartate transcarbamoylase) and periplasmic space (alkaline phosphatase and phospholipase C) were assayed to determine their proximity in relation to the NHs. Determination of activities in the spent medium fraction was highly variable due to low protein concentration and the presence of pigments produced in phosphate starvation (a condition needed for induction of alkaline phosphatase and phospholipase C); this fraction was not used further in this study. As is seen in Figure 3.16 and 3.17, a significant percentage of the NH activity is localized in the periplasmic fractions, along with alkaline phosphatase and phospholipase C activity. Due to the localization of known periplasmic enzyme activities with nucleoside hydrolase, the NHs are concluded to be exported into the periplasmic space.

Figure 3.15 – Alignments of signal peptide sequences.

- a) Alignments of signal peptide sequences showing sequence conservation. Shading indicates degree of homology (red – 100%, orange – 80%, blue – 60%). Amino acids are grouped based upon evolutionary relatedness as determined by the PAM 250 matrix (Dayhoff, 1978).

```

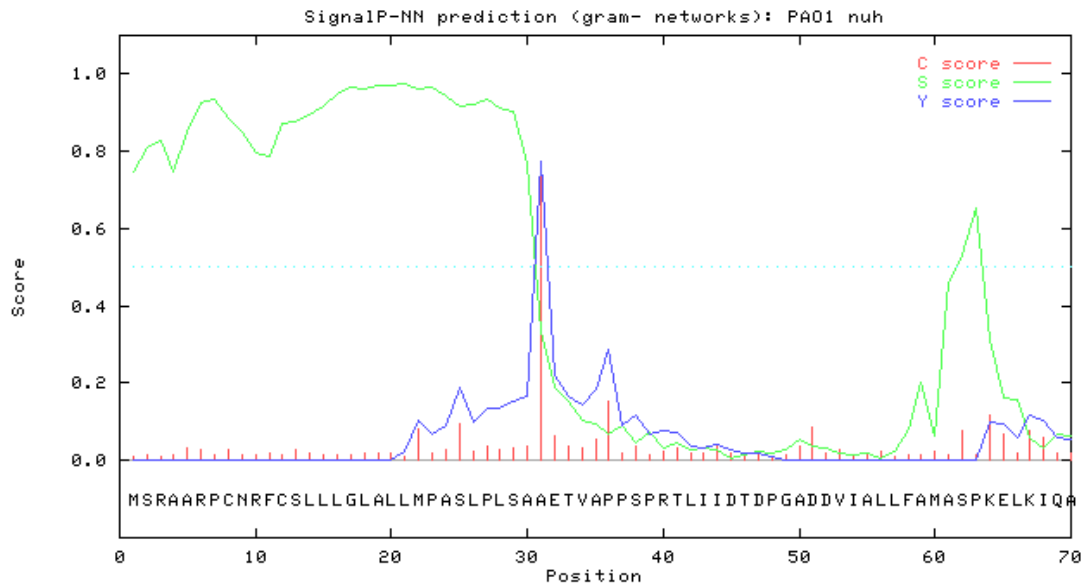
P_aerugino : .MSRAARPCNRFCSLLGLALLMPASLPLSAAETVA
P_f_Pf0-1_ : ...MHR YAQKLHQLIRGLLLLSVITATGAQAAEKID
P_f_SBW25_ : ...MQRGLPTLKNLFRSVLLLSALTAA SAQAAEKID
P_syringae : ...MTLIQFSRQFIRGALLLSLSTAAVQAAEKRD
P_putida_N : .....MLKSLIQGVVFMA..AASTLQAA.PID
R_solan_NH : MATFPNVPRRAFLNLVSLFAGGALLPASSQAVGLSA
  
```

- b) Alignment showing conservation of amino acid characteristics between sequences. Red background – charge (white text = positive, green = negative). Light green background – hydrophobic (red text = aliphatic, white =aromatic).

		Basic	Hydrophobic	Cleavage
		┌───────────┐		┌───────────┐
		└───────────┘		└───────────┘
P_aerugino	:	.MSRAARPCNRFCSLLGLALLMPASLPLSAAETVA		
P_f_Pf0-1_	:	...MHR YAQKLHQLIRGLLLLSVITATGAQAAEKID		
P_f_SBW25_	:	...MQRGLPTLKNLFRSVLLLSALTAA SAQAAEKID		
P_syringae	:	...MTLIQFSRQFIRGALLLSLSTAAVQAAEKRD		
P_putida_N	:MLKSLIQGVVFMA..AASTLQAA.PID		
R_solan_NH	:	MATFPNVPRRAFLNLVSLFAGGALLPASSQAVGLSA		

Figure 3.16 – SignalP prediction. The C score represents the raw cleavage site score; S score represents probable signal peptide score; Y score represents the combined score of the above two (Nielsen et al., 1999)

Pseudomonas aeruginosa



Pseudomonas fluorescens

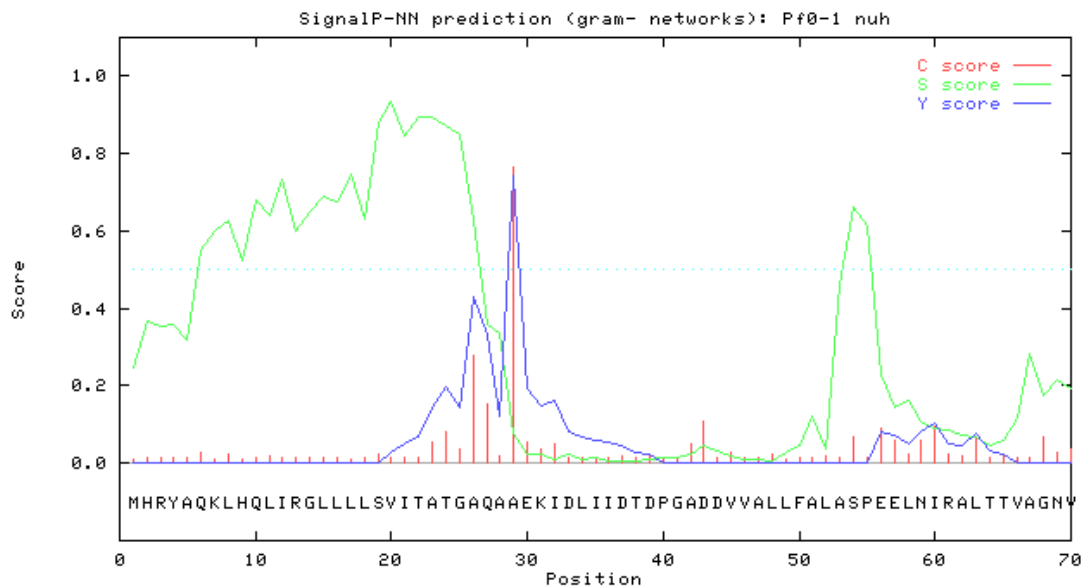


Figure 3.17 – Localization of *P. aeruginosa* NH. Results shown are assays from two independent samples.

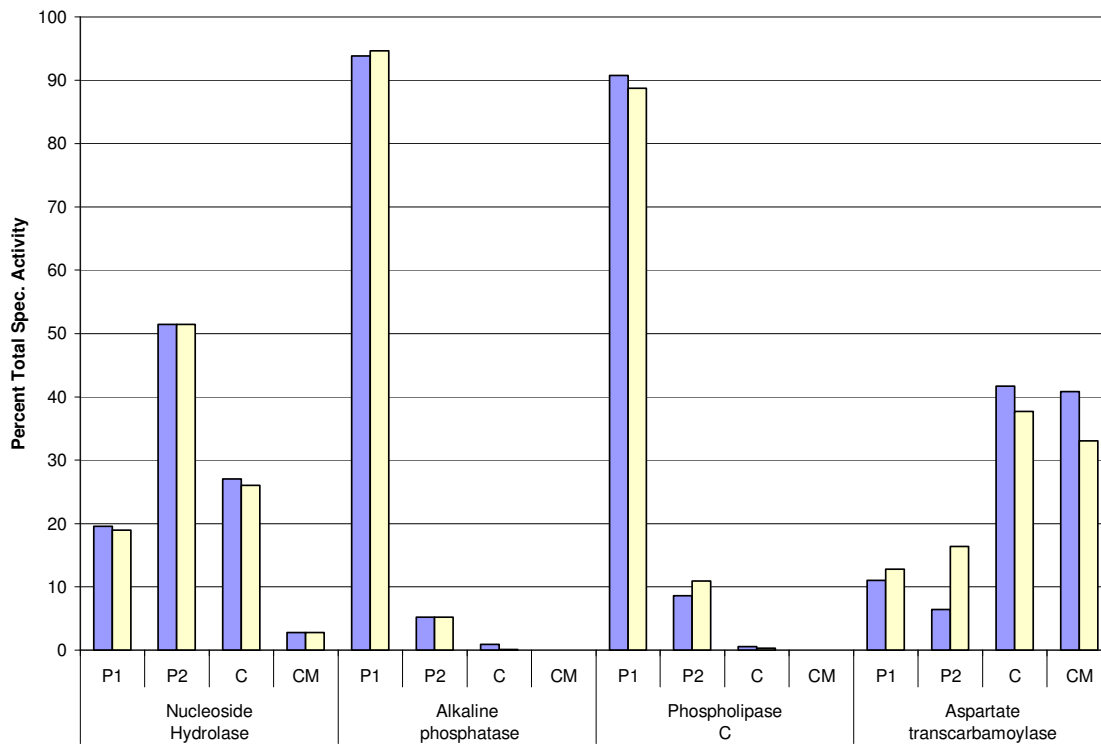
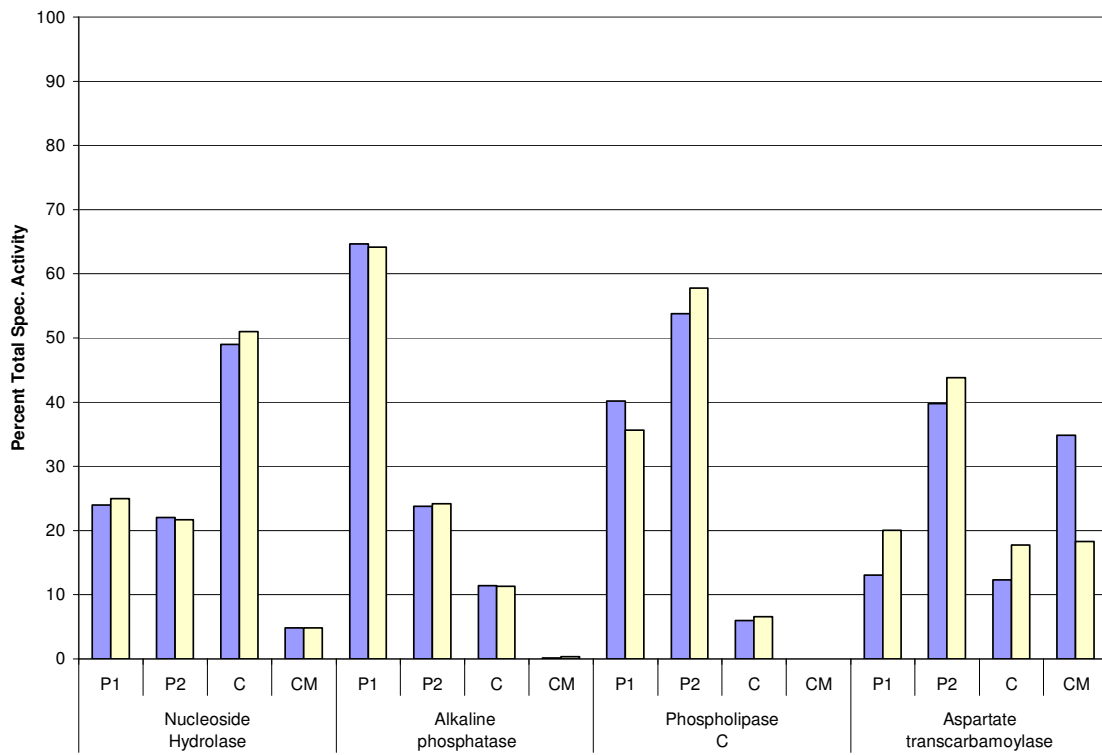


Figure 3.18 – Localization of *P. fluorescens* NH. Results shown are assays from two independent samples.



Conclusions

Unlike the *E. coli* NHs, whose existence remains an enigma (Chapter 2), the *Pseudomonas* NHs seem to play a specific role in nucleoside catabolism. This has been previously stated by others (West and Chu, 1986; West, 1988; Lee, 1991; Beck, 1995; West, 1996). The finding that the pseudomonads have significant problems in transporting nucleosides, though, had become evident in recent studies (West, 1996); the genome annotation also revealed that *P. aeruginosa* lacked all known homologues currently known to transport nucleosides (Munch-Peterson and Mygind, 1983; Wang and Giacomini, 1999). This represents an interesting quandary, as one now has to explain how *Pseudomonas* is able to utilize nucleosides as nitrogen and carbon sources without being able to transport them into the cytoplasm. This would be solved if the nucleoside hydrolase were, instead, exported into the periplasmic space to meet the incoming nucleoside. The permeability of the *Pseudomonas* periplasmic space is variable and is dependent on the conditions presented to the cell, such as the presence of antibiotics (Hancock and Bellido, 1992; Hancock, 1998). In *E. coli*, the protein Tsx is involved with outer membrane permeability for nucleosides (Munch-Peterson and Mygind, 1983). A close homologue for Tsx is not present in the *Pseudomonas aeruginosa* genome (Stover et al., 2000). However, significant matches (expectation values of $< 10^{-80}$) have been found for Tsx in the unfinished genomes of two other pseudomonads, including *P. fluorescens* Pf0-1 and *P. syringae*, suggesting that they are able to transport nucleosides efficiently into the periplasmic space. A distant homologue is found in *P. aeruginosa* (expectation value of 10^{-7}), but the gene, designated PA0165, is highly divergent and may not play an active role in

transporting nucleosides, as a BLASTP search (Altschul et al., 1997) using PA0165 only picked up homologues involved in atrazine degradation (GenBank # AAK50329).

Cleavage of nucleosides in the periplasmic space would allow for ribose and the respective bases to be imported into the cytoplasm by their specific transporters (Munch-Peterson and Mygind, 1983; Iida et al., 1984). The respective bases could be further utilized as sources of nitrogen or nucleotides (Vogels and Van der Drift, 1976; Neuhard, 1983; Nygaard, 1983). The ribose moiety is phosphorylated to form ribose-5-phosphate upon entry into the cytoplasm (Iida et al., 1984; Lopilato et al., 1984). In *E. coli*, ribose-5-phosphate is required to form PRPP (via the action of phosphoribosylpyrophosphate synthetase) or is metabolized by the pentose phosphate pathway through which fructose-6-phosphate, glyceraldehyde-3-phosphate, and other carbon sources are made. In *Pseudomonas*, ribose catabolism is likely to occur through the formation of glyceraldehyde-3-phosphate, which can be utilized in glycolysis, and fructose-6-phosphate, which can be catabolized by conversion into glucose-6-phosphate and further processing via the Entner-Doudoroff pathway (Temple et al., 1998).

If the transport of ribose were defective, growth would be severely impaired. In *P. fluorescens*, the gene immediately upstream is *rbsD*, a protein known to play a role in ribose catabolism but with an unknown function. Impairment in *rbsD* has been found to cause a defect in the transport of ribose (Oh et al., 1999), leading to a dramatic decrease in ribose import prior to phosphorylation by the enzyme ribokinase. The fact that the *nuh* gene is located quite far from the *rbs* genes in *P. aeruginosa* (approximately 2 Mbp), and that the *rbsBACKRD-nuh* operon organization is conserved in all other sequences *Pseudomonas* species indicates that a major gene rearrangement has occurred. Upon closer inspection, it was determined that the *rbsD* gene is no longer present at the 3' end of the *rbs* operon in *P. aeruginosa* and, through a BLAST

homology search, is not located anywhere on the chromosome. It may have been lost as a consequence of the rearrangement of *nuh* in the genome. This explains the longer generation time (26.4 days in *P. aeruginosa* compared to 130 minutes in *P. fluorescens*) as ribose import would be decreased, analogous to the *rbsD* mutants in *E. coli*, leading to a longer generation time due to the decreased growth rate.

Another potential reason for *Pseudomonas* to have a periplasmic NH is from catabolism of RNA breakdown products. Any carbon and nitrogen source in a nutrient-poor environment would be utilized. When cells lyse, massive amounts of nucleic acids are released. RNases are found everywhere (Regnier and Arraiano, 2000); therefore it would be expected that extracellular nucleotide monophosphates would increase over time. Conversion of these into nucleosides would occur through the action of extracellular or cytoplasmic 5' nucleotidase (Bhatti et al., 1976). NH would break down these into bases and ribose to obtain carbon and nitrogen. As DNA has recently been found to sustain *E. coli* as a carbon source (Finkel and Kolter, 2001), one would expect that the catabolically diverse pseudomonads would be able to do the same and more. A summary of the proposed physiological scheme is shown in Figure 3.19.

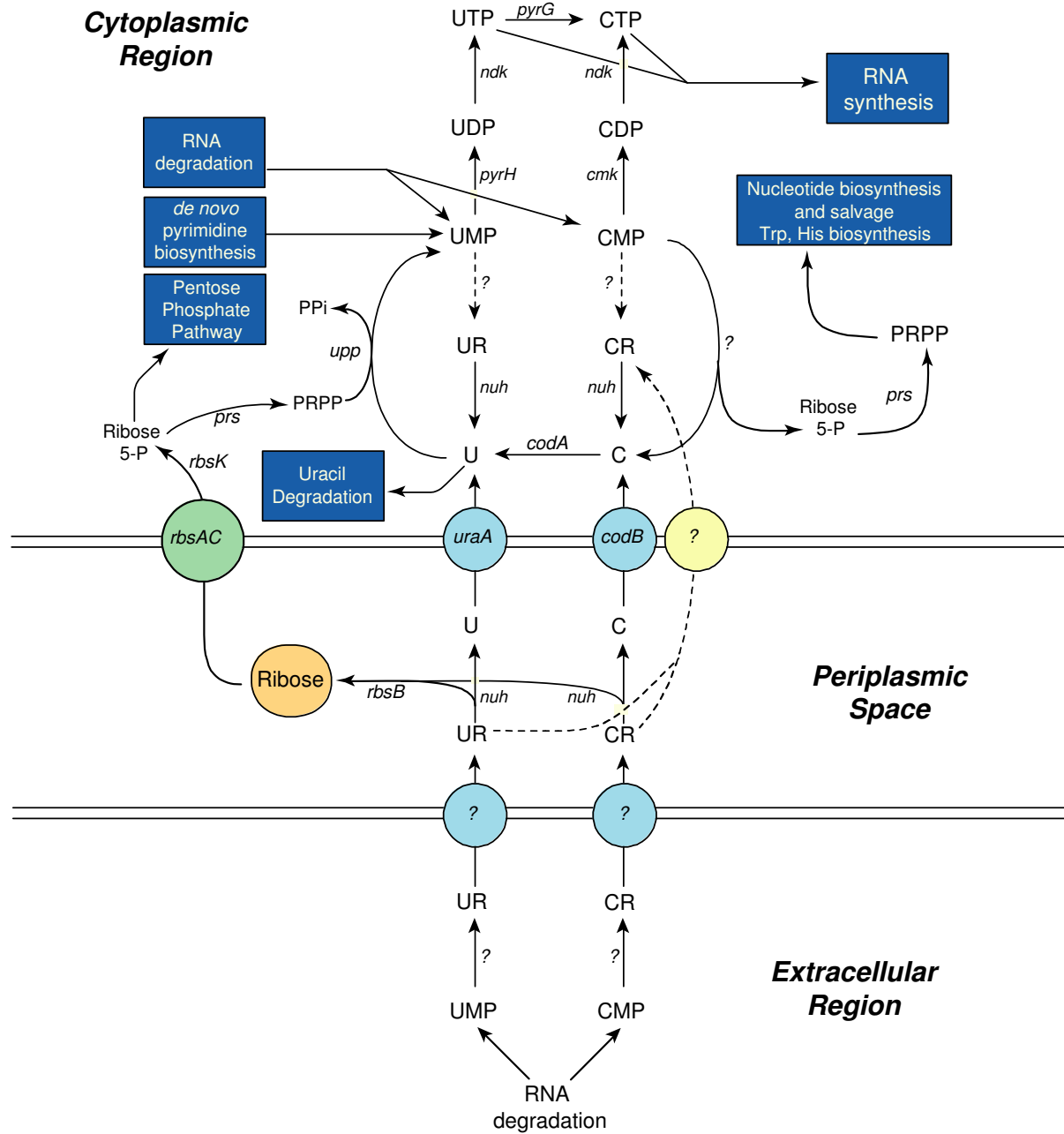


Figure 3.19 – Proposed mode of nucleoside breakdown in *Pseudomonas*.

References

- Altschul, S. F., T. L. Madden, A. A. Schaffer, J. Zhang, Z. Zhang, W. Miller, and D. J. Lipman.** 1997. Gapped BLAST and PSI-BLAST: a new generation of protein database search programs. *Nucleic Acids Res.* **25**:3389-3402.
- Anderson, P. M.** 1977. Binding of allosteric effectors to carbamyl-phosphate synthetase from *Escherichia coli*. *Biochemistry* **16**:587-593.
- Barton, G. J.** 1993. ALSRIPT: a tool to format multiple sequence alignments. *Protein Eng.* **6**:37-40.
- Beck, D. E.** 1995. Pyrimidine salvage enzymes in microorganisms : labyrinths of enzymatic diversity. Ph.D. dissertation. The University of North Texas.
- Bhatti, A. R., I. W. DeVoe, and J. M. Ingram.** 1976. The release and characterization of some periplasm-located enzymes of *Pseudomonas aeruginosa*. *Can.J.Microbiol.* **22**:1425-1429.
- Bradford, M. M.** 1976. A rapid and sensitive method for the quantitation of microgram quantities of protein utilizing the principle of protein-dye binding. *Anal.Biochem.* **72**:248-254.
- Casaz, P., A. Happel, J. Keithan, D. L. Read, S. R. Strain, and S. B. Levy.** 2001. The *Pseudomonas fluorescens* transcription activator AdnA is required for adhesion and motility. *Microbiology* **147**:355-361.

Charlier, D., G. Weyens, M. Roovers, J. Piette, C. Bocquet, A. Pierard, and N. Glansdorff.

1988. Molecular interactions in the control region of the *carAB* operon encoding *Escherichia coli* carbamoylphosphate synthetase. *J.Mol.Biol.* **204**:867-877.

Chu, C. P. and T. P. West. 1990. Pyrimidine ribonucleoside catabolism in *Pseudomonas fluorescens* biotype A. *Antonie Van Leeuwenhoek* **57**:253-257.

Cui, L., G. R. Rajasekariah, and S. K. Martin. 2001. A nonspecific nucleoside hydrolase from *Leishmania donovani*: implications for purine salvage by the parasite. *Gene* **280**:153-162.

Dayhoff, M. O. 1978. Survey of new data and computer methods of analysis, *In Atlas of protein sequence and structure*. National Biomedical Research Foundation, Georgetown University, Washington, D.C.

Degano, M., S. C. Almo, J. C. Sacchettini, and V. L. Schramm. 1998. Trypanosomal nucleoside hydrolase. A novel mechanism from the structure with a transition-state inhibitor. *Biochemistry* **37**:6277-6285.

Degano, M., D. N. Gopaul, G. Scapin, V. L. Schramm, and J. C. Sacchettini. 1996. Three-dimensional structure of the inosine-uridine nucleoside N-ribohydrolase from *Crithidia fasciculata*. *Biochemistry* **35**:5971-5981.

Farinha, M. A., S. L. Ronald, A. M. Kropinski, and W. Paranchych. 1993. Localization of the virulence-associated genes *pilA*, *pilR*, *rpoN*, *fliA*, *fliC*, *ent*, and *fbp* on the physical map of *Pseudomonas aeruginosa* PAO1 by pulsed-field electrophoresis. *Infect.Immun.* **61**:1571-1575.

- Finkel, S. E. and R. Kolter.** 2001. DNA as a nutrient: novel role for bacterial competence gene homologs. *J.Bacteriol.* **183**:6288-6293.
- Gopaul, D. N., S. L. Meyer, M. Degano, J. C. Sacchetti, and V. L. Schramm.** 1996. Inosine-uridine nucleoside hydrolase from *Crithidia fasciculata*. Genetic characterization, crystallization, and identification of histidine 241 as a catalytic site residue. *Biochemistry* **35**:5963-5970.
- Guex, N. and M. C. Peitsch.** 1997. SWISS-MODEL and the Swiss-PdbViewer: an environment for comparative protein modeling. *Electrophoresis* **18**:2714-2723.
- Hancock, R. E.** 1998. Resistance mechanisms in *Pseudomonas aeruginosa* and other nonfermentative gram-negative bacteria. *Clin.Infect.Dis.* **27 Suppl 1**:S93-S99.
- Hancock, R. E.** 9-19-1999. Hancock Laboratory Methods. Department of Microbiology and Immunology, University of British Columbia, British Columbia, Canada. Accessed 10-1-2001. <http://www.cmdr.ubc.ca/bobh/methodsall.html>
- Hancock, R. E. and F. Bellido.** 1992. Antibiotic uptake: unusual results for unusual molecules. *J.Antimicrob.Chemother.* **29**:235-239.
- Harold, F. M.** 1963. Accumulation of inorganic phosphate in *Aerobacter aerogenes*. *J.Bacteriol.* **86**:216-221.
- Hengge-Aronis, R.** 1999. Interplay of global regulators and cell physiology in the general stress response of *Escherichia coli*. *Curr.Opin.Microbiol.* **2**:148-152.

- Hu, P. and R. L. Switzer.** 1995. Evidence for substrate stabilization in regulation of the degradation of *Bacillus subtilis* aspartate transcarbamylase *in vivo*. Arch.Biochem.Biophys. **316**:260-266.
- Iida, A., S. Harayama, T. Iino, and G. L. Hazelbauer.** 1984. Molecular cloning and characterization of genes required for ribose transport and utilization in *Escherichia coli* K-12. J.Bacteriol. **158**:674-682.
- Kim, S. and T. P. West.** 1991. Pyrimidine catabolism in *Pseudomonas aeruginosa*. FEMS Microbiol.Lett. **61**:175-179.
- Kunz, D. A., J. L. Chen, and G. Pan.** 1998. Accumulation of alpha-keto acids as essential components in cyanide assimilation by *Pseudomonas fluorescens* NCIMB 11764. Appl.Environ.Microbiol. **64**:4452-4459.
- Lee, Y.-S.** 1991. Pyrimidine metabolism in bacteria : physiological properties of nucleoside hydrolase and uridine kinase. Masters thesis. The University of North Texas.
- Leger, D. and G. Herve.** 1988. Allostery and pKa changes in aspartate transcarbamoylase from *Escherichia coli* - analysis of the pH-dependence in the isolated catalytic subunits. Biochemistry **27**:4293-4298.
- Lindenbaum, P.** 1998. CloneIt: finding cloning strategies, in-frame deletions and frameshifts. Bioinformatics. **14**:465-466.

- Lopilato, J. E., J. L. Garwin, S. D. Emr, T. J. Silhavy, and J. R. Beckwith.** 1984. D-ribose metabolism in *Escherichia coli* K-12: genetics, regulation, and transport. *J.Bacteriol.* **158**:665-673.
- MacGregor, C. H., S. K. Arora, P. W. Hager, M. B. Dail, and P. V. Phibbs, Jr.** 1996. The nucleotide sequence of the *Pseudomonas aeruginosa* *pyrE-crc-rph* region and the purification of the *crc* gene product. *J.Bacteriol.* **178**:5627-5635.
- Mauzy, C. A. and M. A. Hermodson.** 1992. Structural and functional analyses of the repressor, RbsR, of the ribose operon of *Escherichia coli*. *Protein Sci.* **1**:831-842.
- McGuire, A. M., J. D. Hughes, and G. M. Church.** 2000. Conservation of DNA regulatory motifs and discovery of new motifs in microbial genomes. *Genome Res.* **10**:744-757.
- Merrick, M. J.** 1993. In a class of its own--the RNA polymerase sigma factor sigma 54 (sigma N). *Mol.Microbiol.* **10**:903-909.
- Miczak, A., V. R. Kaberdin, C. L. Wei, and S. Lin-Chao.** 1996. Proteins associated with RNase E in a multicomponent ribonucleolytic complex. *Proc.Natl.Acad.Sci.U.S.A.* **93**:3865-3869.
- Mohr, C. D., J. H. Leveau, D. P. Krieg, N. S. Hibler, and V. Deretic.** 1992. AlgR-binding sites within the *algD* promoter make up a set of inverted repeats separated by a large intervening segment of DNA. *J.Bacteriol.* **174**:6624-6633.

- Munch-Peterson, A. and B. Mygind.** 1983. Transport of nucleic acid precursors, p. 259-305. *In* A. Munch-Peterson (ed.), *Metabolism of Nucleotides, Nucleosides, and Nucleobases in Microorganisms*. Academic Press, London.
- Nakai, K. and P. Horton.** 1999. PSORT: a program for detecting sorting signals in proteins and predicting their subcellular localization. *Trends Biochem.Sci.* **24**:34-36.
- Neuhard, J.** 1983. Utilization of preformed pyrimidine bases and nucleosides, p. 95-148. *In* A. Munch-Peterson (ed.), *Metabolism of Nucleotides, Nucleosides, and Nucleobases in Microorganisms*. Academic Press, London.
- Nguyen, L. H. and R. R. Burgess.** 1997. Comparative analysis of the interactions of *Escherichia coli* sigma S and sigma 70 RNA polymerase holoenzyme with the stationary-phase-specific *bolAp1* promoter. *Biochemistry* **36**:1748-1754.
- Nicholas, K. B. and Nicholas, H. B.** 7-1-2001. Genedoc : a tool for editing and annotating multiple sequence alignments. Pittsburg Supercomputing Center Biomedical Initiative. Accessed 8-25-2001. <http://www.psc.edu/biomed/genedoc/>
- Nielsen, H., S. Brunak, and G. von Heijne.** 1999. Machine learning approaches for the prediction of signal peptides and other protein sorting signals. *Protein Eng.* **12**:3-9.
- Nygaard, P.** 1983. Utilization of preformed purine bases and nucleosides, p. 27-93. *In* A. Munch-Peterson (ed.), *Metabolism of Nucleotides, Nucleosides, and Nucleobases in Microorganisms*. Academic Press, London.

- Ogawa, J., S. Takeda, S. X. Xie, H. Hatanaka, T. Ashikari, T. Amachi, and S. Shimizu.** 2001. Purification, characterization, and gene cloning of purine nucleosidase from *Ochrobactrum anthropi*. *Appl. Environ. Microbiol.* **67**:1783-1787.
- Oh, H., Y. Park, and C. Park.** 1999. A mutated PtsG, the glucose transporter, allows uptake of D-ribose. *J. Biol. Chem.* **274**:14006-14011.
- Parkin, D. W., B. A. Horenstein, D. R. Abdulah, B. Estupinan, and V. L. Schramm.** 1991. Nucleoside hydrolase from *Crithidia fasciculata*. Metabolic role, purification, specificity, and kinetic mechanism. *J. Biol. Chem.* **266**:20658-20665.
- Petersen, C. and L. B. Moller.** 2001. The RihA, RihB, and RihC ribonucleoside hydrolases of *Escherichia coli*. Substrate specificity, gene expression, and regulation. *J. Biol. Chem.* **276**:884-894.
- Poole, K. and R. E. Hancock.** 1984. Phosphate transport in *Pseudomonas aeruginosa*. Involvement of a periplasmic phosphate-binding protein. *Eur. J. Biochem.* **144**:607-612.
- Prescott, L. M. and M. E. Jones.** 1969. Modified methods for the determination of carbamyl aspartate. *Anal. Biochem.* **32**:408-419.
- Regnier, P. and C. M. Arraiano.** 2000. Degradation of mRNA in bacteria: emergence of ubiquitous features. *Bioessays* **22**:235-244.
- Rice, P., I. Longden, and A. Bleasby.** 2000. EMBOSS: the European Molecular Biology Open Software Suite. *Trends Genet.* **16**:276-277.

- Rost, B., C. Sander, and R. Schneider.** 1994. PHD--an automatic mail server for protein secondary structure prediction. *Comput.Appl.Biosci.* **10**:53-60.
- Shi, W., V. L. Schramm, and S. C. Almo.** 1999. Nucleoside hydrolase from *Leishmania major*. Cloning, expression, catalytic properties, transition state inhibitors, and the 2.5-Å crystal structure. *J.Biol.Chem.* **274**:21114-21120.
- Stover, C. K., X. Q. Pham, A. L. Erwin, S. D. Mizoguchi, P. Warrener, M. J. Hickey, F. S. Brinkman, W. O. Hufnagle, D. J. Kowalik, M. Lagrou, R. L. Garber, L. Goltry, E. Tolentino, S. Westbrook-Wadman, Y. Yuan, L. L. Brody, S. N. Coulter, K. R. Folger, A. Kas, K. Larbig, R. Lim, K. Smith, D. Spencer, G. K. Wong, Z. Wu, and I. T. Paulsen.** 2000. Complete genome sequence of *Pseudomonas aeruginosa* PA01, an opportunistic pathogen. *Nature* **406**:959-964.
- Temple, L. M., A. E. Sage, H. P. Schweizer, and P. V. J. Phibbs.** 1998. Carbohydrate catabolism in *Pseudomonas aeruginosa*, p. 35-72. *In* T. Montie (ed.), *Pseudomonas*. Plenum Press, New York.
- Terada, M., M. Tatibana, and O. Hayaishi.** 1967. Purification and properties of nucleoside hydrolase from *Pseudomonas fluorescens*. *J.Biol.Chem.* **242**:5578-5585.
- Thompson, J. D., T. J. Gibson, F. Plewniak, F. Jeanmougin, and D. G. Higgins.** 1997. The CLUSTAL_X windows interface: flexible strategies for multiple sequence alignment aided by quality analysis tools. *Nucleic Acids Res.* **25**:4876-4882.
- Vogels, G. D. and C. Van der Drift.** 1976. Degradation of purines and pyrimidines by microorganisms. *Bacteriol.Rev.* **40**:403-468.

- Wang, J. and K. M. Giacomini.** 1999. Serine 318 is essential for the pyrimidine selectivity of the N2 Na⁺-nucleoside transporter. *J.Biol.Chem.* **274**:2298-2302.
- Werner, T.** 2000. Computer-assisted analysis of transcription control regions. Matinspector and other programs. *Methods Mol.Biol.* **132**:337-349.
- West, T. P.** 1988. Metabolism of pyrimidine bases and nucleosides by *Pseudomonas fluorescens* biotype F. *Microbios* **56**:27-36.
- West, T. P.** 1996. Degradation of pyrimidine ribonucleosides by *Pseudomonas aeruginosa*. *Antonie Van Leeuwenhoek* **69**:331-335.
- West, T. P. and C. P. Chu.** 1986. Utilization of pyrimidines and pyrimidine analogues by fluorescent pseudomonads. *Microbios* **47**:149-157.